

# **IMPROVED MEMBRANE ABSORBERS**

**Robert Oldfield**

Research Institute for the Built and Human Environment, Acoustics  
Department, University of Salford, Salford, UK

Submitted in Fulfillment of the Requirements of the Degree of Master of  
Science by Research, September 2006

## CONTENTS

<i>Acknowledgements</i>	v
<i>Abstract</i>	vi
<i>Nomenclature</i>	vii
<i>List of Tables and Figures</i>	ix
1. INTRODUCTION .....	1
2. ABSORPTION METHODS .....	5
2.1 INTRODUCTION.....	5
2.2 PRINCIPLES OF ABSORPTION .....	6
2.2.1 <i>Reflection Factor</i> .....	6
2.2.2 <i>Absorption Coefficient</i> .....	7
2.2.3 <i>Surface Impedance</i> .....	8
2.3 POROUS ABSORBERS .....	9
2.3.1 <i>Characterising and Modelling Porous Absorbers</i> .....	11
2.3.1.1 Material Properties .....	11
2.3.1.1.1 Measuring Flow Resistivity .....	13
2.3.1.2 Prediction Models .....	14
2.3.1.2.1 Acoustic Impedance Modelling of Multiple Porous Layers .....	16
2.4 RESONANT ABSORPTION .....	19
2.4.1 <i>Helmholtz Absorbers</i> .....	19
2.4.1.1 Predicting the Performance of Helmholtz Absorbers .....	20
2.4.2 <i>Membrane Absorbers</i> .....	22
2.4.2.1 Predicting the Performance of Membrane Absorbers.....	23
2.4.2.1.1 Transfer Matrix Modelling.....	25
2.5 CONCLUSION.....	29
3. MEASURING ABSORPTION COEFFICIENT AND SURFACE IMPEDANCE	30
3.1 INTRODUCTION.....	30
3.2 REVERBERATION CHAMBER METHOD.....	31
3.3 IMPEDANCE TUBE METHOD .....	33
3.3.1 <i>Standing Wave Method</i> .....	33
3.3.2 <i>Transfer Function Method</i> .....	36
3.3.3 <i>General Considerations for Impedance Tube Testing</i> .....	38
3.4 THE DESIGN, BUILD AND COMMISSIONING OF A LOW FREQUENCY IMPEDANCE TUBE .....	39
3.4.1 <i>Design</i> .....	40
3.4.2 <i>Construction</i> .....	41
3.4.3 <i>Processing the Data and Commissioning the Tube</i> .....	42
3.4.3.1 Least Squares Optimization Technique .....	42
3.5 CONCLUSION.....	47
4. USING LOUDSPEAKER SURROUND AS THE MOUNTING FOR A MEMBRANE ABSORBER .....	48
4.1 INTRODUCTION.....	48

4.2	THEORY .....	49
4.2.1	<i>Traditional Mounting Conditions</i> .....	49
4.2.1.1	Simply Supported.....	50
4.2.1.2	Clamped .....	50
4.2.1.3	Freely Supported.....	51
4.2.2	<i>The Pistonic Case</i> .....	51
4.3	MEASUREMENTS .....	53
4.3.1	<i>Initial Measurements Using an Accelerometer</i> .....	53
4.3.2	<i>Impedance Tube Tests</i> .....	56
4.4	MODELLING .....	61
4.4.1	<i>Equivalent Circuit Model</i> .....	62
4.4.1.1	Finding Parameters .....	62
4.4.1.1.1	Determining $C_{AD}$ .....	63
4.4.1.1.2	Finding the Equivalent Piston of a Clamped Plate .....	64
4.4.1.2	Results.....	65
4.4.2	<i>Transfer Matrix Model</i> .....	66
4.5	CONCLUSION.....	68
5.	USING A LOUDSPEAKER AS A RESONANT ABSORBER .....	69
5.1	INTRODUCTION.....	69
5.2	BASIC PREMISE FROM LOUDSPEAKER THEORY .....	70
5.3	LUMPED PARAMETER MODELLING .....	71
5.3.1	<i>Theory</i> .....	71
5.3.1.1	Equivalent Circuits.....	72
5.3.2	<i>Analysis</i> .....	77
5.3.2.1	Electrical Section .....	77
5.3.2.2	Mechanical Section.....	78
5.3.2.3	Acoustical Section.....	82
5.3.2.4	Combining the Sections .....	83
5.3.3	<i>Defining the Parameters</i> .....	88
5.3.4	<i>Calculating the Absorption of the System</i> .....	91
5.4	IMPLEMENTING THE MODEL.....	92
5.4.1	<i>Discussion</i> .....	92
5.5	CONCLUSION.....	95
6.	CHANGING THE RESONANT CHARACTERISTICS OF A LOUDSPEAKER- ABSORBER USING PASSIVE ELECTRONICS .....	97
6.1	INTRODUCTION.....	97
6.2	CHANGING THE LOAD RESISTANCE.....	100
6.2.1	<i>Theory and Prediction</i> .....	100
6.2.2	<i>Measurements</i> .....	103
6.2.3	<i>Summary</i> .....	109
6.3	CHANGING THE CAPACITIVE LOAD .....	109
6.3.1	<i>Theory and Prediction</i> .....	109
6.3.2	<i>Measurements</i> .....	111
6.3.3	<i>Discussion</i> .....	112
6.3.4	<i>Summary</i> .....	112
6.4	MODELLING OTHER SCENARIOS .....	113
6.4.1	<i>Resistors and Capacitors in Series</i> .....	113
6.4.2	<i>Resistors and Capacitors in Parallel</i> .....	116

6.4.3	<i>Applying an Variable Inductor</i> .....	117
6.4.4	<i>A Variable Inductor and Capacitor in Series</i> .....	119
6.4.5	<i>A Variable Inductor and Capacitor in Parallel</i> .....	121
6.4.6	<i>Summary</i> .....	122
6.5	OPTIMISING THE PASSIVE ELECTRONIC LOAD FOR A GIVEN SET OF DRIVER PARAMETERS .....	123
6.5.1	<i>Determining the Capacitance Needed for a Certain Resonant Frequency</i> 124	
6.5.2	<i>Determining How the Q-factor Changes With Resistance</i> .....	127
6.5.3	<i>Determining the Optimum Shunt Inductance of a Capacitor</i> .....	128
6.6	CONCLUSION.....	129
7.	FINAL CONCLUSIONS AND FURTHER WORK.....	131
7.1	FINAL CONCLUSIONS .....	131
7.2	FURTHER WORK .....	133
	<i>References</i> .....	135
	<i>Appendices</i> .....	139
	<i>Bibliography</i> .....	172

## **ACKNOWLEDGEMENTS**

I would like to express my thanks to Prof. Trevor Cox for his inspirational supervision, guidance and time during this project. Also I would like to thank everyone in the Acoustics department at the University of Salford for their continual support, encouragement and suggestions with particular thanks to Fouad and the team of G61. Thanks also to Dr. Mark Avis for his practical suggestions and willingness to offer help whenever it was needed.

Thanks also to my wonderful parents for their ever present wisdom and encouragement which have never been in short supply and have always been an example to me. Finally praise goes to the Almighty God, ‘Great is His faithfulness!’

## **ABSTRACT**

This thesis presents research into two novel techniques for improving the low frequency performance, tunability and efficiency of membrane absorbers. The first approach uses a loudspeaker surround as the mounting for the membrane, increasing the moving mass, thereby lowering the resonant frequency of the system. Using a loudspeaker surround also allows for more accurate prediction of the absorber's performance as the mounting conditions are such that the membrane can be more accurately represented by a lumped mass moving as a piston.

The second approach expands upon this technique and uses a loudspeaker within a sealed cabinet to act as the membrane absorber. Passive electronic components can be connected across the terminals of the loudspeaker to adapt the mechanical resonance properties of the system. Tests were performed on the absorber systems using a specially constructed low frequency impedance tube. It was found that varying a complex electrical load connected to the driver terminals enabled the range of obtainable resonant frequencies of the system to be dramatically increased. Varying a solely resistive load has also been shown to alter the absorption bandwidth. An analogue circuit analysis of the absorber system is presented and demonstrates good agreement with impedance tube measurements. A final model is shown that allows for the system to be optimised using different resistive and reactive components given a specific driver.

## GLOSSARY OF SYMBOLS

$B$	Magnetic flux density (T)
$Bl$	Force factor (Tm)
$C_A$	Acoustic compliance ( $\text{m}^5\text{N}^{-1}$ )
$C_{AB}$	Acoustic compliance of the cabinet ( $\text{m}^5\text{N}^{-1}$ )
$C_{AD}$	Compliance in acoustic units of the diaphragm ( $\text{m}^5\text{N}^{-1}$ )
$C_{AEV}$	Capacitance in acoustical units as a result of variable inductor $L_{EV}$
$C_{AT}$	Total acoustic compliance ( $\text{m}^5\text{N}^{-1}$ )
$C_{AE1}$	Capacitance in acoustical units as a result of inductor $L_1$
$C_{AE2}$	Capacitance in acoustical units as a result of inductor $L_2$
$C_E$	Electrical capacitance (F)
$C_{EV}$	Variable electrical capacitance (F)
$C_M$	Mechanical compliance
$C_{MD}$	Mechanical compliance of the diaphragm without an air load ( $\text{mN}^{-1}$ )
$C_{MS}$	Mechanical compliance of the diaphragm with an air load ( $\text{mN}^{-1}$ )
$F$	Force (N)
$f$	Frequency (Hz)
$i$	Electrical current ( $\Omega$ )
$j$	$\sqrt{-1}$
$k$	Wavenumber ( $\text{m}^{-1}$ )
$k_M$	Mechanical stiffness ( $\text{Nm}^{-1}$ )
$l$	Length of coil (m)
$L_E$	Electrical inductance (H)
$L_{AEV}$	Inductance in acoustical units as a result of capacitor $C_{EV}$
$M$	Mass (kg)
$M_{AB}$	Acoustic mass at the back of the diaphragm ( $\text{kgm}^4$ )
$M_{AD}$	Acoustic mass of the diaphragm without an air load ( $\text{kgm}^4$ )
$M_{AF}$	Acoustic mass at the front of the diaphragm ( $\text{kgm}^4$ )
$M_{AS}$	Acoustic mass at of the diaphragm with an air load ( $\text{kgm}^4$ )

$M_{AT}$	Total acoustic mass ( $\text{kgm}^4$ )
$M_{MD}$	Mechanical mass of diaphragm without air load (kg)
$M_{MS}$	Mechanical mass of diaphragm with air load (kg)
$p_{in}$	Input acoustic pressure (Pa)
$q$	Electrical charge (C)
$R_{AB}$	Acoustic resistance/damping at the back of the diaphragm ( $\text{Nsm}^{-5}$ )
$R_{AD}$	Acoustic resistance/damping of the diaphragm without an air load ( $\text{Nsm}^{-5}$ )
$R_{AE}$	Resistance in acoustical units as a result of resistor $R_E$
$R_{AEV}$	Resistance in acoustical units as a result of resistor $R_{EV}$
$R_{AE2}$	Resistance in acoustical units as a result of resistor $R_2$
$R_{AF}$	Acoustic resistance/damping in front of the diaphragm ( $\text{Nsm}^{-5}$ )
$R_{AS}$	Acoustic resistance/damping of the diaphragm with an air load ( $\text{Nsm}^{-5}$ )
$R_{AT}$	Total acoustic resistance/damping ( $\text{Nsm}^{-5}$ )
$R_E$	Electrical resistance of loudspeaker coil ( $\Omega$ )
$R_{EV}$	Variable electrical resistance ( $\Omega$ )
$R_M$	Mechanical resistance/damping ( $\text{Nsm}^{-1}$ )
$R_{MD}$	Mechanical resistance/damping of diaphragm without air load ( $\text{Nsm}^{-1}$ )
$R_{MS}$	Mechanical resistance/damping of diaphragm with air load ( $\text{Nsm}^{-1}$ )
$S$	Area ( $\text{m}^2$ )
$S_D$	Area of diaphragm ( $\text{m}^2$ )
$t$	Time (s)
$U$	Volume velocity ( $\text{m}^3\text{s}^{-1}$ )
$u$	Particle velocity ( $\text{ms}^{-1}$ )
$V$	Volume ( $\text{m}^3$ )
$v$	Voltage (V)
$v_{in}$	Input voltage (V)
$V_B$	Volume of cabinet ( $\text{m}^3$ )
$x$	Displacement (m)
$Z_A$	Acoustic impedance ( $\text{Pasm}^{-1}$ or MKS rayl)
$Z_{AB}$	Acoustic impedance at the back of the diaphragm ( $\text{Pasm}^{-1}$ or MKS rayl)



$Z_{AF}$	Acoustic impedance at the front of the diaphragm ( $\text{Pasm}^{-1}$ or MKS rayl)
$Z_E$	Electrical impedance ( $\Omega$ )
$Z_M$	Mechanical impedance ( $\text{Nsm}^{-1}$ )
$\alpha$	Absorption coefficient
$\lambda$	Wavelength (m)
$\rho$	Density ( $\text{kgm}^{-3}$ )
$\rho_0$	Density of air ( $1.21\text{kgm}^{-3}$ )
$\omega$	Angular frequency ( $\text{s}^{-1}$ )

For the rules of equivalent circuit nomenclature see Appendix A.

## LIST OF TABLES

<i>Table 5.1</i> Summary of the impedance analogue .....	75
<i>Table 5.2</i> Summary of the mobility analogue .....	76

## LIST OF FIGURES

<i>Figure 2.1</i> Reflection of a sound wave incident normal to a surface .....	7
<i>Figure 2.2</i> a) Closed cell foam, no propagation path through absorbent as pores are closed and unconnected. b) Open celled foam, interconnected pores allow for acoustic propagation and consequent thermal/viscous losses. (From Cox and D'Antonio [8]) .....	10
<i>Figure 2.3</i> Test apparatus for measurement of flow resistivity .....	13
<i>Figure 2.4</i> Diagram of sound propagation through multiple layers.....	16
<i>Figure 2.5</i> Schematic representation of a typical Helmholtz absorber.....	20
<i>Figure 2.6</i> Diagram of a Helmholtz type acoustic resonator.....	20
<i>Figure 2.7</i> Schematic representation of a standard membrane absorber .....	22
<i>Figure 2.8</i> Diagrammatic representation of the transfer matrix modeling of sound incident to a membrane absorber .....	26
<i>Figure 2.9</i> Transfer matrix modeling of porous absorbent with a rigid backing using the Delany and Bazley model .....	27
<i>Figure 2.10</i> Transfer matrix prediction of a simple membrane absorber .....	28
<i>Figure 3.1</i> Diagram of the typical setup of an impedance tube using the standing wave method.....	33
<i>Figure 3.2</i> Diagram of the typical setup of an impedance tube using the transfer function method .....	36
<i>Figure 3.3</i> a) Photograph of completed impedance tube b) Schematic of completed impedance tube .....	41
<i>Figure 3.4</i> Impedance tube for the transfer function method with modeled image source technique .....	43
<i>Figure 3.5</i> Image source technique for multiple microphone positions .....	44
<i>Figure 3.6:</i> Plot showing the validity of the generalised version of Cho's least-square optimisation method. Note that the measured plot was obtained by manually overlapping the measured data for each microphone pair according to the corresponding frequency range each best describes. ....	46
<i>Figure 3.7:</i> Results for absorption coefficient of a 12cm thick sample of mineral wool as measured in the large low frequency impedance tube and a smaller high frequency tube.....	47
<i>Figure 4.1</i> Schematic representation of a simply supported plate.....	50
<i>Figure 4.2</i> Schematic representation of a clamped plate .....	51
<i>Figure 4.3</i> Schematic representation of a freely supported plate.....	51
<i>Figure 4.4</i> Schematic presentation of piston mounting .....	52
<i>Figure 4.5</i> Photos of membrane mounting .....	54
<i>Figure 4.6</i> Experimental setup for the accelerometer tests.....	55
<i>Figure 4.7</i> Results from the accelerometer tests.....	56
<i>Figure 4.8</i> Results from impedance tube tests with and without surround in large sample holder .....	57
<i>Figure 4.9</i> Illustration of differing clamping conditions in accelerometer and impedance tube tests.....	58

<i>Figure 4.10</i> Samples mounted in impedance tube, demonstrating how mounting rings can support modal behaviour .....	59
<i>Figure 4.11</i> Results from impedance tube tests with and without surround in small sample holder .....	60
<i>Figure 4.12</i> Results from impedance tube tests on hardboard with and without surround in small and large sample holders .....	61
<i>Figure 4.13</i> Equivalent circuit for a membrane absorber .....	62
<i>Figure 4.14</i> Experimental setup for measuring compliance of surround.....	63
<i>Figure 4.15</i> Results from experiment to determine compliance of surround .....	64
<i>Figure 4.16</i> Absorption curve from equivalent circuit model of membrane with and without surround .....	66
<i>Figure 4.17</i> Comparison of measured absorption curves with predictions from a transfer matrix model .....	67
<i>Figure 5.1</i> Simple representation of the electrical section of a loudspeaker .....	77
<i>Figure 5.2</i> More complicated representation of the electrical section of a loudspeaker .....	78
<i>Figure 5.3</i> Mechanical representation of a loudspeaker .....	80
<i>Figure 5.4</i> Impedance analogue circuit of the mechanical section of a loudspeaker .....	81
<i>Figure 5.5</i> Mobility analogue circuit of the mechanical section of a loudspeaker .....	81
<i>Figure 5.6</i> Impedance analogue circuit of the acoustical section of a loudspeaker.....	82
<i>Figure 5.7</i> Mobility analogue circuit of the acoustical section of loudspeaker used as a membrane absorber .....	83
<i>Figure 5.8</i> Idealised transformer.....	84
<i>Figure 5.9</i> Simplified idealised transformer .....	84
<i>Figure 5.10</i> Equivalent circuit linking electrical, mechanical and acoustical sections with transformers .....	86
<i>Figure 5.11</i> Equivalent circuit of membrane absorber with electrical and mechanical sections combined .....	86
<i>Figure 5.12</i> Equivalent circuit of membrane absorber with electrical, mechanical and acoustical sections combined .....	87
<i>Figure 5.13</i> Equivalent circuit of membrane absorber in impedance analogue .....	87
<i>Figure 5.14</i> Simplified equivalent circuit of membrane absorber .....	90
<i>Figure 5.15</i> Comparison of equivalent circuit model with impedance tube measurements.....	92
<i>Figure 5.16</i> Real part of surface impedance from both predicted and measured data....	93
<i>Figure 5.17</i> First three vibrational modes of a circular plate.....	94
<i>Figure 5.18</i> Multi-plot of absorption and surface impedance showing the first two resonant modes of the loudspeaker .....	95
<i>Figure 6.1</i> Electrical section of the absorber equivalent circuit with an additional variable resistor across terminals <i>A</i> and <i>B</i> .....	101
<i>Figure 6.2</i> Full equivalent circuit of absorber with additional variable resistor across terminals.....	101
<i>Figure 6.3</i> Simplified equivalent circuit of absorber .....	101
<i>Figure 6.4</i> Changes in absorption curves with a variable resistor connected across loudspeaker terminals.....	103
<i>Figure 6.5</i> Mounting of loudspeaker in large sample holder for impedance tube testing .....	104
<i>Figure 6.6</i> Measurements made on absorber in impedance tube changing resistive load on loudspeaker terminals .....	105
<i>Figure 6.7</i> Real part of the measured surface impedance of absorber with a variable resistive load without porous absorption in the cabinet.....	106

<i>Figure 6.8</i> Predicted absorption coefficient changing the resistive load on the absorber without porous absorption in cabinet. ....	107
<i>Figure 6.9</i> Measured absorption coefficient of absorber with variable resistive load with porous absorption in the cabinet .....	108
<i>Figure 6.10</i> Equivalent circuit with additional variable capacitor connected to loudspeaker terminals.....	110
<i>Figure 6.11</i> Predicted absorption curves with a variable capacitor connected to loudspeaker terminals.....	111
<i>Figure 6.12</i> Measured absorption curves, changing the load capacitance connected across loudspeaker terminals.....	111
<i>Figure 6.13</i> Equivalent circuit modelling a variable resistor in series with a variable capacitor connected to the terminals of the loudspeaker .....	114
<i>Figure 6.14</i> Multi-plot showing changes in the trend of absorption for different combinations of resistors in series with capacitors.....	115
<i>Figure 6.15</i> Equivalent circuit modelling a variable capacitor in parallel with a variable resistor connected to the terminals of the loudspeaker .....	116
<i>Figure 6.16</i> Equivalent circuit modelling a variable inductor connected to the terminals of the loudspeaker .....	117
<i>Figure 6.17</i> Absorption curves changing inductive load on loudspeaker.....	118
<i>Figure 6.18</i> Equivalent circuit modelling a variable inductor in series with a variable capacitor connected to the terminals of the loudspeaker .....	119
<i>Figure 6.19</i> Multi-plot of absorption trends with a variable inductive and capacitive load connected in series .....	120
<i>Figure 6.20</i> Equivalent circuit modelling a variable capacitor in parallel with a variable inductor connected to the terminals of the loudspeaker.....	121
<i>Figure 6.21</i> Multi-plot showing predicted absorption trends with a variable inductor and capacitor connected in parallel to the terminals of the loudspeaker .....	122
<i>Figure 6.22</i> Equivalent circuit of absorber system with simplified motor impedance terms and variable capacitor connected to terminals .....	125
<i>Figure 6.23</i> Resonant frequency versus capacitance value to determine the component value needed for a given resonant frequency.....	127
<i>Figure 6.24</i> Standard deviation changes in absorption curve for different load resistances on loudspeaker terminals, a comparison between measurement and prediction .....	128
<i>Figure 6.25</i> Resonant frequencies of absorber with varying capacitance and inductance in parallel connected to the loudspeaker terminals .....	129

# 1. INTRODUCTION

This thesis is focused primarily upon low frequency absorption for room acoustic applications. Absorption is paramount in room acoustics for reducing the intensity of reflections from the boundaries of, or objects within, a given room. Without sufficient absorption, these reflections cause the reverberant level in the room to be high as a result of long decay times. Absorption will reduce the reverberation time in the room and consequently will reduce the level of the reverberant field enabling the direct sound to be heard at sufficiently high amplitude in comparison to the reverberant field thus aiding speech intelligibility. Absorption also helps to reduce colouration i.e. a change in frequency content or timbre between the radiated and received signal as a result of strong reflections at discrete frequencies [1]. Absorption can thus help to produce a room with a flatter response with respect to frequency. In many situations creating a completely reflection free listening environment is undesirable as reflections tend to enhance the enjoyment of listening; adding to the perceived spaciousness of the room [2]. Creating an entirely anechoic room by using too much absorption has a rather eerie quality which impedes the perceived enjoyability of a performance.

A room will have a different temporal and frequency response at different frequencies so it is important that acoustic treatment is considered across the entire audio bandwidth. The absorption of mid to high frequency sound can be achieved relatively easily and cheaply with the use of porous absorbers, low frequency absorption however is harder to achieve and is often the most necessary, with the particular problem of room modes. Room modes occur when standing waves are set up between the boundaries of a room; these standing waves lead to regions in space of higher and lower amplitude at discrete frequencies governed by the geometrical dimensions of the room. Thus the room will have an uneven response both spatially and with respect to frequency. There are also temporal problems as at modal frequency the decay times are longer, subjectively this is commonly the most noticeable consequence of room modes. Problems with room modes occur primarily at longer wavelengths, as here the modes are subjectively further apart in frequency with respect to each other and are subsequently detected more easily as discrete modes by the ear.

Many precautions can be taken in order to prevent the occurrence, and to control the extent, of room modes. Placing loudspeakers and sound sources in places where they will not excite the antinodes and optimising the geometry of room [3, 4] can both help, however repositioning sources only tackles half the problem and it is not always possible, practical or cost efficient to resize and shape a room. Work has been done on treating room modes by active equalization using digital signal processing [5], however this only deals with sound reproduction systems and not problems as a result of acoustic stimuli, it is therefore an incomplete solution. Attempting to diffuse these low frequency reflections, thereby preventing room modes, is by and large unfeasible as the scattering surfaces needed have to have deep irregularities to be optimally effective for longer wavelength sound; thus where space is a premium this is seldom a practical solution. Absorption is therefore often the best way to treat room modes. By absorbing sound at the discrete modal frequencies of a room, the magnitude of boundary reflections is reduced thus lessening the severity of the standing waves i.e. decreasing the pressure ratio between antinodes and nodes, resulting in a flatter frequency and spatial response. Absorption at modal frequencies can be achieved using either active [6] or passive techniques however active techniques often fraught with practical difficulties and are

therefore not widely used; consequently this project focuses primarily on passive low frequency absorption techniques.

Low frequency absorption can be difficult to achieve without using very large and cumbersome absorbers due to the large wavelengths involved. One method of absorption is to use porous absorbers, where viscous and thermal losses of sound passing through small pores in a material generate absorption. Porous absorption is a broadband solution but the depth of material needed for it to be effective increases as the wavelength gets longer, thus it is often impractical for treating low frequency problems. Another method is to use damped resonators to provide absorption such as with membrane absorbers which provide a smaller/shallower solution. Incident sound forces a cavity backed membrane into oscillation, the energy of which is absorbed using acoustic damping. As membrane absorbers are resonant systems they tend to have a narrow bandwidth of effective absorption, controlled in frequency by the physical and geometrical properties of the device. These absorbers also suffer from poor tunability, which can only be achieved by reconstruction with different materials and/or geometry. However because of their small size and relatively simple design membrane absorbers are commonly used in the control of low frequency sound in rooms.

Designing a room where membrane absorbers are to be used can be rather problematic as there are no accurate prediction models available for predicting their performance, simple relationships do exist [7] that can predict the resonant frequency but these often rely on the assumption that the membrane in question is moving as a piston, in most cases this is not true and the exact boundary conditions are very difficult to accurately predict. The first question of this thesis addresses this problem by considering the possibility of using loudspeaker surround as the mounting for a membrane in a membrane absorber. Loudspeaker surround is designed so that the diaphragm of a loudspeaker can move like a piston i.e. each point on the diaphragm moves with the same velocity and phase. In loudspeaker technology this is useful both in terms of predicting the behaviour of loudspeakers and also in ensuring the radiation characteristics are as flat with respect to frequency as possible. Using loudspeaker surround means that approximating the movement of the membrane to that of a piston will be more accurate and thus prediction models will be more useful when designing an absorber for a specific application. The use of a loudspeaker surround will also

increase the moving mass of the membrane thus lowering its resonant frequency, allowing absorbers to be built with smaller dimensions whilst still achieving the same low frequency performance.

The second part of the project expands this theme, using an entire loudspeaker as an absorber system. Loudspeakers are already designed to be mass-spring systems with damping in the cabinet, thus they have the potential to work as membrane absorbers if used in reverse. There are a number of advantages in using loudspeakers as absorbers, firstly they are cheap, readily available and are already configured to absorb. Secondly they can be tuned by connecting a passive electronic load to the terminals of the driver. By adding a reactive electronic component, the resonance of the induced current produced as the coil oscillates within the magnetic field can be changed; this will then result in a change in the mechanical resonant frequency, allowing for a tunable absorber. In addition, adding electrically resistive components will alter the electrical and mechanical damping and hence the Q-factor of the system. Using these techniques leads to an absorber that could be moved from room to room and tuned to meet the requirements of that room, i.e. tuned to the frequency of a troublesome room mode and damped to the required level in order to produce the optimally flat frequency response.

This thesis will, in chapter two, highlight the main principles of both porous and resonant absorption and, in chapter three, how these absorbers can be tested including the design and build of a specially constructed low frequency impedance tube. Chapter four will consider using loudspeaker surround as the mounting of a membrane, looking first at the theory and prediction and later at experimental studies undertaken in order to verify this theory. Chapters five and six will look at using a loudspeaker as an absorber and how it can be tuned and optimized by the use of a passive electronic load on the driver; again theory, prediction and experimentation are included. Chapter seven concludes and outlines any further work and commercial possibilities that could result from this research.



## **2. ABSORPTION METHODS**

### **2.1 Introduction**

Absorbing mid band and high frequency sound is easily achieved and is done with high efficiency using porous absorbers, such as mineral wool. Porous absorbers make use of the movement of the air particles in acoustic waves through the pores of the material and absorb energy through viscous and thermal losses as sound propagates through these small orifices. Absorption in this case is greater when there is a larger particle velocity. The positioning of these absorbers for maximum efficiency reflects this, such that the surface of the absorbent should be in a region of higher particle velocity. Here lies the reason why this technique is well suited to the absorption of mid to high frequency sound. At a boundary the pressure will be a relative maximum, the particle velocity however will be a relative minimum, this means that the porous material will not be effective if on the boundary itself, it will have to protrude from the wall to such an extent that its surface will be in the place of a higher, or ideally, maximum particle velocity. This is not a problem for higher frequency waves but when the incident wavelength is larger, problems occur as the material needed has to be very thick to

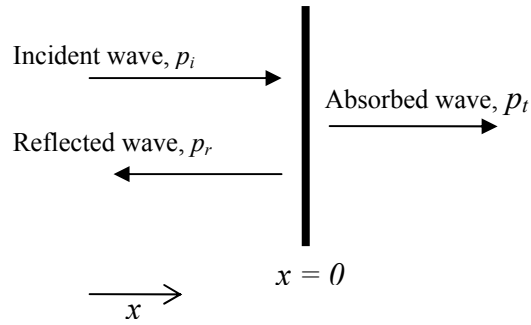
absorb efficiently. This is undesirable as the useable volume of the room is reduced to make space for the acoustic treatment. A solution to this problem is to create an absorber that would exhibit maximum absorption in a region where the pressure was a maximum rather than particle velocity i.e. a solution that could be used close to the boundary of a room. This would reduce the need for thick porous absorbers to treat longer wavelengths. A technique that fits this criterion is resonant absorption, so called because it utilises damped resonators to absorb sound. Acoustic pressures induce the vibration of a mass-spring system which, at a given frequency will resonate, producing maximum excursion of the mass. Damping this movement will introduce loss of energy into the system and consequently absorb the incident sound. The mass in resonant absorbers is usually in the form of a semi-rigid plate or membrane in the case of membrane absorbers or a plug of air in Helmholtz absorbers, the spring in both cases is usually an air spring as a result of an enclosed volume. Damping is introduced into the system usually by adding some porous absorbent either in the holes of Helmholtz absorbers or at the rear of the membrane in a membrane absorber. Resonant absorbers are effectively velocity transducers, as they convert incident pressure into movement of a membrane that creates a high particle velocity through the porous absorbent thus absorbing sound at the resonant frequency of the system. This project is primarily concerned with resonant absorption but as porous materials are needed in resonant absorbers to provide greatest efficiency across a larger bandwidth, the theory of both methods has been detailed in this chapter.

## **2.2 Principles of Absorption**

Several parameters of absorbent materials and systems can be derived or measured that give good indication as to its acoustic performance, chiefly these are the surface impedance, the reflection factor and the absorption coefficient. A brief theory of each of these terms is presented here as it is important for subsequent analysis.

### **2.2.1 Reflection Factor**

For the definition of these terms it is considered that a plane wave is incident normal to a surface as shown in *Figure 2.1*:



**Figure 2.1** Reflection of a sound wave incident normal to a surface

On incidence to a surface the energy of a plane wave is split into reflected and absorbed energies. The absorbed energy could be as a result of acoustic transmission through the surface or as heat conversion in the material. The proportion of energy that is not absorbed is reflected, this reflected wave will have both a different amplitude and phase from the incident wave such that the reflected wave can be given as:

$$p_r(x, t) = R\hat{p}_0 e^{j(\omega t + kx)} \quad (2.1)$$

where  $R$  is the reflection factor of the surface. The reflection factor is a complex ratio of the reflected and incident pressures given by:

$$R = |R|e^{j\phi} = \frac{p_r(x, t)}{p_i(x, t)} \quad (2.2)$$

### 2.2.2 Absorption Coefficient

The reflection factor of a surface can be used to determine the absorption coefficient of a surface. The absorption coefficient of a surface is a very useful parameter as it states the fraction of energy that is absorbed when sound is incident to a surface. Absorption coefficient it is a unitless quantity between zero and unity, zero meaning that no acoustic energy is absorbed resulting in total reflection of the sound wave. An absorption coefficient of unity means that all of the incident energy is absorbed leaving no reflected energy.

To derive the absorption coefficient the intensity of a plane wave is considered as given by:

$$I = \frac{p^2}{\rho_0 c} \quad (2.3)$$

Therefore on reflection, the reflected wave is reduced in intensity by a fraction of  $|R|^2$  and consequently the fraction of energy absorbed can be given by  $1 - |R|^2$ . The absorption coefficient of a surface is therefore expressed as:

$$\alpha = 1 - |R|^2 \quad (2.4)$$

The absorption coefficient of a material is probably the most widely used quantity when describing absorbent materials and systems and an absorber's performance is often given by a graph of absorption coefficient versus frequency.

### 2.2.3 Surface Impedance

The surface impedance is a very useful parameter as it is very closely linked to the physical properties of a surface so it provides clear indication of how the surface behaves given an incident wave. The surface impedance is given by the ratio of pressure and the particle velocity normal to the surface:

$$z = \frac{p(x, t)}{u(x, t)} \quad (2.5)$$

With the surface at  $x = 0$  the combined pressure and velocity normal to the surface can be given by:

$$\begin{aligned} p(0, t) &= \hat{p}_0 (1 + R) e^{j\omega t} \\ u(0, t) &= \frac{\hat{p}_0}{\rho_0 c} (1 - R) e^{j\omega t} \end{aligned} \quad (2.6)$$

The surface impedance becomes:

$$z = \rho_0 c \frac{1 + R}{1 - R} \quad (2.7)$$

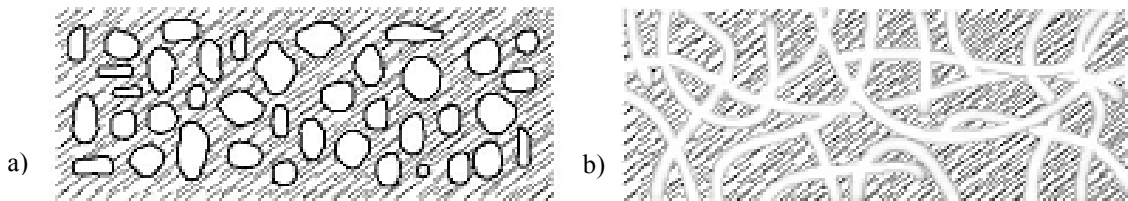
Separating the surface impedance into its real and imaginary components reveals information as to the magnitude of absorption and its resonant characteristics which can be very useful in analysis.

### 2.3 Porous Absorbers

When most people think of acoustic absorbers they commonly think of porous absorbers, this is because there are so many materials that are naturally porous and consequently absorb sound. Many people, in the pursuit of constructing a home studio or attempting some rudimentary acoustic treatment of an existing room, will use common materials such as thick curtains, carpets and sofa's to control the reverberation time within the room, these all constitute porous absorbers. Porous absorbers must have open pores as in *Figure 2.2* i.e. pores that can support acoustic propagation where the orifice is at the surface of the absorber. Porous absorbers can be either granular or fibrous providing they have these open pores. Granular absorbers can be made from small pieces of almost any rigid or semi rigid material bound together with glues that do not block pores. Loose granular materials such as sand also constitute porous absorbers as the gaps between grains provide a complex path for the acoustic waves to propagate through, but their loose nature often means they are impractical to use, especially in room acoustics. An example of a fibrous porous absorbent is mineral wool, made by spinning molten minerals such as sand and weaving the spun fibres together to form a complicated structure of pores. This complex pore structure leaves a material that is highly porous and is commonly used for both acoustic and fire insulation as its open pores allow restricted airflow through the material thus absorbing sound and also preventing efficient heat exchange.

When sound propagates in small spaces there are losses in energy, primarily caused by viscous boundary layer effects, i.e. the friction of the viscous air fluid passing through the orifice of a small hole/pore. It is this friction that causes viscous and heat losses in

porous absorbers making them efficient for room acoustic applications. For a porous absorber to be effective, it is important that the pores are open rather than closed. The diagram below shows the differences between closed and open cell foam:



**Figure 2.2** a) Closed cell foam, no propagation path through absorbent as pores are closed and unconnected. b) Open celled foam, interconnected pores allow for acoustic propagation and consequent thermal/viscous losses. (From Cox and D'Antonio [8])

Many manmade types of foam can be classified as closed cell foams, these foams have either closed pores so there is no propagation path or pores that are too small for the sound wave to propagate through. As waves cannot propagate through the material there will be no viscous and thermal losses so there will be very little absorption and the material will act as a reflector. Open cell foams as depicted in *Figure 2.2b* have a propagation path either through all or part of the foam generating losses as sound propagates through the pores. In general the longer and more tortuous the pores, the greater the viscous and thermal losses generated as sound propagates through them; hence there will be more absorption. The most efficient porous absorbers have many tortuous and interconnected pores resulting in what could be considered as a complex system of pipes in which the acoustic wave can propagate. Obviously if these pores become too small the acoustic wave can no longer propagate within them as there is not sufficient volume for pressure changes to occur and the material then can be classified as closed cell. Conversely if the pores become too large the viscous boundary layer effects become negligible resulting in no significant absorption. In order for viscous losses to be effective, the particle velocity has to be high, the higher the particle velocity the larger the viscous and heat losses. This means that the most effective way to use porous absorption is where the particle velocity is at a maximum. This occurs away from a rigid boundary by a quarter of a wavelength as at the boundary the particle velocity would be a minimum. Figures often quoted are that for significant acoustic absorption the porous material should be at least one tenth of a wavelength thick, and for maximum absorption the material should be one quarter of a wavelength thick (or away from the boundary with an air gap such that the surface is a quarter of a

wavelength from the boundary). With this in mind it becomes clear that as the wavelength of the incident sound increases, the porous material must increase in depth if satisfactory absorption is to be achieved. This is the reason that porous absorption is unsuitable for treating low frequency modal problems in rooms, because the wavelengths are sufficiently large that much of the room would be taken up by the porous absorption, which is impractical. An exception to this is in the construction of anechoic chambers where broadband absorption is needed across the entire audio spectrum; porous absorption is used here so the absorption coefficient is roughly equal across a large bandwidth (a useful characteristic of porous absorption). Very thick porous absorption is used to tackle even the low frequencies in this case as low frequency resonant absorption would reflect and cause problems at higher frequencies.

### **2.3.1 Characterising and Modelling Porous Absorbers**

It is often important to be able to predict accurately the performance of porous absorbers both for use on their own and also when used as part of a resonant absorber (see section 2.4). Being able to predict the reverberation time of a room and even to auralise its response before building or before acoustic treatment is added is becoming increasingly important in room acoustic design. With the increase in building regulations governing the acoustic insulation requirements of buildings, it is also imperative that the absorption characteristics of materials is known before building to ensure the building will reach the necessary standards on completion. This task is only possible when accurate information can be given about the absorption within the room. For these reasons and to aid research into the development of new absorptive materials much attention has been placed on defining the characteristics of materials and also predicting their acoustic performance. In order to accurately model porous materials it is important to determine certain physical properties of the material.

#### **2.3.1.1 Material Properties**

The performance of a porous absorber is governed by two main characteristics; the material's porosity and flow resistivity. The porosity is the fraction of the amount of air volume in the absorbent material, it is calculated by the ratio of pore volume to the total volume of the absorbent material i.e. a porosity of 0.5 means that half of the volume of

the material constitutes the air in the pores, the other half (the material that supports the pore structure) would be the ‘frame’ of the material. Closed pores do not count in measurements of porosity as they cannot be accessed by incident sound waves and are therefore ineffective for absorption. Foam with entirely closed pores would have a porosity of zero.

Flow resistivity is a metric that defines how easily air can enter a material and the resistance to flow that it experiences as it passes through, analogous to electrical resistivity. It is a measure of how much energy will be lost due to propagation through the pores. Flow resistivity can be defined as the resistance to flow per unit thickness of the material. The viscous resistance to air flow through a porous material causes a pressure drop across the material which at low frequencies is proportional to the flow velocity,  $U$  and thickness of the material,  $d$ . The ratio of this drop in pressure with the product of the flow velocity and material thickness gives the material’s flow resistivity:

$$\sigma = \frac{\Delta p}{Ud} \tag{2.8}$$

The flow resistance of a material can also be useful and is given by multiplying the flow resistivity by the material thickness. However flow resistivity is more useful in the modeling of acoustic materials and is the property used throughout this thesis.

Both porosity and flow resistivity are very important factors but it is the flow resistivity that varies the most from material to material and therefore is considered the most important factor. The porosity of an effective porous absorbent is often very close to unity and varies very little with different materials.

Another factor that will affect the performance of porous absorbers is the tortuosity, which states how tortuous or ‘wiggly’ the pores of a material are. Tortuosity is basically a metric of the complexity of the propagation path through the absorbent. A material with a higher tortuosity will exhibit greater absorption, as a more tortuous path of propagation makes it harder for the acoustic wave to pass through the material so more energy is lost through heat as the viscous air fluid is forced through the small pores. Pore shape is also a factor that influences the amount of absorption from a porous

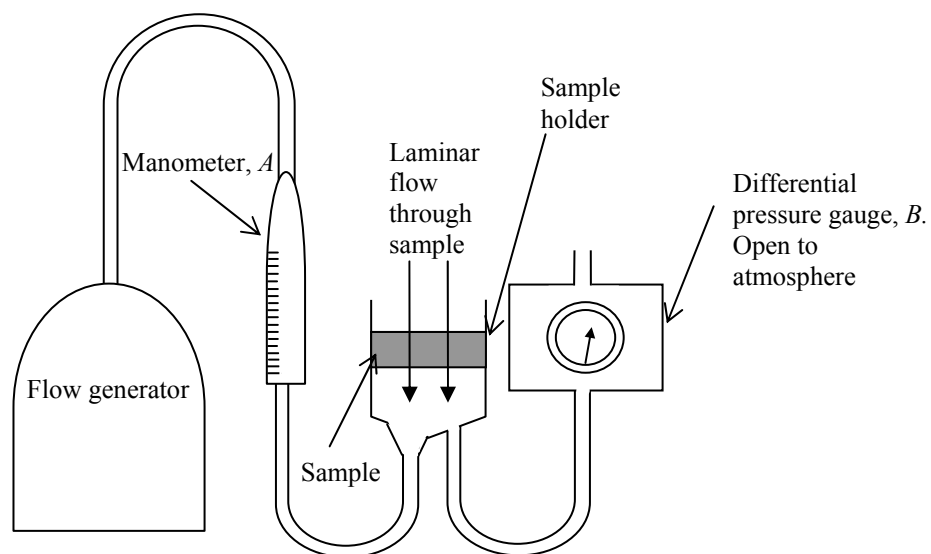


absorber. Pore shape is difficult to define as materials often exhibit many pores with very different shapes and as such it is a difficult parameter to accurately define.

There are many different strategies for the modeling of porous materials using a variety of different approaches with varying degrees of complexity and overview of some of these can be found in [9]. The primary model used in this thesis is a one parameter empirical approach by Delany and Bazley [10]. In this model the porosity is considered to be unity and the material parameter needed is the flow resistivity. It is therefore important that the flow resistivity of the material used is accurately measured; the following describes the process of this measurement.

#### 2.3.1.1.1 Measuring Flow Resistivity

Flow resistivity can be measured using a relatively simple experimental setup as shown in *Figure 2.3*. The premise is to induce airflow through the test sample and to measure the resulting pressure difference across the sample. Details of this procedure are outlined in an international standard [11]. The standard outlines two different methods for the measurement of flow resistivity, the first utilising unidirectional airflow and the other an alternating airflow. The apparatus chosen here typified an apparatus to measure flow resistivity using unidirectional laminar flow.



**Figure 2.3** Test apparatus for measurement of flow resistivity

In *Figure 2.3* the manometer,  $A$  is used to calculate the airflow velocity through the sample, this is achieved in the test apparatus using the calibration chart for this particular set up which can be found in Appendix A. From this manometer reading the volumetric airflow rate,  $q_v$  can be determined in cubic meters per second. When divided by area this gives the linear airflow velocity,  $V$ . The pressure difference across the sample with respect to the atmosphere can be deduced from the differential pressure gauge,  $B$ . from these values the specific airflow resistance,  $R_s$  can be written as:

$$R_s = \frac{\Delta p A}{q_v} = \frac{\Delta p}{V} \quad (2.9)$$

Where  $\Delta p$  is the pressure drop across the sample measured with the differential pressure gauge, and  $A$  is the cross sectional area of the sample. The flow resistivity  $\sigma$  of the sample is the specific flow resistance per meter:

$$\sigma = \frac{R_s}{d} = \frac{\Delta p}{Vd} \quad (2.10)$$

where  $d$  is the depth of the sample.

This gives a measure of flow resistivity which can be used in many acoustic models and will be used in subsequent sections of this work in a basic one parameter model for rigid frame porous materials as part of a transfer matrix model presented later.

### 2.3.1.2 Prediction Models

Attempting to predict the performance of a porous absorber using an analytical approach is not easy, many models assume that pores are either slits, circular or at least have a simple geometry but this is rarely the case in reality and consequently models are fraught with inaccuracies even when many material parameters are considered; as a result empirical models such as Delany and Bazley [10] have been formulated, which provide a good basis for modeling porous materials. The Delany and Bazley model is based on many measurements taken of fibrous porous absorbents. Using curve-fitting

techniques they then put an empirical formula together to allow the prediction of both the characteristic impedance and the complex wavenumber of fibrous absorbent materials. The formulae assume porosity close to unity and include the material's flow resistivity, accurate only between 1000 and 50000 MKS raylm<sup>-1</sup>. Delany and Bazley's is a single parameter model meaning only the material's flow resistivity is needed for calculation. The model can be summed up in the following three equations. First they define a dimensionless variable  $X$ , dependent on the density of air within the pores  $\rho_0$ , the frequency  $f$  and the flow resistivity  $\sigma$ :

$$X = \frac{\rho_0 f}{\sigma} \quad (2.11)$$

Then the Characteristic Impedance  $z_c$  and the complex wavenumber  $k$  are defined:

$$z_c = \rho_0 c_0 (1 + 0.0571X^{-0.754} - j0.087X^{-0.732}) \quad (2.12)$$

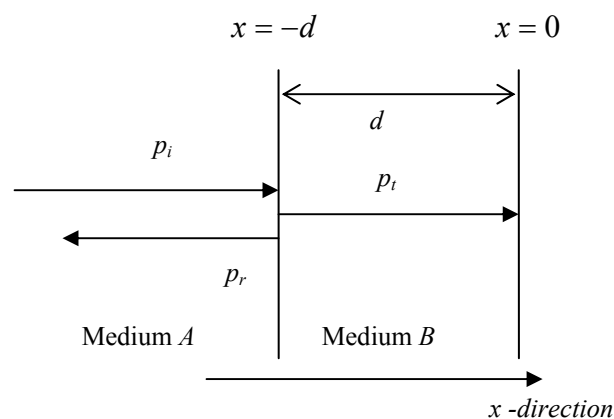
$$k = (\omega / c_0) (1 + 0.0978X^{-0.700} - j0.189X^{-0.595}) \quad (2.13)$$

where  $\omega$  is the angular frequency and  $c_0$  is the speed of sound in air. This model is extremely useful and is widely used as it has proved to accurately predict the performance of fibrous materials with minimal information of the material needed. It is however only accurate within a given frequency bandwidth as it may only be used for materials with a flow resistivities within the aforementioned limits enabling  $X$  to be within the allowed limits of 0.01 and 1.0. The effect of these conditions is that the low frequency accuracy of the formulation is compromised. This can be a problem and consequently there is a wealth of more complex models [12, 13] both analytical and empirical that seek to improve the low frequency predictability of porous absorbents. These are often manifested in multi parameter models that can be cumbersome to use and lack satisfactory accuracy. Consequently it is often thought, that the differences between the new formulations and the original Delany and Bazley formulation are not large enough to cause concern and many use their model anyway, as is the case in this thesis.

### 2.3.1.2.1 Acoustic Impedance Modelling of Multiple Porous Layers

Often important in acoustic modeling and applications is the behaviour of acoustic waves propagating through layers of different media. This encapsulates many scenarios, ranging from sound traveling through a porous absorbent mounted on a rigid backing through to more complicated situations where there are many layers all with different characteristic impedances and the overall impedance needs to be found. In order to study accurately the behaviour of sound in these cases a modeling system needs to be formulated. Considering a wave approach enables a simple model to be put together, often called a two port model as it has just two ports (both a single input and single output). This type of model can also be extended to work for more complicated situations where further resonant layers are introduced (see section 2.4.2.1.1).

Considering plane waves incident only normal to the surface, a diagram of an acoustic wave incident to a multiple layered absorber can be represented by *Figure 2.4*:



**Figure 2.4** Diagram of sound propagation through multiple layers

At any point the total pressure can be seen as simple addition of the incident, reflected and transmitted pressures such that:

$$p_t(x) = p_i e^{-jkx} = p_i e^{-jkx} + p_r e^{jkx} \quad (2.14)$$

So when  $x = 0$ :

$$p_t(0) = p_i + p_r \quad (2.15)$$

Velocity is a vector quantity therefore the addition of the velocities before and after the boundary of the layer is:

$$u_t(0) = u_i - u_r = \frac{1}{z_c}(p_i - p_r) \quad (2.16)$$

where  $z_c$  is the characteristic impedance of material  $A$ .

From equations 2.14 and 2.15, the incident and reflected pressures at the boundary  $x = 0$  can be expressed as:

$$\begin{aligned} p_i &= p_r + u_t(0)z_c \\ p_r &= p_i - u_t(0)z_c \end{aligned} \quad (2.17)$$

Therefore:

$$\begin{aligned} p_i &= \frac{1}{2}(p_t(0) + u_t(0)z_c) \\ p_r &= \frac{1}{2}(p_t(0) - u_t(0)z_c) \end{aligned} \quad (2.18)$$

So the sound pressure at any point  $x$  in space (assuming normal incidence) can be given by equation 2.19:

$$p(x) = p e^{-jkx} = p_i e^{-jkx} + p_r e^{jkx} = \frac{1}{2}(p_t(0) + u_t(0)z_c)e^{-jkx} + \frac{1}{2}(p_t(0) - u_t(0)z_c)e^{jkx} \quad (2.19)$$

Expanding this gives the transmitted pressure as:

$$\begin{aligned}
p_t(x) &= p_t e^{-jkx} = \left[ \frac{1}{2} (p_t(0) + u_t(0)z_c) (\cos(kx) - j \sin(kx)) \right] + \dots \\
&\quad \left[ \frac{1}{2} (p_t(0) - u_t(0)z_c) (\cos(kx) + j \sin(kx)) \right] \\
p_t(x) &= p_t e^{-jkx} = p_t(0) \cos(kx) - z_c u_t(0) j \sin(kx)
\end{aligned} \tag{2.20}$$

And the transmitted velocity as:

$$\begin{aligned}
u_t(x) &= u_t e^{-jkx} = \frac{1}{Z_c} (p_t e^{-jkx} - p_r e^{jkx}) = \frac{1}{z_c} \left[ \frac{1}{2} (p_t + u_t z_c) e^{-jkx} + \frac{1}{2} (p_t - u_t z_c) e^{jkx} \right] \\
u_t(x) &= u_t e^{-jkx} = u_t \cos(kx) - \frac{1}{z_c} p_t j \sin(kx)
\end{aligned} \tag{2.21}$$

The ratio of the transmitted pressure and velocity at a point  $x$  gives the acoustic impedance at that point. So in order to find the impedance at the boundary of material  $A$ ,  $x = -d$ . Substituting this into the above equations gives:

$$\begin{aligned}
z_t(-d) &= \frac{p_t(-d)}{u_t(-d)} = \frac{p_t(0) \cos(kd) + j z_c u_t(0) \sin(kd)}{u_t(0) \cos(kd) + \frac{j}{z_c} p_t(0) \sin(kd)} \\
&= \frac{-j p_t(0) z_c \cot(kd) + z_c^2 u_t(0)}{-j u_t(0) z_c \cot(kd) + p_t(0)} \\
&= \frac{-j z_t(0) z_c \cot(kd) + z_c^2}{z_t - j z_t(0) z_c \cot(kd)}
\end{aligned} \tag{2.22}$$

Where  $z_t$  is the surface impedance at  $x = 0$  (termination impedance) given by  $p_t(0)/u_t(0)$ ,  $z_c$  is the characteristic impedance of the layer with thickness  $d$ .  $z_t(-d)$  is the surface impedance at the point  $x = -d$ .  $k$  is the wavenumber in the material, this can often be determined by a simple empirical model for porous absorbents or as  $2\pi f / c$  if in air.

Equation 2.22 can be used in any general case as long as the wavenumber within and characteristic impedance of the materials are known. It can also be written in matrix form which as part of a transfer matrix [14] as represented by equation 2.32:

## 2.4 Resonant Absorption

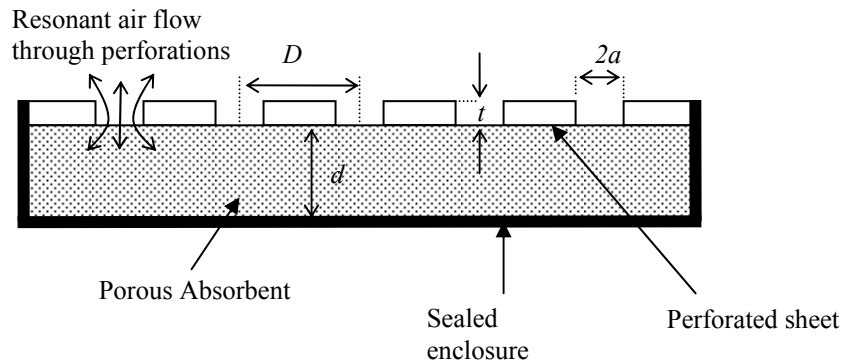
Unlike porous absorption, which is used primarily for absorption of mid to high frequency sound, resonant absorption is most commonly used for treating low frequency acoustic problems. Resonant absorption is sometimes used for higher frequency applications where porous absorbers are impractical i.e. where weather or fumes could damage or clog the pores. It is however not common to use resonant absorption for higher frequency problems because the bandwidth of absorption is commonly a lot lower than porous absorption if high absorption coefficients are to be achieved. This narrow bandwidth corresponds to a very small fraction of an octave band at higher frequencies so is often considered impractical.

Resonant absorbers are essentially mass-spring systems where sound pressure incident on the absorber causes a mass element to vibrate on a spring which is damped to introduce energy loss and consequently absorption. Resonant absorbers are most efficient if placed in areas where acoustic pressures are high, as higher pressures induce greater movement of the mass. As a result, resonant absorbers are often placed on the boundaries of a room and often in the corners where room modes have maximum pressure amplitude so maximally efficient absorption can be achieved. This contrasts with porous absorbers, which are most effective in areas of maximum particle velocity i.e. away from boundaries.

There are two main types of resonant absorption, namely Helmholtz absorbers named after Hermann Von Helmholtz (1821-1894) and membrane absorbers. Both are commonly used in room applications and also as silencers in engines and ventilation ducts *et cetera*. Theory of both techniques is presented in the following sections.

### 2.4.1 Helmholtz Absorbers

Helmholtz absorbers consist of a plate with many holes equally spaced in both the  $x$  and  $y$  plane, which are usually damped with porous absorption, unless the holes are sufficiently small as to generate absorption without it. The resonating mass is the plug of air that is in the holes and the spring is the air compliance of the volume between the front and back plates. *Figure 2.5* shows the construction of a typical Helmholtz absorber:

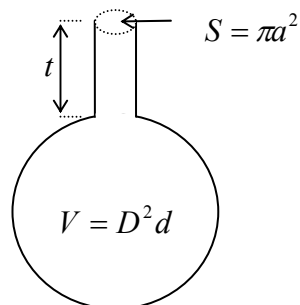


**Figure 2.5** Schematic representation of a typical Helmholtz absorber

Both membrane and Helmholtz resonant absorption attempt to convert areas of high acoustic pressure into a region of high particle velocity that can be absorbed by intelligently positioned porous absorption. In the case of a Helmholtz absorber, incident pressure causes highest particle velocity in the neck of each orifice so porous materials are often placed there to maximise absorption efficiency, in practical applications however the porous absorbent is usually placed in between the two plates for ease of manufacture and cost efficiency.

#### 2.4.1.1 Predicting the Performance of Helmholtz Absorbers

The performance and resonant frequency of Helmholtz absorbers is easy to predict and can be done to a high degree of accuracy by considering each orifice to be a short tube forming individual Helmholtz resonators as shown in *Figure 2.6*:



**Figure 2.6** Diagram of a Helmholtz type acoustic resonator



A short tube terminated with a low impedance behaves like an inert mass, [7] therefore the acoustic mass per unit area of the Helmholtz absorber is given by equation 2.23 assuming the geometry given in *Figure 2.5*:

$$m = \frac{\rho_0 D^2 t}{\pi a^2} = \frac{\rho_0 t}{\varepsilon} \quad (2.23)$$

where  $\varepsilon = \frac{\pi a^2}{D^2}$  and is termed the fractional open area or ‘porosity’ of the perforated sheet.

Each plug of air is considered to behave like a baffled piston such that it is subject to a radiation impedance given by equation 5.19, [15]. The value of this radiation impedance depends on whether or not the holes are flanged. Considering a flanged termination introduces an end correction as a result of the radiation impedance which adds an apparent extra length of  $8a/3\pi \approx 0.85a$  to each end of the plug of air thus equation 2.23 becomes:

$$m = \frac{\rho_0(t + 1.7a)}{\varepsilon} = \frac{\rho_0 t'}{\varepsilon} \quad (2.24)$$

where  $t'$  is the apparent length of each plug as a result of end corrections. The mechanical impedance of a Helmholtz resonator is the sum of the impedance due to radiation resistance  $R_r$ , stiffness  $K$ , and mass per unit area  $m$ , such that:

$$Z_M = j\omega m + \frac{K}{j\omega} + R_r \quad (2.25)$$

Considering just one plug,  $\varepsilon$  becomes unity and the stiffness of the plug can be expressed as [15]:

$$K = \rho_0 c^2 \frac{S^2}{V} \quad (2.26)$$

The resonant frequency can therefore be determined by setting the imaginary part to zero. The resonant frequency can then be found by:

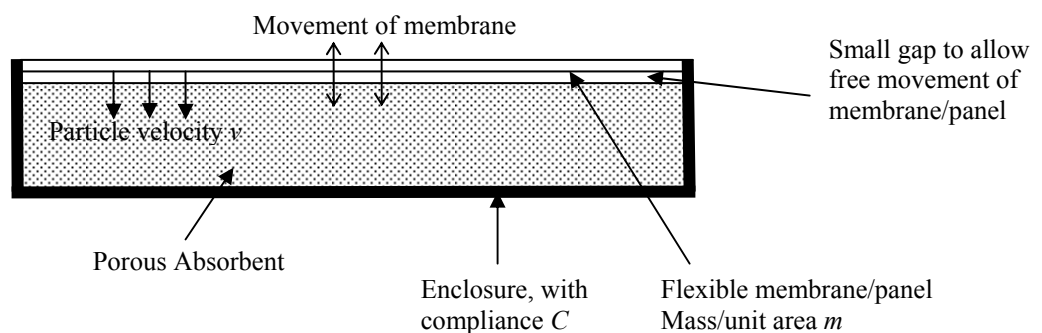
$$f_0 = \frac{1}{2\pi} \sqrt{\frac{\rho_0 c^2 (s^2 / V)}{\rho_0 t'}}$$

$$f_0 = \frac{c}{2\pi} \sqrt{\frac{S}{Vt'}} = \frac{c}{2\pi} \sqrt{\frac{\varepsilon}{dt'}}$$
(2.27)

To formulate the absorption of a Helmholtz absorber it is possible to define a lumped element model as in chapter 5, it is often more helpful however to consider in the entire acoustic system as a combination of layers as part of a transfer matrix model (see section 2.4.2.1.1). In this case the impedance of the perforated sheet is simply added onto the impedance of the backing to find the overall impedance; from here the absorption coefficient can easily be found from equations 2.7 and 2.4.

#### 2.4.2 Membrane Absorbers

Membrane or panel absorbers are also mass-spring systems, this time however the vibrating mass is a flexible membrane or plate and the spring is the compliance of the sealed air cavity of the box backing the membrane. A standard design of membrane absorber is shown below:



**Figure 2.7** Schematic representation of a standard membrane absorber

High pressure acoustic waves meeting the surface of a membrane cause it to oscillate at a frequency governed by its mass, and the stiffness of the air spring of the cavity. The air spring is considered linear as long as there are no standing waves in the cavity within

the fundamental frequency range, which is almost always the case with membrane absorbers. The vibration of the membrane creates high particle velocities at its rear that effectively force air through the porous absorbent thus generating high levels of absorption. This however is only over a limited bandwidth i.e. the resonance peak of absorption has a high Q-factor. The bandwidth can be increased by increasing the damping, but as with any mass-spring system, this has the effect of decreasing the maximum efficiency of the absorber. A trade off therefore ensues between bandwidth and maximum absorption.

Unlike Helmholtz absorbers, prediction of the behavior of membrane absorbers is difficult and often inaccurate this is because the exact mounting conditions and properties of the membrane are hard to predict and model. Not being able to model the mounting conditions accurately is problematic as membrane absorbers often exhibit losses and hence absorption from the edges. Many common formulations also assume that the membrane cannot support higher order modes than the fundamental resonant frequency i.e. they assume that the membrane moves as a lumped mass system in much the same way as a piston does. These simpler models do not allow for the membrane to support bending waves and consequently don't result in accurate predictions especially at oblique incidence, when bending waves are more easily excited.

#### 2.4.2.1 Predicting the Performance of Membrane Absorbers

If the membrane is considered to oscillate as a piston and its bending stiffness is ignored such that the restoring force is entirely due to the compliance per unit area  $C$  of the air volume where:

$$C = \frac{d}{\rho_0 c^2} \tag{2.28}$$

An equation of the impedance of the cavity backed membrane can then be written as:

$$Z = j \left( \omega M - \frac{1}{\omega C} \right) + R_M \tag{2.29}$$

where  $M$  is the mass per unit area of the membrane or plate and  $R_M$  is the mechanical losses of the mounting. The resonant frequency of this system can be found by setting the imaginary part to zero thus:

$$\omega_0 = \left( \frac{\rho_0 c^2}{Md} \right)^{\frac{1}{2}}, \quad \text{so} \quad f_0 \approx \frac{60}{\sqrt{Md}} \quad (2.30)$$

Equation 2.30 is a useful first approximation but it only defines the condition with an empty cavity. If the cavity contains porous absorbent as is common in the design of such absorbers the resonant frequencies predicted by this formula tend to be too high. This formula can therefore be altered to account for the adiabatic case as [7]:

$$f_0 = \frac{50}{\sqrt{Md}} \quad (2.31)$$

These provide a useful first approximation but often yield inaccurate results with errors of up to 10 per cent. This inaccuracy is largely because the mechanical properties of the panel are not taken into account. With the edges of the panel fixed its bending stiffness will, especially for thicker panels, contribute considerably to the restoring force of the system such that it cannot be approximated simply by equation 2.28. Accurately predicting this bending stiffness is particularly difficult especially when the exact boundary conditions of the membrane or plate are uncertain.

Other formulations and methods are also often used [16,17], these techniques have the disadvantage of being complex and need extensive knowledge of the material properties to be accurate. However even with accurate determination of these properties assumptions are still made for the mounting conditions which are often inaccurate, leading to errors in the predicted performance. A more simplistic method for prediction of resonant absorbers is the transfer matrix method which builds upon the theory of sound traveling through different layers of porous media mentioned in section 2.3.1.2.1. This technique is often thought better as it is adaptable for many scenarios of construction and yields results with reasonable accuracy.

### 2.4.2.1.1 Transfer Matrix Modelling

The transfer matrix approach is a very useful tool as it allows surface velocities, pressures to be calculated this enables the more useful determination of the surface impedance.

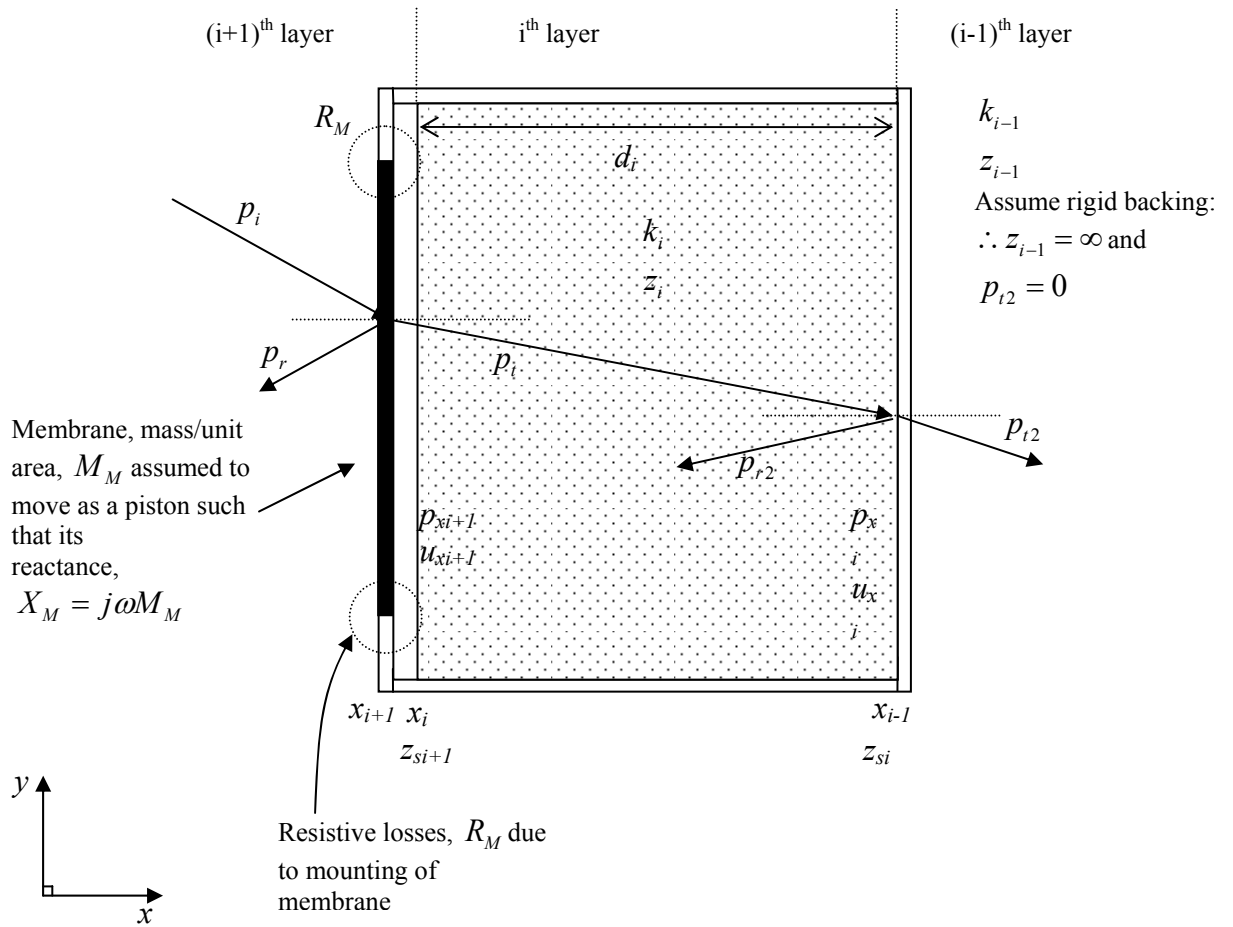
Writing equation 2.22 in matrix form gives the pressure and velocity at a point  $x$  as:

$$\begin{Bmatrix} p_t(x) \\ u_t(x) \end{Bmatrix} = \begin{Bmatrix} \cos(kd) & jz_c \sin(kd) \\ \frac{j}{z_c} \sin(kd) & \cos(kd) \end{Bmatrix} \begin{Bmatrix} p_t(0) \\ u_t(0) \end{Bmatrix} \quad (2.32)$$

This is part of a transfer matrix that can be found in Allard [14]. The transfer matrix method uses the surface impedance of one layer as the backing impedance of the next enabling any number of layers to be combined and the final surface impedance found. It is a very useful tool for designing absorbers as it eliminates the need for iterative development which is both costly and time consuming in the design of absorber systems. The transfer matrix method allows many different systems to be predicted ranging from the simple case of a porous material mounted on a rigid wall up to multiple porous layers including membrane and Helmholtz layers. In order to perform calculations, the characteristic impedance of the material of each layer must be known. This can be achieved easily in many cases such that a porous layer can be represented by empirical or semi-empirical formulations like the Delany and Bazley model as mentioned in section 2.3.1.1. The characteristic impedance of membrane and Helmholtz layers can be more problematic to predict with accuracy as often boundary conditions are not known and as such approximations have to be made. For the membrane case the membrane is assumed to be very thin such that there are no bending waves present. It is thereby assumed to move as a piston mass. The impedance in this case can be considered as a series combination (that is the simple addition) of a single resistive and reactive term. In general membranes are assumed to move pistonically with a nominal resistance to motion made up from the mounting and resistive losses in the material. The impedance therefore is given by equation 2.35.

Assuming that only plane waves are incident on the multi-layered absorber system and only considering propagation in the  $x$  and  $y$  direction, the propagation through the

system can be represented by *Figure 2.8*. The initial case is considered with a membrane mounted on a cabinet filled with absorbent material.



**Figure 2.8** Diagrammatic representation of the transfer matrix modeling of sound incident to a membrane absorber

The equation that links all of the surface pressures and velocities and allows hence the calculation of the surface impedance is the same as in section 2.3.1.2.1 but with different notation equation 2.22 can therefore be written as:

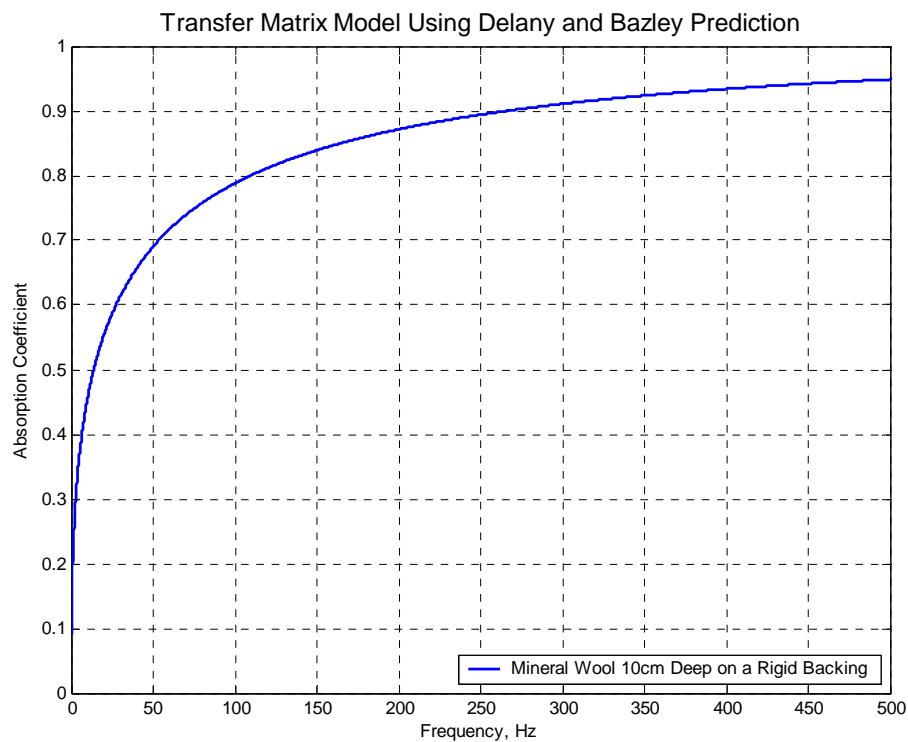
$$z_{si+1} = \frac{-jz_{si}z_i \cot(k_i d_i) + z_i^2}{z_{si} - jz_i \cot(k_i d_i)}$$

(2.33)

Using this notation it is easier to keep track of multiple layered systems. Applying this to the  $i^{\text{th}}$  layer, the backing is considered to have infinite impedance such that  $z_{s_i} \approx \infty$  and the above equation simplifies to:

$$z_{s_{i+1}} = -jz_i \cot(k_i d_i) \quad (2.34)$$

Where  $k_i$  can be determined from a model for porous media such as Delany and Bazley and  $d_i$  is the depth of the porous material. This value can then be used as  $z_{s_i}$  for the next layer and the impedance calculated for further layers of materials. From this the absorption coefficient can be calculated and plotted against frequency yielding the standard result for mineral wool as shown in *Figure 2.9*:



**Figure 2.9** Transfer matrix modeling of porous absorbent with a rigid backing using the Delany and Bazley model

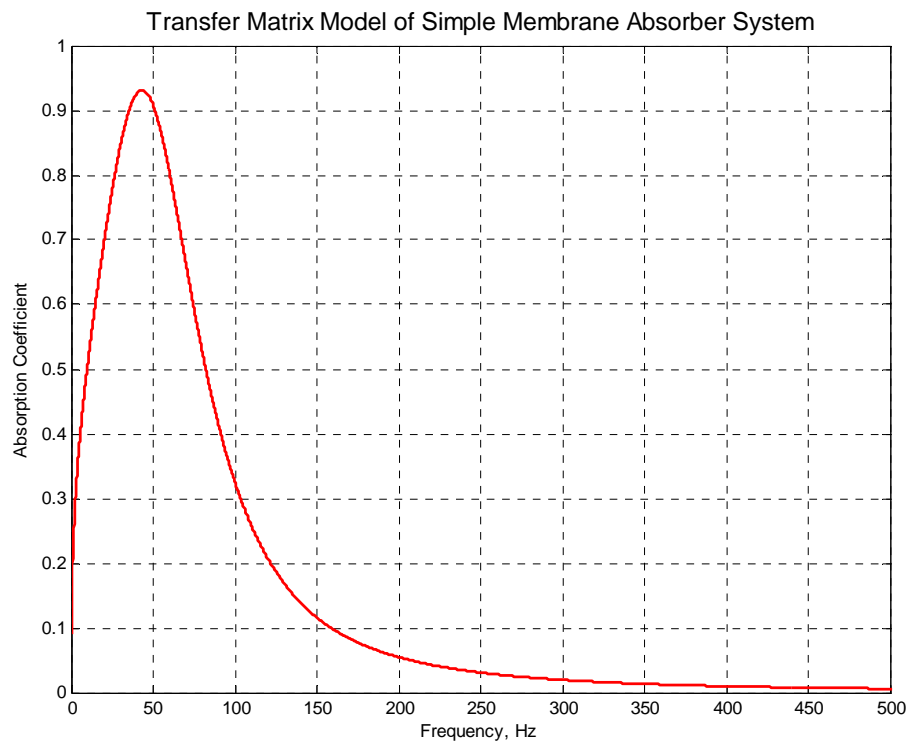
When adding a membrane to the front of the absorber system the impedances work in series with each other such that the overall impedance can be determined simply by the addition of the resistive and reactive impedances of the membrane:

$$z_M = j\omega M_M + R_M \quad (2.35)$$

The surface impedance of the system is then the series addition of the impedance of the membrane layer and the porous layer:

$$z_{si+1} = z_{si} + z_M \quad (2.36)$$

More complex solutions can be obtained if air gaps and/or Helmholtz layers are included, for now the simplest case is considered as shown in *Figure 2.8* with a membrane layer added to the porous absorber with a small air gap between the layers to allow for the membrane's movement. Plotting this in MATLAB yields the prediction in *Figure 2.10*:



**Figure 2.10** Transfer matrix prediction of a simple membrane absorber

The graph shows a typical absorption graph for a membrane absorber, exhibiting a resonant peak with high absorption at lower frequency with less absorption at higher frequencies.



The predictions so far have dealt only with waves incident normal to the surface of an absorber, this is a useful case and matches closely to the testing of an absorber in an impedance tube and therefore is very useful for comparison of predictions and measurements. There is however scope for extending the transfer matrix approach for oblique incidence waves by considering the wavenumber in materials as a vector quantity with components in the  $x$  and  $y$  direction. Such that:

$$\mathbf{k}^2 = k_x^2 + k_y^2 \quad (2.37)$$

Using Snell's law it is then possible to define the refractive effect as the acoustic waves propagate through each medium. The equation then becomes:

$$z_{si+1} = \frac{-jz_{si}z_i \frac{k_i}{k_{xi}} \cot(k_{xi}d_i) + \left(z_i \frac{k_i}{k_{xi}}\right)^2}{z_{si} - jz_i \frac{k_i}{k_{xi}} \cot(k_{xi}d_i)} \quad (2.38)$$

For most porous absorbents the  $x$  component of the wavenumber vector,  $\mathbf{k}$  is equal to the scalar wavenumber in that material as the angle of incidence tends to the normal. Thus often the angle of incidence is not needed. For the purposes of this project only normal incidence will be modeled.

## 2.5 Conclusion

It has been seen how both porous materials and damped acoustic resonators can be used in the field of room acoustics to absorb sound in high and low frequency bands. Theory of these methods has been outlined along with the relevant prediction models that will be used in subsequent sections of this work. The theory presented in this chapter will serve as a useful background to the analysis, modeling and development of more complicated absorber systems presented in chapters 4, 5 and 6.

### **3. MEASURING ABSORPTION COEFFICIENT AND SURFACE IMPEDANCE**

#### **3.1 Introduction**

The previous chapter outlined some theory and prediction techniques for the performance of acoustic absorbers. This chapter describes and demonstrates some useful techniques for the measurement of absorption characteristics. Of primary interest is the surface impedance of an absorber, be it porous or resonant. From this quantity, the reflection factor and the absorption coefficient can be found giving a good idea of the absorber's performance with respect to frequency.

Two main methods are used for measuring these absorber characteristics, namely the reverberation room method and impedance tube method. The former, measures random incidence absorption coefficient and the latter, the normal incidence absorption coefficient and surface impedance. In general, the reverberation chamber method is

used to test larger areas of absorbers such as carpets where samples with large surface area can easily be obtained. Impedance tubes require much smaller samples and are often used when developing new absorbers as small samples are more cost effective to produce. The normal incidence absorption coefficient measured in this case is also easier to compare with theoretical models than the random incidence absorption coefficient which is very difficult to predict so is less useful for comparisons.

Both techniques are presented in this chapter along with the design, construction and commissioning of a low frequency impedance tube especially designed for the measurement of low frequency absorbers. The cross sectional area of the tube was such that the entire membrane absorber could fit into it thus allowing accurate testing of its normal incidence absorption coefficient.

### 3.2 Reverberation Chamber Method

The basic premise of the reverberation method is to determine how much difference an absorber makes to the reverberation time in a room, and therefore to determine the absorption coefficient of the material that would result in this difference. The reverberation time is measured before and after the addition of the absorption and from this, the absorption coefficient is derived. The reverberation chamber method is based on Sabine's equation for the reverberation time in a room [18]:

$$T = \frac{55.3V}{cA} \quad (3.1)$$

Where  $T$  is the time for the noise source within the room to decay by 60dB from a steady level,  $V$  is the volume of the room,  $c$  is the speed of sound and  $A$  is the total absorption area of all surfaces. Rearranging this formula and adding a term for the absorption due to the air (this becomes significant for larger rooms) gives an equation for the equivalent sound absorption area of the empty reverberation room,  $A_1$ :

$$A_1 = \frac{55.3V}{cT_1} - 4m_1 \quad (3.2)$$

The equation for the equivalent sound absorption area of the reverberation room with the absorption present,  $A_2$  is then given by:

$$A_2 = \frac{55.3V}{cT_2} - 4m_2 \quad (3.3)$$

where  $T_1$  and  $T_2$  are the reverberation times and  $m_1$  and  $m_2$ , the power attenuation coefficients of the room, without and with the sample respectively. Combining these equations gives a formula for the equivalent sound absorption area of the sample as follows:

$$A_T = A_2 - A_1 = 55.3V \left( \frac{1}{c_2T_2} - \frac{1}{c_1T_1} \right) - 4V(m_2 - m_1) \quad (3.4)$$

The random incidence absorption coefficient of the test sample can then be easily calculated by:

$$\alpha_s = \frac{A_T}{S} \quad (3.5)$$

A more detailed description of this method can be found in an international standard [19]. The random incidence absorption coefficient measured by the reverberation chamber method is more true to life than the normal incidence coefficient as sound is commonly incident to a surface from all angles so this method can be useful to see how absorbers behave in real applications like determining how much sound energy a carpet will absorb if used in a domestic setting. Consequently it is the random incidence absorption coefficient that is most commonly used to define the performance of materials used in architectural acoustics. A disadvantage of this method is that it doesn't allow the impedance of the material to be measured which prevents a complete understanding of how the material behaves acoustically. Further to this, the method requires a reverberation chamber and large samples so it can be expensive to undertake.

This method has not been used for any measurements carried out in this project as the large samples required makes testing of membrane absorbers difficult as such it is the

impedance tube method outlined in section 3.3 that is used for measurements throughout this work.

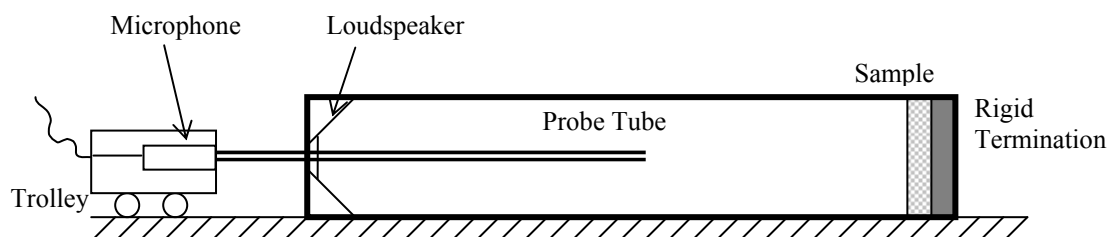
### 3.3 Impedance Tube Method

Impedance tubes offer a more controlled test environment and have the advantage over the reverberation method that they enable the measurement of the acoustic impedance of a sample or system. Impedance tubes are cheaper to use than the reverberation chamber technique because less specialist equipment is needed; also the sample sizes can be much smaller, cutting down on waste. There are two techniques for using impedance tube; the standing wave method and the transfer function or ‘two-microphone method’. Both methods are outlined below and can also be found in the relevant International Standards [20, 21]. Brief theory of both methods is given below.

#### 3.3.1 Standing Wave Method

The standing wave method was the earliest method devised for measuring absorption using a tube it evolved from August Kundt’s (1839-1894) tube for measuring the speed of sound and is simpler in principle than the transfer function approach. The basic premise is as follows. Plane waves propagate down the tube from the loudspeaker and are reflected from the other end of the tube where the sample is mounted, consequently setting up standing waves in the tube. Measuring the relative amplitudes of the maxima and minima of the standing waves using a moving probe microphone enables the absorption coefficient to be calculated, for discrete frequencies. A diagram showing the construction and operation of a standing wave tube is shown in

*Figure 3.1:*



**Figure 3.1** Diagram of the typical setup of an impedance tube using the standing wave method

With the loudspeaker source on, a standing wave will be set up in the tube. The probe microphone can be moved up and down the tube in order to find the first pressure maximum and the first pressure minimum from the sample. This can be done by simply connecting the output from the microphone to a voltmeter. Noting down the values and

their position relative to the sample allow for both magnitude and phase data to be determined and used to calculate the absorption coefficient and the surface impedance of the sample. As this procedure has to be done separately for each frequency of interest it can be rather time consuming and doesn't give continuous data. It is however a reliable method and simple equations can be used to calculate the necessary parameters of the sample as shown below.

The pressure at any point in the tube, assuming plane wave propagation, will be given by:

$$p = p_i + p_r \quad (3.6)$$

where  $p_i = Ae^{jkz}$  and  $p_r = AR e^{-jkz}$ . Therefore:

$$p = A(e^{jkz} + R e^{-jkz}) \quad (3.7)$$

$z$  is the distance from the sample,  $k$  is the wavenumber,  $R$  is the reflection factor and  $A$  is a complex constant. For a pressure maximum the incident and reflected waves interfere constructively and are therefore in phase. For a pressure minimum the incident and reflected waves interfere destructively and are therefore 180 degrees out of phase, therefore equations for  $p_{max}$  and  $p_{min}$  can be given as follows:

$$\begin{aligned} p_{max} &= 1 + |R| \\ p_{min} &= 1 - |R| \end{aligned} \quad (3.8)$$

Knowing only the magnitudes of  $p_{max}$  and  $p_{min}$  the reflection factor can be calculated by finding the standing wave ratio (SWR) between the two pressures.

$$SWR = \frac{p_{max}}{p_{min}} = \frac{1 + |R|}{1 - |R|} \quad (3.9)$$

$$\Rightarrow |R| = \frac{SWR - 1}{SWR + 1}$$

$$(3.10)$$

From this, the absorption coefficient of the sample can be found using equation 2.4.

If the surface impedance is wanted then the position of the first minimum can be noted and used in equation 3.11 to calculate the argument of  $R$  which can then be used to derive the surface impedance of the sample:

$$\phi + (2n - 1)\pi = 2kZ_{\min,n} \quad (3.11)$$

$$R = |R|e^{j\phi} \quad (3.12)$$

Here  $n$  is the number of the pressure minimum measured. From this the complex impedance is given by:

$$Z = \rho_0 c \frac{1 + R}{1 - R} \quad (3.13)$$

Although this method does allow for any of the pressure minimums to be measured it is better to use only the first minima as this will eliminate effects from losses in the tube walls.

Calibration isn't necessary for the standing wave method because pressure values have a constant offset, which appears in the complex amplitude,  $A$ , and cancels out in the pressure ratio. This makes things simpler and results in an easy method for measuring absorption of samples.

There is a low frequency limit of a standing wave tube, which is governed by its length i.e. ensuring that a maximum and a minimum can be found. The standard dictates that at least two minima should be able to be found, this imposes a low frequency limit on the tube of:

$$f_l = \frac{0.75c}{l}$$

(3.14)

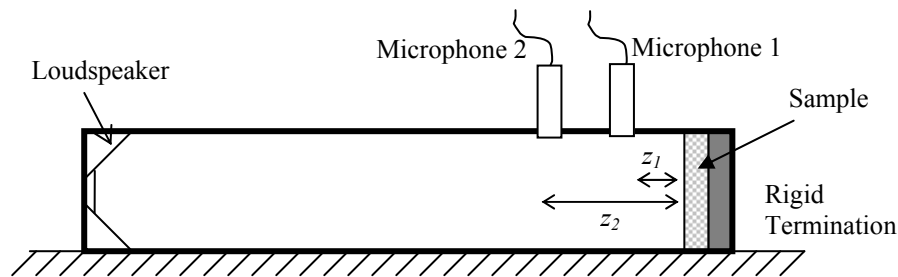
Where  $l$  is the length of the tube and  $c$  is the wave speed in the tube.

The standing wave method is more reliable and failsafe than the transfer function method mentioned in section 3.3.2 but it is rather tedious as it can be time consuming to locate and measure the positions of the minima in order to obtain the phase data, and to do this for each frequency of interest.

### 3.3.2 Transfer Function Method

This method is often thought superior to the standing wave method because it allows all frequencies to be calculated simultaneously thereby producing continuous data in the frequency domain with just two measurements. As such, this method is less time consuming and can be easier to verify results with predictions.

*Figure 3.2* shows a diagram of a typical setup of a transfer function impedance tube:



**Figure 3.2** Diagram of the typical setup of an impedance tube using the transfer function method

The transfer function method operates within a certain frequency range, depending on the microphone positions and diameter of the tube governed by equations 3.17, 3.18 and 3.19. The lower of the two upper frequency limits should be chosen so that both equations are satisfied. Although often called the ‘two microphone method’ (as it uses at least two microphone positions) the transfer function method is a better name as it describes the process by which the results can be obtained.

The steady state pressure at a point in the tube is given by equation 3.7 where units and symbols have their usual meanings,  $z$  being the distance from the sample to the microphone. There are two unknowns in this equation namely the magnitude and the phase of the complex reflection factor. The two microphone positions are used to get



two pressure equations that can be solved simultaneously in order to obtain the two unknowns. Taking the transfer function of these two pressures gives:

$$H_{12} = \frac{p_2}{p_1} = \frac{A(e^{jkz_2} + R.e^{-jkz_2})}{A(e^{jkz_1} + R.e^{-jkz_1})} = \frac{e^{jkz_2} + R.e^{-jkz_2}}{e^{jkz_1} + R.e^{-jkz_1}} \quad (3.15)$$

Therefore:

$$R = \frac{He^{jkz_1} - e^{jkz_2}}{e^{-jkz_2} - He^{-jkz_1}} \quad (3.16)$$

From this the impedance and hence the absorption coefficient can easily be derived, using equations 2.7 and 2.4 respectively.

There are frequency limitations imposed on this method as a consequence of the microphone positions. If the microphones are too close together the pressure difference between them is too small to be accurately measured and the method breaks down, the low frequency limit is usually given by the following equation:

$$f_l > \frac{0.05c}{|z_1 - z_2|} \quad (3.17)$$

If the microphones are too far apart this leads to an upper frequency limit. As the distance between the microphones becomes equal to a wavelength the pressures at the two microphones will be the same at the corresponding frequency and the simultaneous equations will not be solvable. The upper frequency limit imposed by this is therefore given by:

$$f_u > \frac{0.45c}{|z_1 - z_2|} \quad (3.18)$$

Both of these upper and lower limits are dictated by the microphone positions, hence often additional microphone positions are used in order to increase the useable frequency range of this method, computing the transfer function separately for each pair of microphone positions.

Microphones cannot be placed too near to the sample or to the source to ensure accurate measurements. The first microphone should be at least two tube diameters from the loudspeaker as by this point any cross modes that have been generated by the loudspeaker will have died away and only plane waves will be incident on the sample, enabling the normal incidence absorption coefficient to be accurately measured. Subsequent microphones should be sufficiently far from the sample (usually by about  $\frac{1}{2}$  diameter of the tube) this is so that any cross modes generated from the reflection of the sample will have also died away. This tends to be more of a problem for anisotropic materials so often greater distances are needed between sample and microphone when these materials are being tested.

Practically, when using the transfer function method it is common to use a deterministic noise source such as a swept sine wave or an MLS noise source [22] rather than simply white noise. This eliminates the need for phase-matched microphones, which would otherwise be needed; these can be expensive and would have to be changed over anyway to verify each measurement for repeatability checking. With a deterministic signal a measurement can be made at one microphone position, the microphone moved and the pressure taken at the second position enabling the transfer function to be calculated.

The diaphragm of the microphone should always be flush with the side of the tube and sealed, to enable accurate results. Of utmost importance is that the unused hole be blocked, with the rubber bung or block being flush with the edge of the tube as these holes can lead to additional absorption due to a Helmholtz effect.

### **3.3.3 General Considerations for Impedance Tube Testing**

Whichever impedance tube method is being used, some important general principles need to be applied. It is imperative that a good seal between sample and tube walls is achieved to prevent extra absorption generated by sound propagating in the small gap or as a result of a Helmholtz resonance if there is a cavity behind the gap. When mounting the sample it is also very important to get rid of any unwanted air gaps at the rear of the sample as these can lead to an increase in low frequency absorption which, if not

intended, could produce misleading results. Samples should also not be squashed into the tube as the squashing alters the mechanical properties of the sample i.e. the density could be altered or additional irregularities in the face of the sample could result, leading to erroneous results. The sample end of the tube should provide a rigid backing of impedance approaching infinity without a sample in place such that only the performance of the sample is tested rather than the combined effect of the absorber and backing.

Losses in the tube need to be minimized, especially for the standing wave method to ensure it is only the effect of the sample that is measured rather than of the tube. A constant cross sectional area down the tube, especially near to the sample, is also required so that only plane waves are incident normal to the surface of the sample.

The diameter of the tube will impose further frequency limits on use of the tube, governed by the first cross modal frequency of the tube such that:

$$f_u = \frac{c}{2d} \tag{3.19}$$

Where  $d$  is the diameter or maximum width of the tube if a square cross section tube is being used. Therefore if low frequency measurements need to be made larger tubes will be needed, this is the case for testing membrane absorbers such as in this project as they are not scalable, for this reason a larger impedance tube was constructed, the design and construction of which can be found in the section 3.4. The membrane absorber in this case had to be designed to fit the diameter of the tube as membrane absorbers are extended reactors therefore the whole sample had to be measured, taking a small section of a membrane absorber would not work as the mounting conditions are so key in the performance of these absorbers.

### **3.4 The Design, Build and Commissioning of a Low Frequency Impedance Tube**

For the purposes of this project it was decided that tests would be carried out in an impedance tube rather than in the reverberation chamber due to ease of testing and the need for just one absorber to be constructed for accurate tests. Of course this only gives the normal incidence absorption coefficient, however after development in the

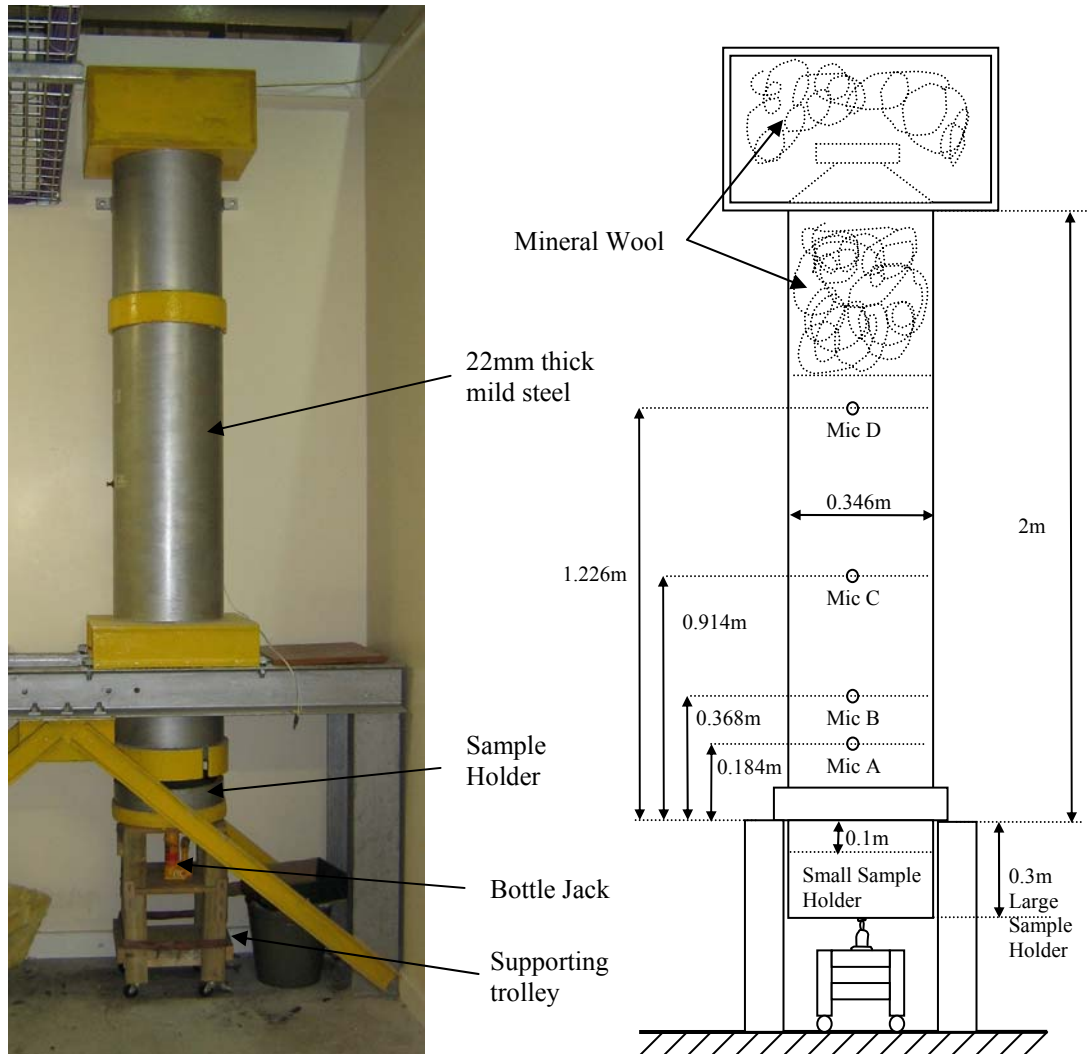
impedance tube the absorber systems could be tested in a reverberation room to obtain data on the random incidence absorption coefficient if desired.

Impedance tubes tend to be designed to such dimensions that they can be used for testing samples in the mid frequency band. In order to enable the low frequency performance of membrane absorbers as in this project a larger tube was commissioned. This section outlines the design, construction and commissioning of a specially built low frequency impedance tube used for the testing in this project.

### 3.4.1 Design

Using an impedance tube to measure the absorption of a membrane absorber presents a few problems that must be overcome in the design stage to prevent experimental inaccuracies and flawed testing. A membrane absorber is an extended reactor, meaning that a small section will not behave in a manner that is representative of the entire system, so sampling a small section of the absorber for testing will not yield good results as it would for most porous absorbers. For this reason the impedance tube had to be made to such dimensions that the membrane in question would fit within the inner walls of the tube, allowing the entire membrane to be tested. A further problem was the frequency limitations of the tube dictated by its dimensions as outlined by equations 3.17, 3.18 and 3.19. This meant that for satisfactorily low frequency performance certain dimensions were imposed upon the construction. For both the purposes of this project and for subsequent projects involving low frequency absorption the tube's dimensions were chosen to enable the accurate measurement to the lower limit of the human auditory range, the lowest measurable frequency of the tube was therefore designed to be 16Hz. The transfer function method was chosen as this provides ease of measurement and also gives results for a continuous frequency spectrum. In order to improve the measurable bandwidth of the tube dictated by the microphone positions, four microphone holes were made allowing six different microphone pairings. This also enabled accuracy of results to be checked as the frequency limits of each position overlap allowing tests of continuity for the overlapping frequency regions. A schematic of the tube's design is shown in *Figure 3.3* with the relevant dimensions labeled as well as a photograph of the completed tube. The tube was designed in an upright position

both for economy of space and also to allow the testing of granular materials for other projects.



**Figure 3.3** a) Photograph of completed impedance tube b) Schematic of completed impedance tube

### 3.4.2 Construction

The tube was constructed from 22mm thick mild steel, this provided enough mass to significantly reduce losses from the walls of the tube even at the low frequency end of the measurement bandwidth. The raw materials were ordered from a local steel merchant and the manufacture performed onsite at The University of Salford. The impedance tube consists of four sections of steel, two making up the main chamber and a further two sections to be used as sample holders (a large one and a smaller one) allowing for different testing conditions i.e. absorbers with different backing volumes. The sample holder is placed on the trolley and then jacked into place using the bottle

jack to allow for a very tight fit, ensuring no small cracks for leaks between the sections of tubing. Holes were drilled using a magnetic pillar drill in the positions as outlined above. Annular rings were welded onto the side of one of the sections of the tube to prevent the sections from coming apart. Further pieces, also welded on, were used to support the tube on a stand made from rolled steel joists. On the end of each of the sample holders a rigid backing was bolted on by drilling and tapping into the end of the tubing. The rigid backing consisted of 4cm thick MDF providing a termination impedance approaching infinity. The structure was craned into place and the stand bolted to the floor as an extra safety measure. The chosen loudspeaker was a 12" Eminence driver within a standard MDF cabinet. The rim of the cabinet was routed so it would fit tightly on the top of the tube and could not fall off. Plugs were made to block the microphone holes not in use during testing so there would be no leaks in the tube. Mineral wool was placed in the top section of the tube in order to reduce any cross modes that might be generated by the loudspeaker especially at higher levels and at higher frequencies when piston motion of the driver can no longer be guaranteed, allowing only plane wave propagating down the tube.

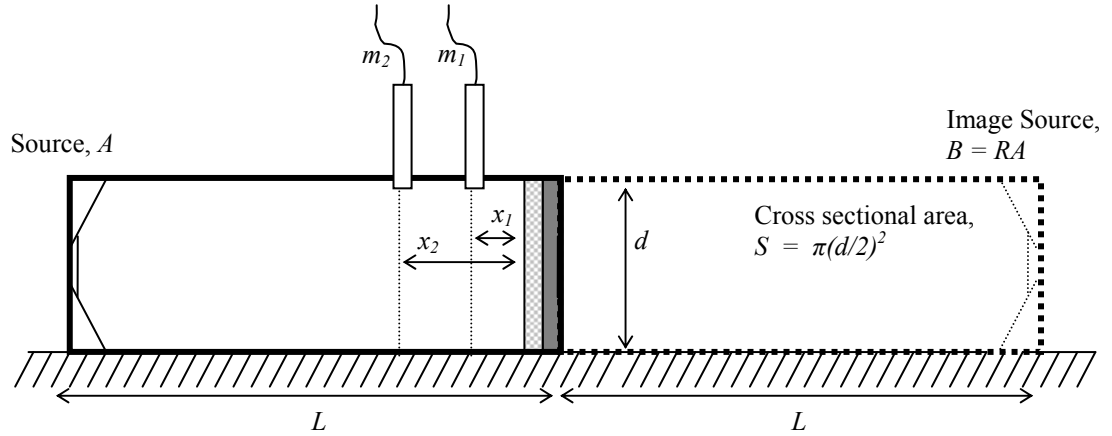
### 3.4.3 Processing the Data and Commissioning the Tube

Using the multiple microphone transfer function method it is possible to plot six separate curves pertaining to the transfer function from each combination of microphone positions. Six plots on a single set of axes does however look rather messy so processing the data from all six combinations together and plotted as one line across the whole frequency range is desirable. There has however, recently been developed a more elegant method of processing results (outlined in section 3.4.3.1) from multi microphone position impedance tubes which allows for greater accuracy at low frequencies and also allows the results to be plotted with a single line. The improved method [23] uses least squares curve fitting to optimize the response from all of the microphone positions to produce a result with minimum error.

#### 3.4.3.1 Least Squares Optimization Technique

The least squares method uses an idea of an imaginary source equidistant from the sample but in the  $-ve$   $x$  direction as shown in *Figure 3.4*. Initially this is considered for

a two microphone case although the theory can be extended to work for multiple microphone measurements.



**Figure 3.4** Impedance tube for the transfer function method with modeled image source technique

Assuming the signal strength from the actual source is of amplitude,  $A$  and the amplitude from the image source is:

$$B = RA \quad (3.20)$$

Where  $R$  is the complex reflection factor, the pressure at each microphone can be deduced from a Green's function relating the output from each microphone to the input of the each source (both actual and image):

$$\begin{aligned} p_1 &= Ag_{1A} + Bg_{1B} = A(g_{1A} + Rg_{1B}) \\ p_2 &= Ag_{2A} + Bg_{2B} = A(g_{2A} + Rg_{2B}) \end{aligned} \quad (3.21)$$

The Green's Functions  $g_{1A}$ , relates the output of microphone 1 to the input source,  $A$ ,  $g_{1B}$ , relates the output of microphone 1 with the input source of the imaginary source,  $B$ .  $g_{2A}$  and  $g_{2B}$  are the same but relate to microphone 2. In an impedance tube these Green's functions can be approximated, as given by Cho, by equation 3.22 as there is plane wave propagation in the tube:

$$\begin{aligned} g_{1A} &= \frac{\rho_0 c}{2S} e^{-jk(L-z_1)}, & g_{1B} &= \frac{\rho_0 c}{2S} e^{-jk(L+z_1)} \\ g_{2A} &= \frac{\rho_0 c}{2S} e^{-jk(L-z_2)}, & g_{2B} &= \frac{\rho_0 c}{2S} e^{-jk(L+z_2)} \end{aligned}$$

(3.22)

where  $s$  is the cross sectional area of the tube in question. Taking the transfer function of the pressures from each microphone as given in equation 3.21 gives:

$$H_{12} = \frac{p_2}{p_1} = \frac{g_{2A} + g_{2B}R}{g_{1A} + g_{1B}R}$$

(3.23)

Rearranging this equation allows the complex reflection factor to be given as:

$$R = \frac{g_{2A} - g_{1A}H_{12}}{g_{1B}H_{12} - g_{2B}}$$

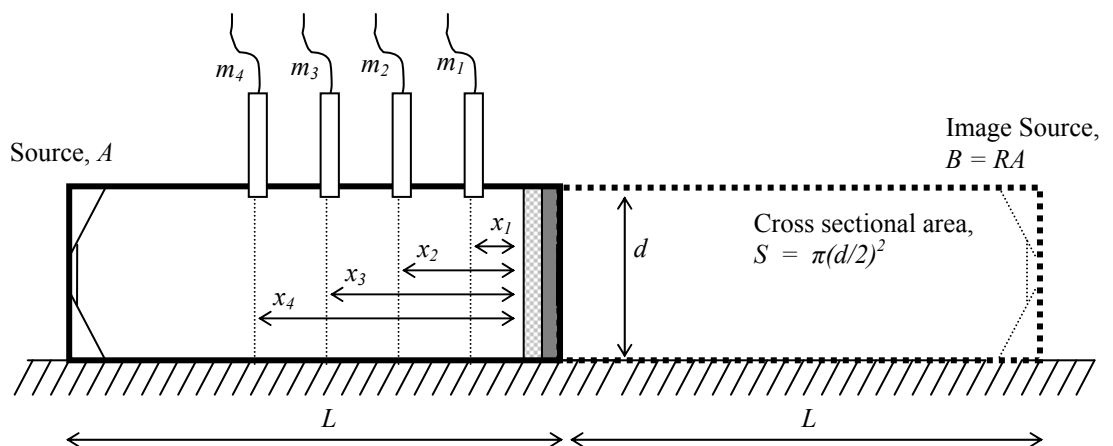
(3.24)

Cho defines both a theoretical and a measured transfer function given as  $H_{12}$  and  $\hat{H}_{12}$  respectively based on the measured and predicted pressures at the microphones. He uses a least squares solution to obtain an optimally estimated reflection factor given as:

$$R_{opt} = \frac{g_{2A} - g_{1A}\hat{H}_{12}}{g_{1B}\hat{H}_{12} - g_{2B}}$$

(3.25)

This is the same as the theoretical equation 3.24 but the theoretical transfer function is replaced with the measured transfer function. The theory is initially applied to a two microphone case but is later extended to work for multiple microphone positions in a tube as shown in *Figure 3.5*:



**Figure 3.5** Image source technique for multiple microphone positions



Using the same method as above gives an optimised reflection factor from the least squares solution for multiple microphone positions as:

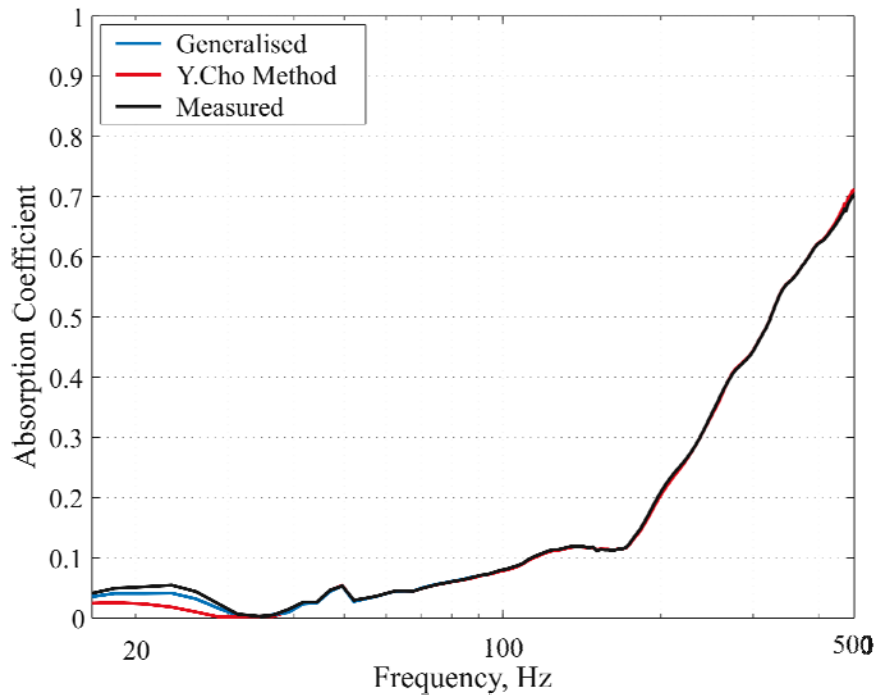
$$R_{opt} = - \frac{\sum_{m=2}^M (g_{1A} \hat{H}_{1m} - g_{mA}) (g_{1B} \hat{H}_{1m} - g_{mB})^*}{\sum_{m=2}^M |g_{1B} \hat{H}_{1m} - g_{mB}|^2} \quad (3.26)$$

This result is obtained by minimising the sum of the errors between the measured and the analytically derived pressures. It can be used for any number of microphone positions,  $M$  where  $m$  is the number of each microphone in the tube. This reflection factor can then be used to determine the acoustic impedance and absorption coefficient in the normal way.

Cho's original method references all of the microphone positions to microphone  $A$  and calculates the least squares results from that. An extended version of this method can also be formulated that references all of the possible permutations of microphone combinations rather than just the three that related to microphone  $A$ . As a result a new equation based on all five of the microphone transfer functions can be given as:

$$R_{opt} = - \frac{\sum_{n=1}^{M-1} \sum_{m=n+1}^M (g_{nA} \hat{H}_{nm} - g_{mA}) (g_{nB} \hat{H}_{nm} - g_{mB})^*}{\sum_{n=1}^{M-1} \sum_{m=n+1}^M |g_{nB} \hat{H}_{nm} - g_{mB}|^2} \quad (3.27)$$

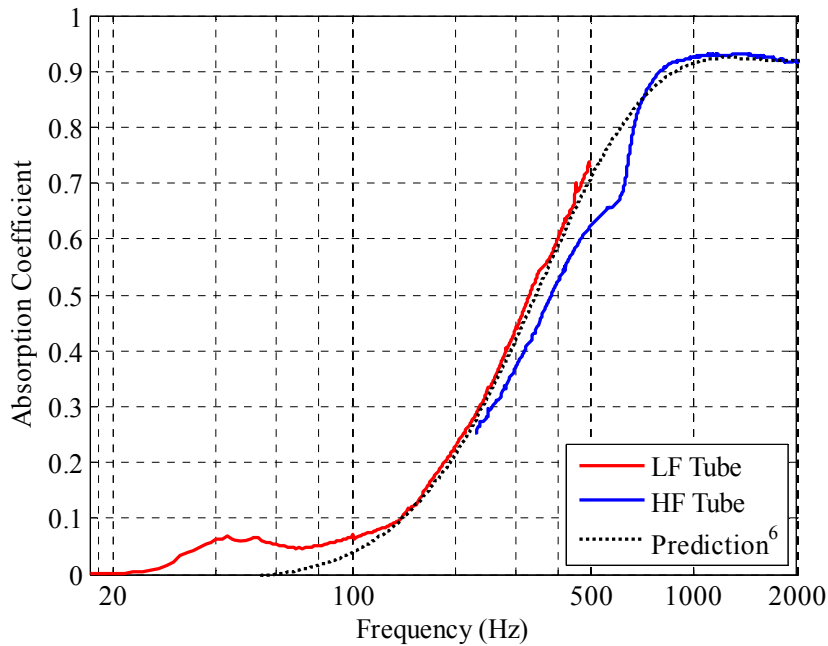
where  $n$  is the number of the reference microphone and  $m$  is the number of the second microphone. Using the extended method increases the number of transfer functions on which the least squares routine can be applied to and therefore is deemed to be a more accurate method for processing impedance tube results. In order to check the validity of the generalised expression for the reflection coefficient, measurements were performed on a sample of 12cm thick mineral wool. Results from the original and generalised Cho method as well as the traditional transfer function method are shown in *Figure 3.7*.



**Figure 3.6:** Plot showing the validity of the generalised version of Cho’s least-square optimisation method. Note that the measured plot was obtained by manually overlapping the measured data for each microphone pair according to the corresponding frequency range each best describes.

The the generalised version of Cho’s estimation method, although very similar to the standard four-microphone version above 40Hz, does achieve a slightly better prediction at the very low frequencies. This is due to the least squares estimation eliminating inaccuracies due to the presence of ‘error frequencies’ caused at frequencies where the wavelength is similar to the microphone spacing. This also allows accurate use of the impedance tube to lower frequencies.

In order to check the validity of the results with other impedance tubes, the same mineral wool sample used above is then tested in a smaller tube, capable of a measurement bandwidth between 200Hz and 1700Hz. An overlap of 300Hz is then covered between the two tubes. Being an uncommon piece of equipment, it was difficult to fully commission the low frequency impedance tube, where usually samples would be tested in other similar devices. Measurement results, presented in *Figure 3.7* below, do however show good correlation between the two impedance tubes used and also with a simple Delany and Bazley prediction model. Results from the large tube, although not exactly similar at the higher frequencies to the low frequency results of the small impedance tube, do show a comparable trend in the absorption coefficient of mineral wool between the two tubes.



**Figure 3.7:** Results for absorption coefficient of a 12cm thick sample of mineral wool as measured in the large low frequency impedance tube and a smaller high frequency tube

Using the extended method increases the number of transfer functions on which the least squares routine can be applied to and therefore is deemed to a more accurate method for processing impedance tube results. As such it is the extended optimised method that has been used throughout this project to process impedance tube results, the code for the extended optimization code is in Appendix D.

### 3.5 Conclusion

Theory of the testing of the surface impedance and the absorption coefficient of materials and systems has been presented. It has been shown that the impedance tube method is of greater practicality for the testing of the membrane absorber in this research than the reverberation chamber method as the latter method needs larger samples and would consequently need more than one membrane absorber to be constructed. A specially designed impedance tube was constructed and commissioned for the purpose of low frequency testing which will be used throughout this project for testing various permutations of design of the membrane absorber. A least squares method of processing the measured data was chosen such that the results from all four microphone positions could be included on one graph for ease of analysis.

## **4. USING LOUDSPEAKER SURROUND AS THE MOUNTING FOR A MEMBRANE ABSORBER**

### **4.1 Introduction**

The main premise of this section of the work was to change the mounting conditions of the membrane or plate used as the vibrating mass in an absorber system. The resonator for a membrane absorber can often be approximated as a simply supported or clamped membrane/plate on an acoustic cavity. This section of the work aimed at changing these conditions such that the resonator more closely approximates a piston oscillation with mass and stiffness controlled solely by its material and cavity properties. Pistonic oscillation or an approximation thereof, can be achieved by utilising a loudspeaker surround designed for such oscillation. Surrounds are used within a loudspeaker system in order to apply a restoring force,  $k\zeta$  to the outer rim of the diaphragm where  $k$  is the stiffness of the spring and  $\zeta$  is the displacement. Loudspeakers have a spider which also acts as a restoring force but on the apex of the diaphragm ensuring equal restoring force

to all parts of the diaphragm so it only moves in one plane. The surround used for measurements in this section was circular as this could be easily obtained from a loudspeaker manufacturer and tested in the specially constructed impedance tube, which has a circular cross section. In practice however, pistonic oscillation could be achieved for any shaped membrane/plate by using other shaped surrounds or with mountings such that it moves as a lumped mass in one plane only.

## **4.2 Theory**

By changing the mounting condition of the membrane in the absorber system it was hoped that the fundamental resonant frequency would be lowered as a consequence of the larger moving mass imposed by the pistonic condition. Pistonic motion means that the entire membrane/plate can oscillate rather than some of it being stationary due to the clamped condition. The efficiency therefore, should also improve as the pistonic condition allows for larger displacements with less impedance to motion (depending on the mechanical properties of the surround used). In order to successfully model, predict and verify tests using a loudspeaker surround mounted plate it was important to look at the basic theory of plate vibrations. The material used for the tests was a vinyl rubber used commonly in domestic floor tiles. It was seen that this behaved more as a plate than a membrane as the Eigen modes were more spread out in frequency suggesting that its restoring force was controlled primarily by its stiffness rather than its tension thus it approximated more accurately to a plate than a membrane [15]. In fact in most practical membrane absorbers the vibrating mass equates more faithfully to a plate rather than a membrane. However the term ‘membrane absorber’ is often used rather loosely and refers primarily to a method of acoustic absorption rather than the type of resonator used i.e. plate or membrane. As such for the purpose of this thesis the absorber system will hereafter be referred to as a membrane absorber, but the resonating mass treated as a plate.

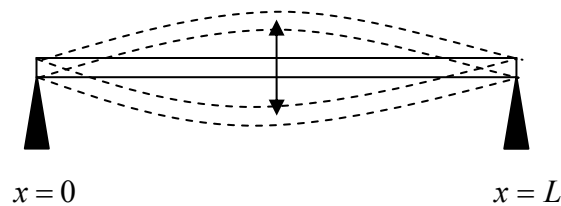
### **4.2.1 Traditional Mounting Conditions**

When looking at the vibrational behaviour of plates and membranes, defining the boundary conditions accurately is of utmost importance if an accurate model is to be devised [24]. There are principally three mounting conditions and any anomalies tend to

be variations upon these three, they are simply supported, clamped and freely supported. The three conditions are briefly summarized below.

#### 4.2.1.1 Simply Supported

The most common representation of the impedance boundary conditions is that of simply supported, this condition can be represented diagrammatically as *Figure 4.1*



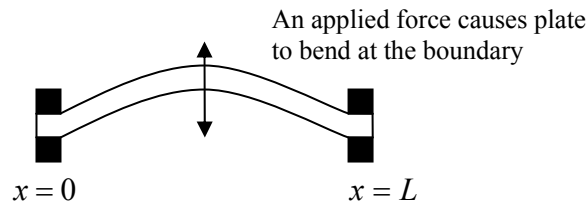
*Figure 4.1* Schematic representation of a simply supported plate

For a simply supported plate it is assumed that the edges are pinned to the support; from this assumption some physical conditions can be determined. A plate mounted with these conditions exhibits no deflection at the edges as it is pinned to the support such that  $\zeta(0) = 0$  and  $\zeta(L) = 0$ . The supports are pin supports so the plate is free to rotate on the pin and doesn't experience any torque/bending moment,  $M$  as a result, therefore  $M(0) = 0$  and  $M(L) = 0$ . In practice only approximations to simple supports exist as there will always be a small bending moment at the pin supports even if they are well greased. However many bars and plates are mounted such that they can be considered to be a close approximation to this boundary condition. Simply-supported plates are often used in the modeling of membrane absorbers as exemplified by Mechel [25].

#### 4.2.1.2 Clamped

The clamped condition is different to the simply supported case in that the edges of the plate cannot pivot on the supporting edges as with the simply supported case there can be no displacement at the edges of the plate so  $\zeta(0) = 0$  and  $\zeta(L) = 0$ . The plate will also be horizontal at its edges such that the derivative of displacement is zero,  $\zeta'(0) = 0$  and  $\zeta'(L) = 0$ .

The clamped condition can be drawn diagrammatically as:



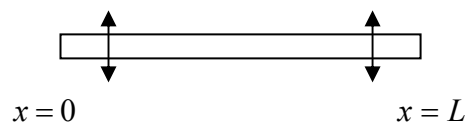
**Figure 4.2** Schematic representation of a clamped plate

A clamped plate is often a good assumption to make when modeling membrane absorbers as panels are often screwed or glued providing a strong fixing at the boundary and allowing no pivotal movement.

#### 4.2.1.3 Freely Supported

This case is probably the theoretically the simplest case although is difficult to create in practice. A freely supported plate has no bending moment at the edges such that,  $M(0) = 0$  and  $M(L) = 0$  and there is no force acting on the edges of the plate as there are no supports.

Diagrammatically a freely supported plate can be drawn as:



**Figure 4.3** Schematic representation of a freely supported plate

#### 4.2.2 The Pistonic Case

Aside from these three common boundary conditions a pistonic case can also be defined. The pistonic case allows the movement of the plate only in one dimension similar to the freely supported case, the difference is that for the pistonic case there is a restoring force introduced by a spring of stiffness,  $k$ . The spring provides a restoring force of  $k\zeta$  to the plate, there will also be a damping associated with the spring applying

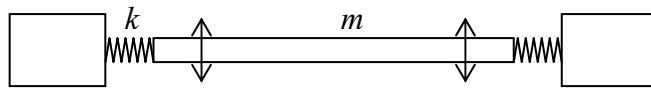
a force  $Ru$  to the system. Finally the mass of the plate will also apply a force of  $M \frac{du}{dt}$ .

This means that the plate will oscillate with motion governed by these parameters such that its resonant frequency can be given by:

$$f = \frac{1}{2\pi\sqrt{\frac{m}{k}}}$$

(4.1)

The pistonic case can be represented diagrammatically as:



**Figure 4.4** Schematic presentation of pistonic mounting

In practice if the plate is mounted on a cabinet, the spring stiffness will also depend on the acoustic compliance of the enclosed volume of air.

Using the pistonic condition for modeling the plate of the membrane absorber is a very useful tool because it enables the plate to be modeled as a lumped mass; that is, there is no need to determine the material constants such as its modulus of elasticity or Poisson ratio. All that is needed is the mass and area of the plate and the stiffness/compliance of any restoring springs. Damping terms are harder to quantify but techniques borrowed from modeling porous media and also from loudspeaker design can help.

A perennial problem associated with the design and application of membrane absorbers is that it is difficult to accurately predict the system's resonant frequency as seen in section 2.4.2.1 The main reason for this is that it is very difficult to quantify exactly what the mounting conditions of the plate are; the interaction between the membrane and the cavity is also a difficulty even with advanced numerical techniques such as finite element modeling. With the mounting condition of the plate approximating a pistonic condition, modeling will be easier and more accurate predictions of the system's resonant behaviour will result. Commercially this could lead to an absorber



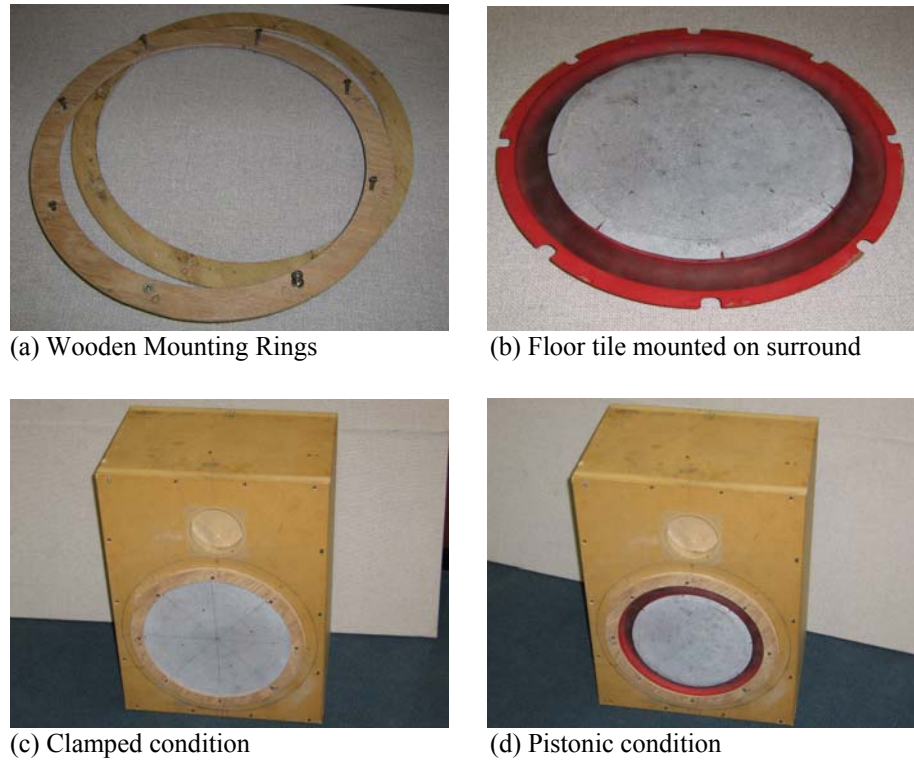
design that would resonate at lower frequency with greater efficiency and be designed more easily such that it would resonate at the designated frequency when built.

### **4.3 Measurements**

The theory of using a loudspeaker surround as the mounting for a membrane absorber was tested using an accelerometer and the impedance tube. Results showed that the resonant frequency of the system was decreased dramatically with the introduction of the surround as a consequence of the additional moving mass.

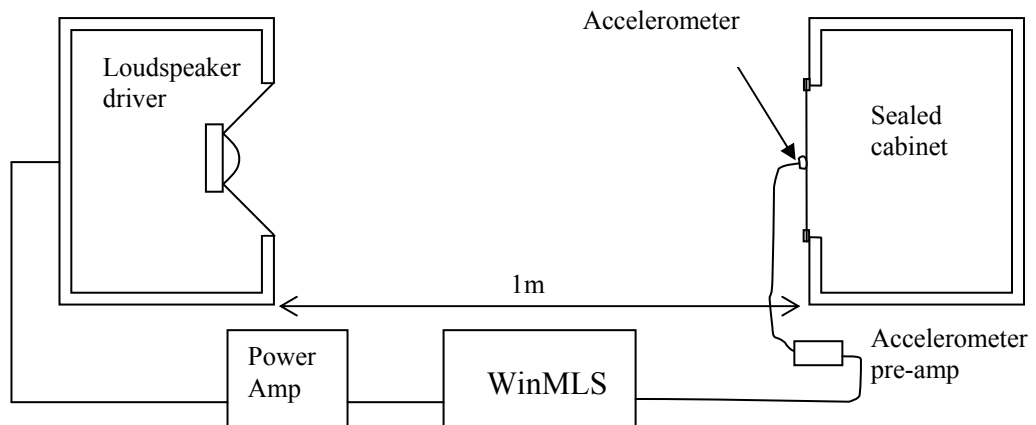
#### **4.3.1 Initial Measurements Using an Accelerometer**

Two scenarios of mounting were tested for the absorber system, firstly with the plate approximating a clamped condition and secondly with the plate approximating a pistonic case. Initial tests were carried out on the two conditions, testing the fundamental resonant frequency of each case using an accelerometer stuck to the centre of the plate in question. A 12" loudspeaker surround was obtained by request from KEF Loudspeakers and the vinyl rubber plate fixed to it to test the pistonic case. The surround's mechanical properties were such that it had a large stiffness and a reasonably heavy damping for a surround of its size. Two mounting rings were cut from a sheet of 3mm plywood, these rings were used to clamp the sample being tested, the rings and sample together then being screwed to a loudspeaker cabinet as per *Figure 4.5*.



**Figure 4.5** Photos of membrane mounting

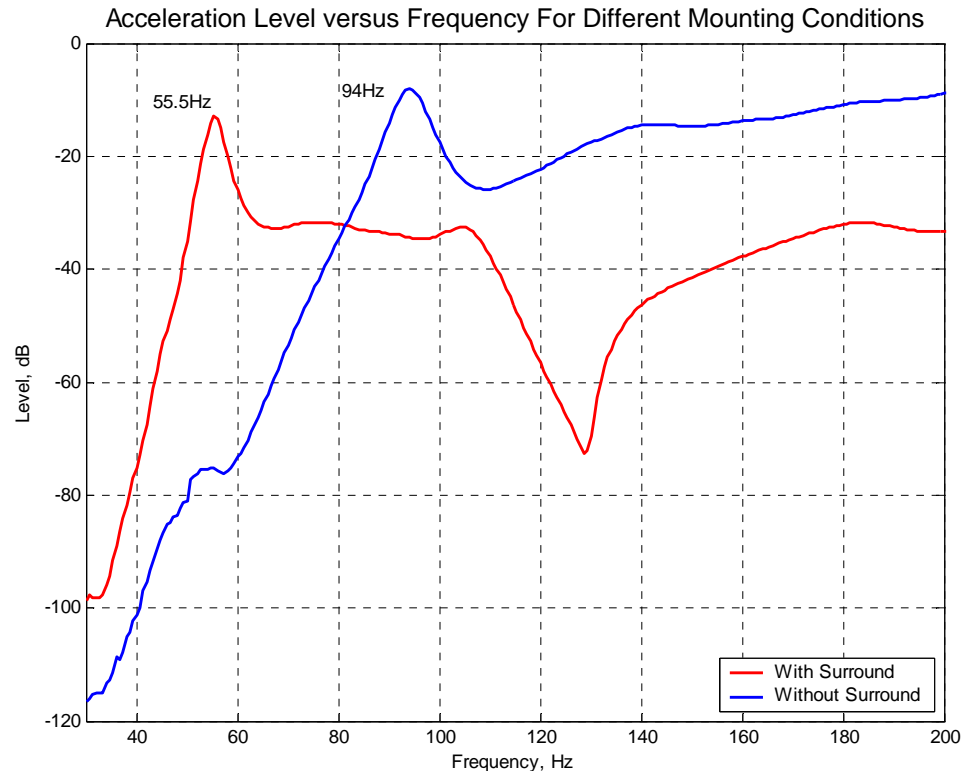
The rings were used so the mounting conditions were the same each time hence it was just the effect of the surround being tested. Using the rings meant that the area being tested was the same for both conditions i.e. the area of the surround with the plate and the plate alone was the same. The surround had a mass/unit area of the  $2.381 \text{ kgm}^{-2}$  and the vinyl membrane of  $2.81 \text{ kgm}^{-2}$ . The membrane system was excited with a 12 inch loudspeaker from a distance of 1 metre, using a swept sine signal from a winMLS controlled computer, an impulse response was generated as measured with the accelerometer, the windowed Fourier Transform was then taken to obtain a frequency spectrum from which the results were analysed.



**Figure 4.6** Experimental setup for the accelerometer tests

Both the driver and the absorber were placed on the ground with absorbent in between to reduce the effect of first order reflections. The experimental setup is shown in *Figure 4.6*.

Results were processed in MATLAB using the script in Appendix E. The accelerometer was a Knowles BU-1771 with a mass of just 0.28g and dimensions 7.9mm by 5.6mm by 4.1mm. As such it was considered that the additional loading of the accelerometer on the plate was negligible. The following graph shows the frequency responses obtained from the measurements.



**Figure 4.7** Results from the accelerometer tests

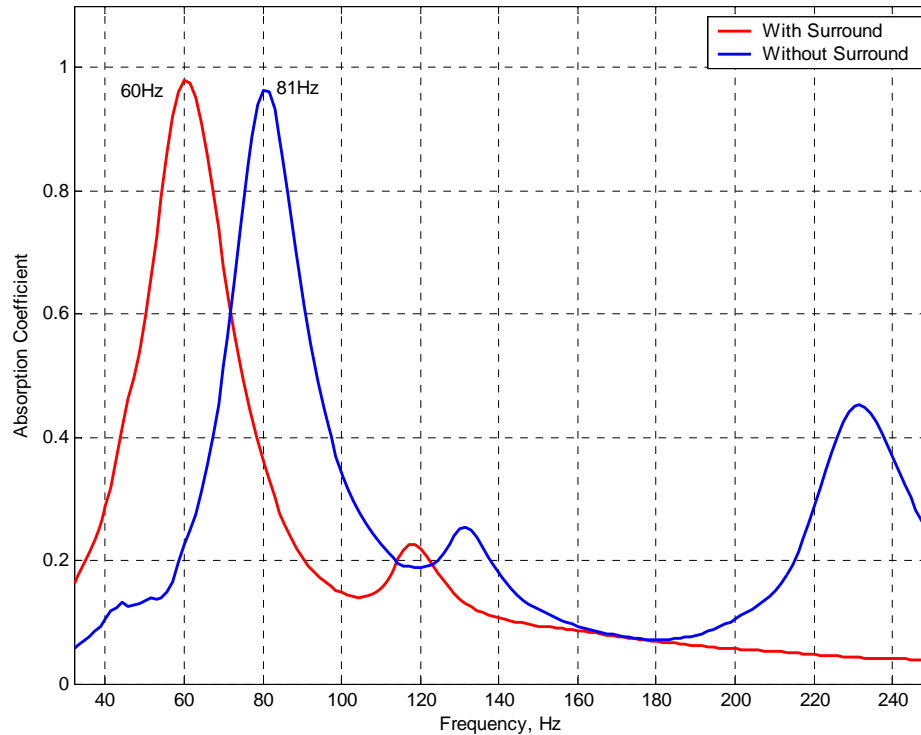
*Figure 4.7* shows clearly the shift in the fundamental resonance frequency of the system between boundary conditions approximating clamped and pistonic. The decrease in resonant frequency is approximately 38.5 Hz, a shift of some 41% confirming the theory that the difference in boundary condition does produce a lower resonant frequency of significant proportion.

### 4.3.2 Impedance Tube Tests

The impedance tube as described in chapter 3 had two sample holders of differing depths (10cm and 30cm), initial tests were carried out using the larger of the two sample holders as this had a similar volume and hence similar compliant load on the plate as the loudspeaker cabinet used for the initial accelerometer tests. The membrane was mounted on the sample holder using two rings (see photo in Appendix F) and jacked up onto the impedance tube to provide a good seal. The rings were like those used previously with the accelerometer tests as this corresponded to the similar boundary conditions, the outer diameter of the rings being larger to allow a tight fit in the tube.

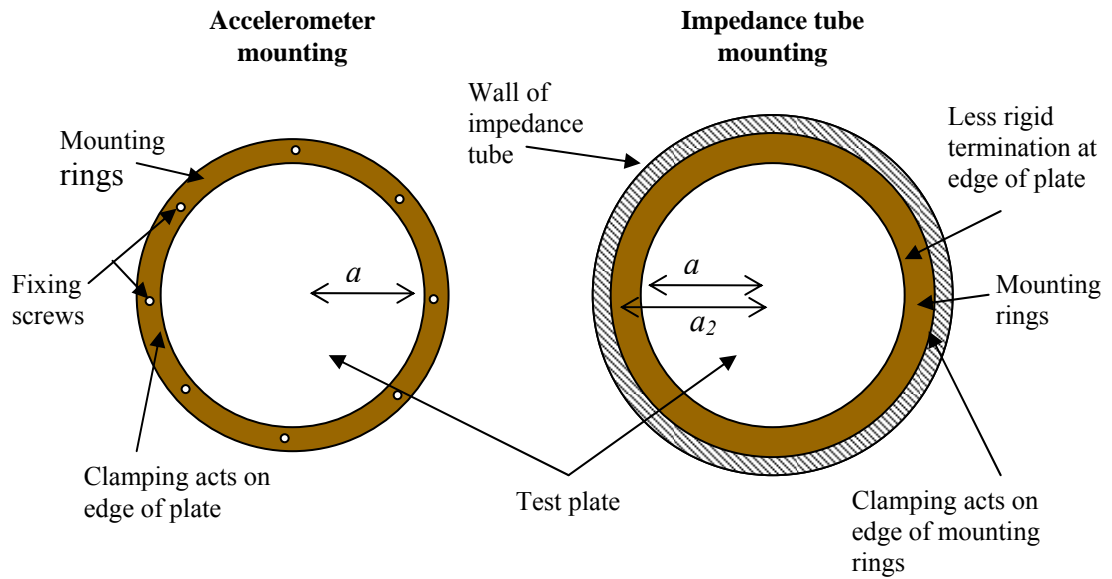
Tests were carried out using a swept sine signal at all four microphone positions and then processed using MATLAB. The tests yielded the following results:

Absorption Versus Frequency for Different Mounting Conditions Measured in Impedance Tube



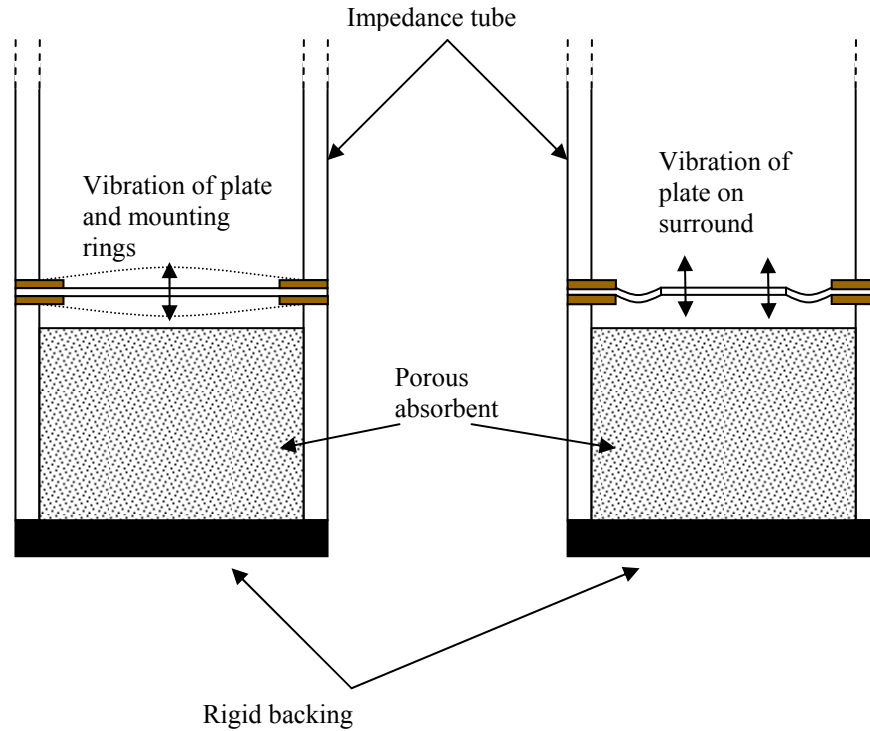
**Figure 4.8** Results from impedance tube tests with and without surround in large sample holder

*Figure 4.8* shows that when measured in the impedance tube the fundamental resonant frequency shifts 21Hz from the clamped condition, without the surround to the piston condition, with the surround. This shift in resonant frequency corresponds to a 26% decrease. This decrease is less than determined from the accelerometer tests; this is due to the differences in the cabinets that acted as the backing volume in each case. The sample holder for the impedance tube had a volume of  $0.0212\text{m}^3$  where as the loudspeaker cabinet had a volume of  $0.0434\text{m}^3$ . An increase in volume corresponds to an increase in compliance which leads to a lower resonant frequency; this explains why the case with the surround in the impedance tube resonates at a higher frequency than when tested on the cabinet with the accelerometer. A further difference seen between the two tests is that with the clamped case, measured in the impedance tube, the resonant frequency is lower than with the accelerometer tests, this is a consequence of the difference in mounting conditions as shown diagrammatically in *Figure 4.9*.



**Figure 4.9** Illustration of differing clamping conditions in accelerometer and impedance tube tests

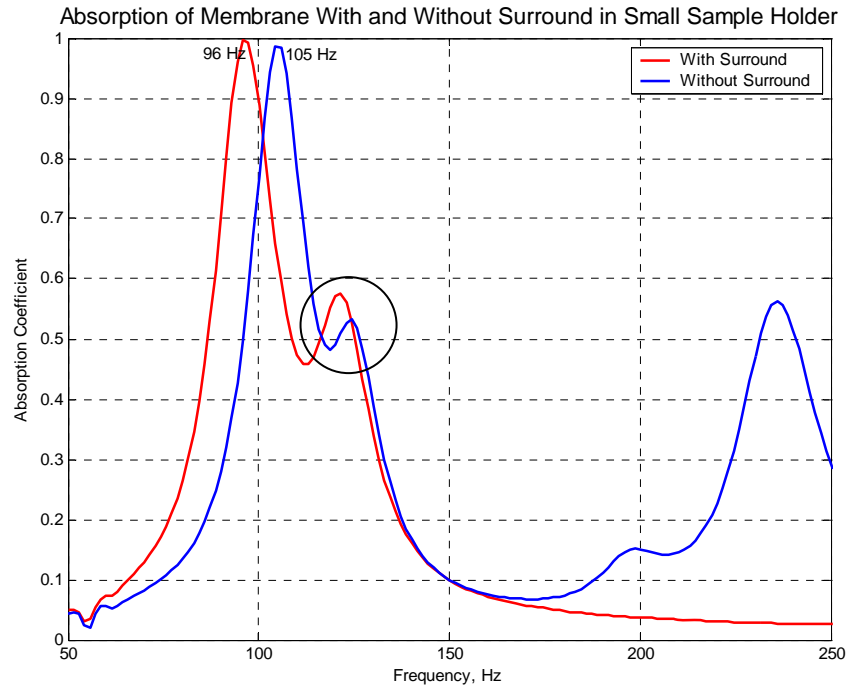
The rings used for the impedance tube tests had a wider outer diameter to account for the diameter of the impedance tube; this provided a larger surface area for reception of the incident wave. The clamping of the sample in the impedance tube acts primarily on the mounting rings rather than on the edge of the membrane, this means that the impedance at the edge of the clamped plate is less than for the accelerometer tests. The mounting rings will therefore also support bending waves (See *Figure 4.10*), thus there will be a greater moving mass, as the plate is effectively larger hence the fundamental frequency is lower in the impedance tube than with the accelerometer.



**Figure 4.10** Samples mounted in impedance tube, demonstrating how mounting rings can support modal behaviour

When the mass of the clamped plate is larger, the change in moving mass will be less when mounted pistonically, thus the frequency shift between the two will not be as great. It can therefore be deduced that the effect of adding the surround is less pronounced at lower frequencies. This is demonstrated more clearly in the tests done on a hardboard plate below.

If the plate is mounted on a cabinet of smaller volume the difference that the additional moving mass makes will be less. This can be seen when the plate was tested in the smaller of the two sample holders:



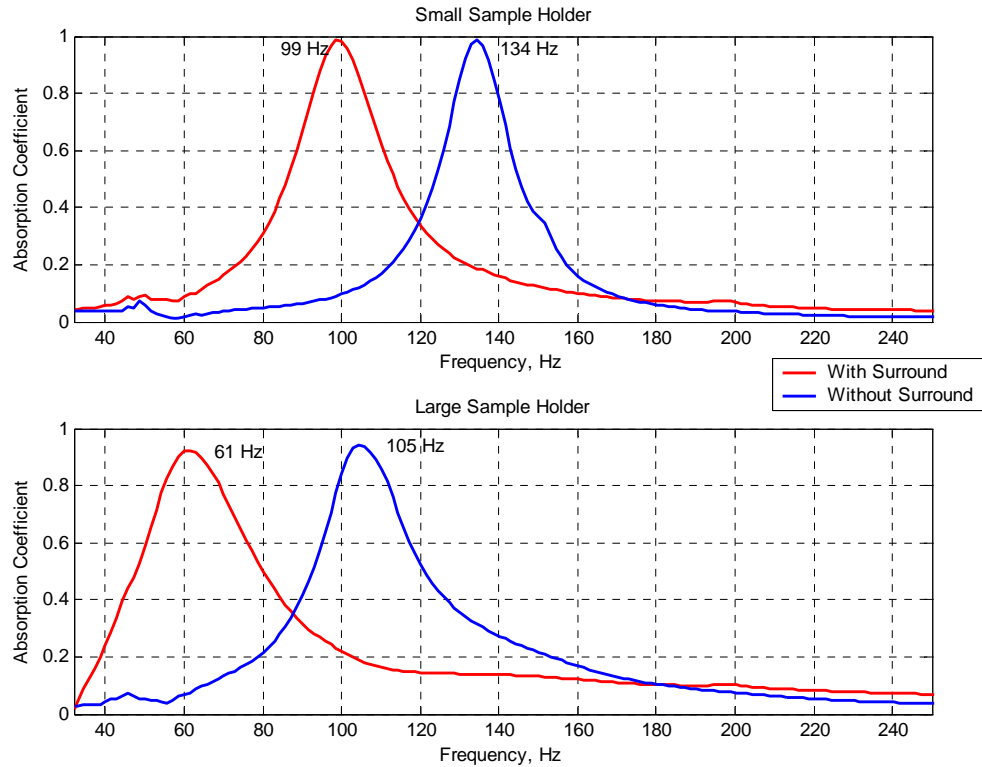
**Figure 4.11** Results from impedance tube tests with and without surround in small sample holder

*Figure 4.11* shows a frequency shift of the fundamental resonant peak of just 9Hz corresponding to shift of just 9%. Secondary peaks have been circled on the graph; these correspond to a double resonance in the material which is made up from two distinct layers. The peaks appear at higher amplitudes than with the larger sample holder case because they are closer in frequency to the fundamental mode of the membrane thus there is a modal superposition such that the combination of the two peaks results in greater amplitude at that frequency. The second resonant mode of the system as a whole can be seen at 230Hz for the clamped condition.

The tests were repeated in the impedance tube using a different material, this time it was 3mm thick hardboard that was tested, results found that the double resonance disappeared confirming that it was a consequence of the material properties rather than the test set up. Results of the hardboard tests in both the large and small sample holder are given in *Figure 4.12*.



Hardboard Tested in Small and Large Sample Holders With and Without Surround Mounting



**Figure 4.12** Results from impedance tube tests on hardboard with and without surround in small and large sample holders

Figure 4.12 shows a frequency shift of 26% for the small sample holder case and 42% for the large sample holder case. It can be observed that the surround mounted hardboard in the small sample holder resonates at a lower frequency than the clamped hardboard resonates on the large sample holder. This provides a very useful case where a membrane absorber can be constructed with much smaller dimensions whilst still retaining the low frequency performance and high absorption coefficients simply by mounting the resonating plate on a loudspeaker surround. In this case the depth of the absorber is a third as thick for with the small sample holder compared to the larger sample holder yet still resonates at a lower frequency with the surround.

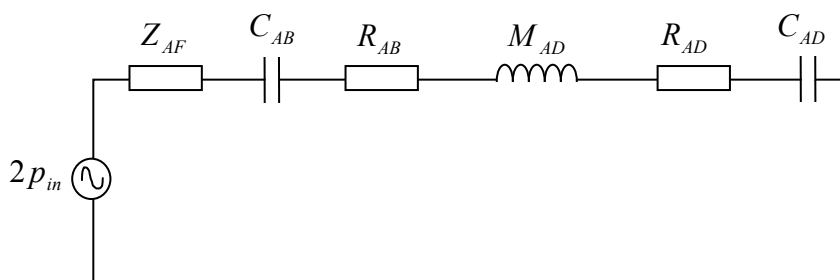
#### 4.4 Modelling

Two types of model were used in this section, an equivalent circuit model and a transfer matrix model, it was seen that the pistonic case could be modelled with a good degree of accuracy using both modelling methods. Comparisons were made between measurements and predictions using the conventional membrane absorber equations

illustrating that greater accuracy in prediction can be made when considering the pistonic rather than the clamped case.

#### 4.4.1 Equivalent Circuit Model

The theory for equivalent circuit modeling is found in section 5.3.1.1. The equivalent circuit for the absorber system described in this section is of a simpler form than that described in chapters five and six. It consists of only a mechanical and acoustical section such that the analogue circuit that describes its motion can be given as:



**Figure 4.13** Equivalent circuit for a membrane absorber

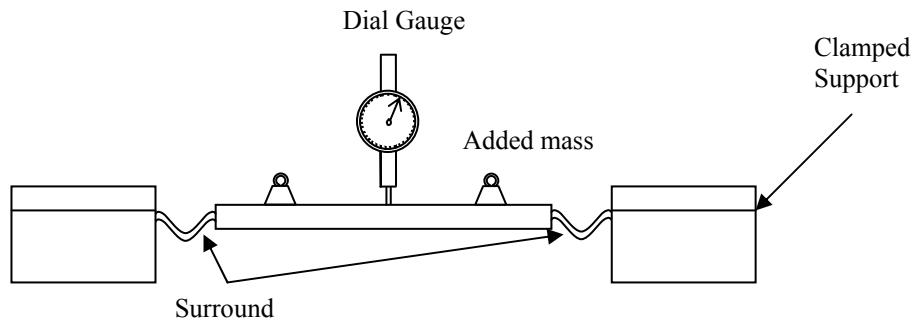
$C_{AB}$  is the compliance of the cabinet,  $R_{AB}$  is the resistive losses in the cabinet,  $M_{AD}$  is the mass of the plate,  $R_{AD}$  is the resistive losses due to the mounting of the plate,  $C_{AD}$  is the compliance of the surround and  $Z_{AF}$  is the radiation impedance which is dependent on whether the absorber is in a tube or in free field conditions (see section 5.3.3). All of the above quantities are in acoustic units.

##### 4.4.1.1 Finding Parameters

Before the above circuit can be modeled and the surface impedance found it is necessary to determine some of the constants in the system.  $M_{AD}$  is easily determined by weighing the plate,  $Z_{AF}$  is equal to  $\rho_0 c / S_D$  if the absorber is within the impedance tube or is given by equation 5.19 if in free field.  $R_{AD}$ , can be estimated from a loudspeaker model,  $R_{AB}$  is determined from the Delany and Bazley model of porous media [10] and  $C_{AB} = V / \rho_0 c^2$ .  $C_{AD}$  is the hardest to determine and requires a simple experimental procedure as described in section 4.4.1.1.1.

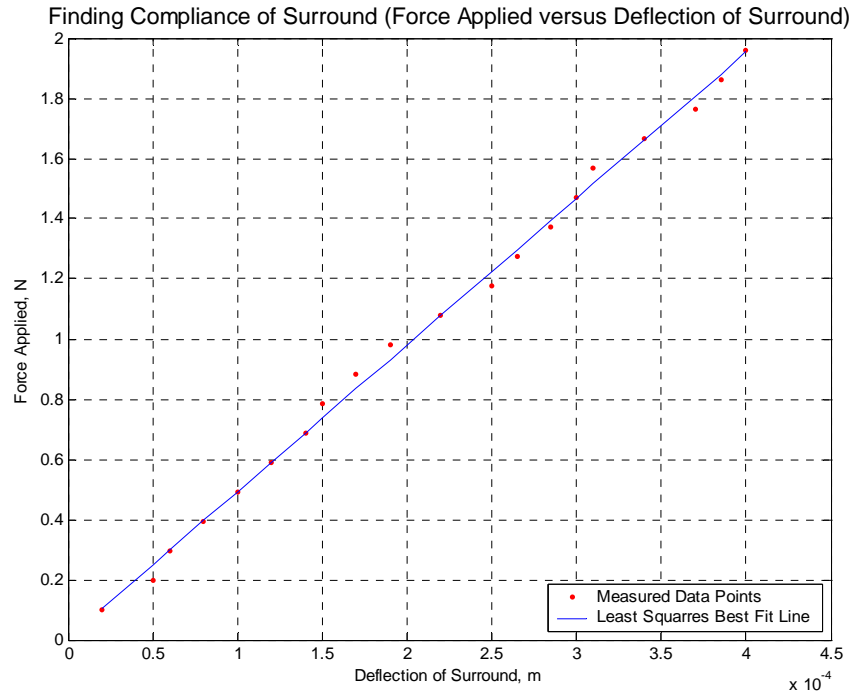
#### 4.4.1.1.1 Determining $C_{AD}$

The compliance of the surround is given by its displacement when given a force  $F$ . Assuming Hook's law the force applied to the spring (surround) should be proportional to its displacement. In order to find the stiffness of the surround and from that to determine its compliance the following test set up was used:



**Figure 4.14** Experimental setup for measuring compliance of surround

Incremental changes in the mass applied to the plate displaced the surround, the displacement was then measured to a hundredth of a millimeter by the dial gauge which was held with a clamp stand to keep it from moving. Masses were positioned carefully such that equal force was applied to the entire surround. The plate used was rigid hardboard so it was only the compliance of the surround being measured rather than that of the plate itself. A graph as shown in *Figure 4.15* was plotted of force applied versus displacement from which the stiffness and hence the compliance could be found.



**Figure 4.15** Results from experiment to determine compliance of surround

A regression analysis was performed on the measured data and the corresponding best fit line plotted. The gradient of the best fit line gives the stiffness of the surround, the reciprocal of which gives the compliance. The compliance of the surround was found to be:

$$C_{AB} = 205.49 \pm 2.59 \mu\text{mN}^{-1} \quad (4.2)$$

The percentage error in this measurement is given as 1.26% which is significantly less than the 10% error often quoted as the error in the compliance as measured by MLSSA in the added mass method of small-signal parameters [26] (see section 5.3.3).

Having determined the parameters governing the pistonic case the equivalent circuit can be solved easily. The equivalent circuit for the clamped case is the same but deriving the compliance and mass are difficult and as such an equivalent piston of the plate can be considered.

#### 4.4.1.1.2 Finding the Equivalent Piston of a Clamped Plate

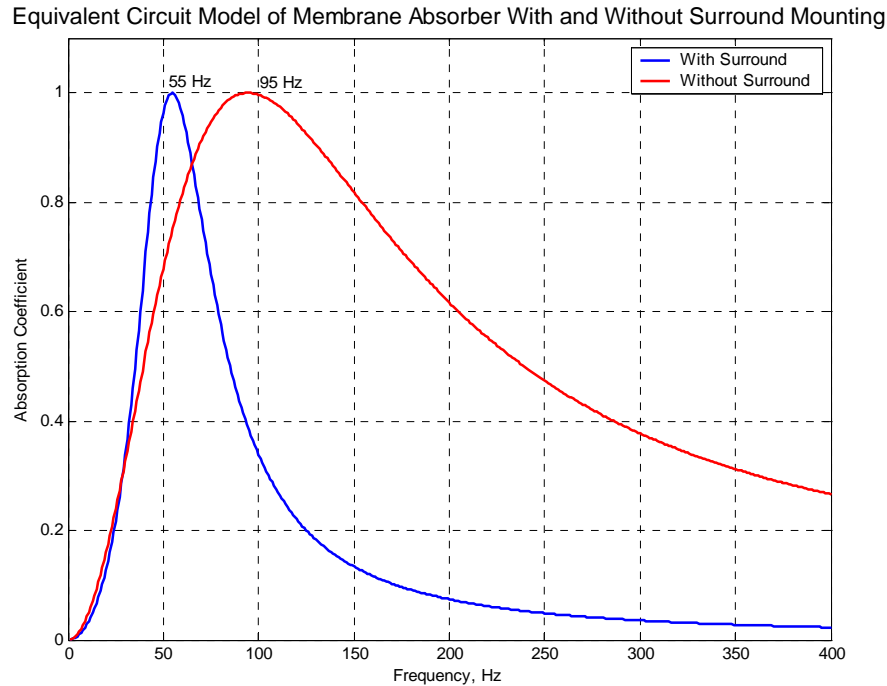
Assuming a clamped plate with a Poisson ratio,  $\mu$  thickness,  $h$  and Young's modulus,  $E$  it is possible to determine the equivalent mass and compliance of the plate as an equivalent piston. Rossi [27] presents such theory. By calculating the kinetic and potential energy of the plate as it is deflected by the standard parabolic deflection and integrating over its area it is possible to find an equivalent mass and compliance as if the plate were a pistonic resonator. Rossi gives the equivalent mass as one fifth of the mass of the clamped plate and the compliance as:

$$C_{ME} = \frac{180(1 - \mu^2)a^2}{Eh^3} \quad (4.3)$$

These values can be put into the equivalent circuit model such that the pistonic case can be compared with the clamped case.

#### 4.4.1.2 Results

The equivalent circuit was implemented in MATLAB using the code in Appendix G plotting the equivalent circuit for the pistonic case and the clamped condition yields *Figure 4.16*. The scenario that was modeled was the same as with the initial accelerometer tests so as to eliminate the uncertainties in the boundary conditions of the mounting rings:

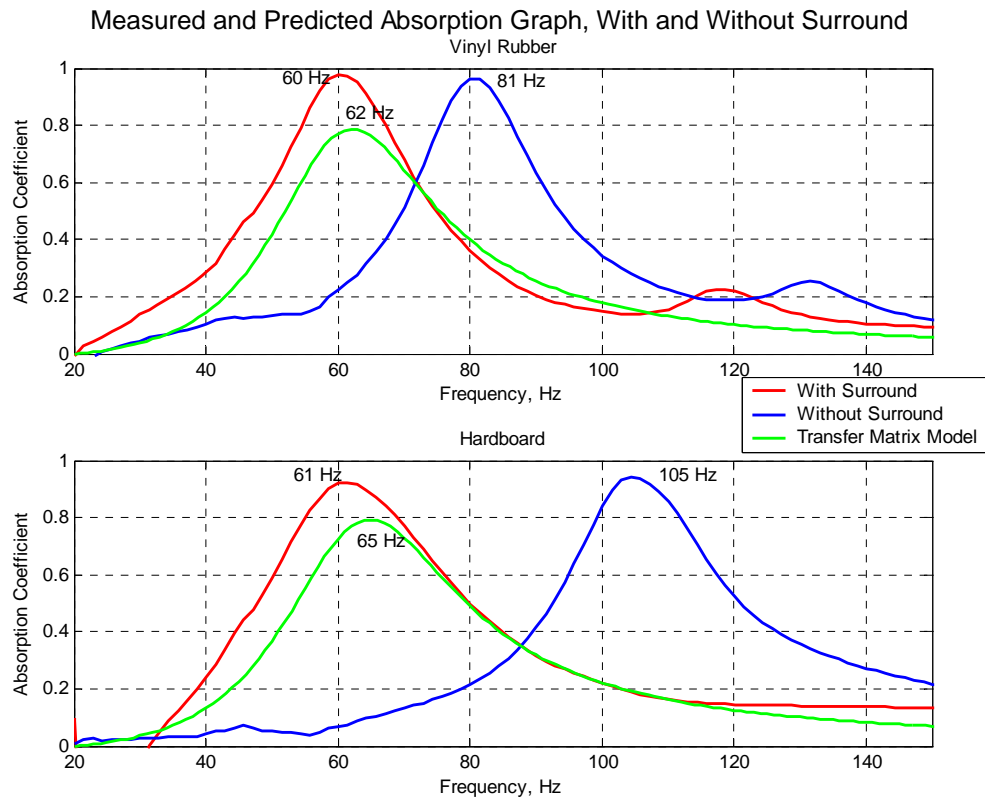


**Figure 4.16** Absorption curve from equivalent circuit model of membrane with and without surround

The model accurately predicts the resonant frequency of both cases suggesting that the change in frequency is almost entirely due to the increase in moving mass of the membrane as a result of the surround mounting. The model demonstrates that the equivalent piston for the vibrating plate can be used to predict the resonant frequency but not the overall absorption of the system as it shows large inaccuracies in prediction of the absorption bandwidth. These inaccuracies result because a plate is a complex element, the equivalent piston model calculated an equivalent compliance and mass assuming the plate was at its fundamental resonance so outside of that range it is unsurprising that the model is inaccurate.

#### 4.4.2 Transfer Matrix Model

A transfer matrix model was formulated using the principles described in section 2.4.2.1.1. The MATLAB script can be found in Appendix H. Results were compared to values as measured in the impedance tube for both the vinyl rubber case and the hardboard case.



**Figure 4.17** Comparison of measured absorption curves with predictions from a transfer matrix model

*Figure 4.17* demonstrates that the accuracy of the transfer matrix modeling approach is far better when predicting the lumped mass pistonic case than with the clamped condition. It illustrates well the problems that are often encountered when designing membrane absorbers to resonate at a specific frequency. Models are often inaccurate which is often due to uncertainties in mounting conditions of the resonating mass. When the plate is mounted on the loudspeaker surround the accuracy of the transfer matrix model increases greatly, thus using a loudspeaker surround will aid accuracy in predicting its performance at the design stage.

Results obtained in this section can also be compared with predictions of resonant frequency from the simple design equation often used for membrane absorbers mentioned in section 2.4.2.1. Applying equation 2.30, to the above examples yields resonant frequencies of 65.3 Hz for the vinyl plate ( $M = 2.81\text{kgm}^{-2}$ ) and 68.3 Hz for the hardboard plate ( $M = 2.57\text{kgm}^{-2}$ ). These match up favourably with the pistonic case but not the clamped case again confirming that greater accuracy in predictions can be

achieved when using a pistonic lumped mass rather than a clamped plate as the mass of a membrane absorber.

#### **4.5 Conclusion**

Two mounting conditions of a membrane absorber have been considered, firstly a clamped case as is typical of most membrane absorbers and secondly a pistonic mounting condition with the use of a loudspeaker surround. Tests were initially performed with an accelerometer on the membrane and results showed a significant decrease in resonant frequency with the membrane mounted on the surround. Further tests were carried out with the low frequency impedance tube confirming the findings of the accelerometer tests. It was shown the decrease in resonant frequency was a result of the increased moving mass introduced by the surround. These effects were more pronounced when the compliance of the cavity was greater i.e. the backing volume was larger and when the initial mass was smaller. Tests demonstrated that frequency shifts in excess of 40% could be obtained by using a surround mounting in preference of a standard clamped condition. It was also shown that a membrane absorber utilising a loudspeaker surround on the small sample holder (a third of the volume of the larger one) could produce a lower resonant frequency than the clamped case using the larger sample holder. This illustrates a significant improvement in the low frequency performance of membrane type absorbers.

An equivalent circuit model was presented, demonstrating that the difference in resonant frequency was indeed a result of the increased moving mass. The model included equivalent mass and stiffness terms of a clamped plate moving as a piston. The pistonic mass modelled as one fifth of the mass of the clamped plate and the compliance as a function of the material constants, Poisson ratio and Young's modulus. The equivalent circuit model predicted accurately the resonant frequency of both clamped and pistonic cases, but approximating the clamped plate as an equivalent piston lead to inaccuracies in predicting the broadband absorption characteristics. A transfer matrix model was also demonstrated showing that the pistonic case could be modelled to a much better degree of accuracy than the clamped case thereby aiding the design of membrane absorbers such that a trial and error approach need not be employed. The Standard membrane absorber design equations were also shown to produce more accurate results for the surround mounted condition.



## **5. USING A LOUDSPEAKER AS A RESONANT ABSORBER**

### **5.1 Introduction**

Having outlined the theory and practice of using a loudspeaker surround as the mounting for a membrane absorber, a logical progression is to attempt to use the entire loudspeaker system as part of the resonant absorber. This is a topic that has been considered previously by Sato and Koyasu [28] although in this case it was the incidental absorption of low frequencies by obsolete loudspeakers within a room, seen as a problem rather than a solution that was considered.

This section aims at the purposeful use of loudspeakers as absorber systems. A loudspeaker within an enclosure very closely approximates a membrane absorber, the

diaphragm as the resonating mass, the compliance of the enclosure as the restoring spring and porous material within the enclosure providing additional damping. Using a loudspeaker as an absorber has several advantages. Firstly loudspeakers already oscillate naturally, as designed, in a pistonic manner allowing the increased low frequency performance and accurate predictions outlined in the previous chapter. Secondly, loudspeakers are cheap and readily available for rudimentary acoustic treatment. Thirdly, and possibly the greatest advantage of using a loudspeaker, is that it is an electromagnetic system, hence the electrical and magnetic coefficients of the system will affect its mechanical behaviour according to Faraday's laws of electromagnetism. This has the consequence of allowing the system to be tuned to a specific resonant frequency, within certain bounds, simply by the addition of resistive and reactive electrical components across the terminals of the driver, an idea previously applied to the field of loudspeaker design [29]; this is the focus of chapter six. For now the simple case of a passive loudspeaker with no additional electronic components is considered as an absorber system.

A lumped element prediction model of a loudspeaker used as an absorber is first presented in this chapter followed by results from impedance tube measurements that confirm the predicted data, demonstrating a loudspeaker-absorber that achieves high absorption coefficients within its resonance region.

## **5.2 Basic Premise from Loudspeaker Theory**

Most loudspeakers work by supplying a varying current  $i$  to a coil of wire length  $l$  within a magnetic field of flux density  $B$  which consequently induces a force  $F = Bil$  on the coil. If some kind of diaphragm is attached to this coil, air is driven into motion causing small localised pressure changes thus producing an audible output. Using a loudspeaker as an absorber uses this system in reverse, similar to a moving coil microphone. Alternating acoustic pressures incident to the diaphragm force it into oscillatory motion thus moving the coil in the magnetic field inducing a voltage in the connected circuitry. As with a typical membrane absorber the system will have a characteristic resonant frequency governed by its mechanical and acoustical properties, such as the volume of the enclosure, stiffness of springs and the mass per unit area of

the membrane. Its resonant characteristics will however also be dependent on its electrical and magnetic coefficients giving the loudspeaker-absorber an extra dimension.

To predict the behaviour of this absorber system a standard lumped parameter technique for loudspeaker analysis can be used. In the next section such a model is presented and used to analyse the behaviour of the absorber.

### **5.3 Lumped Parameter Modelling**

Acoustical systems can contain up to three spatial dimensions the components of which all can change temporally. This leads to very complicated solutions obtainable by the three dimensional wave equation. In the case of the loudspeaker, there is the added complication of the coupling between the mechanical and electrical systems. Solutions using techniques such as Finite Element Analysis can be time consuming and difficult, consequently it is highly desirable to simplify problems such that they can be manipulated and solved more easily. The theory of lumped parameter or lumped element modelling enables such simplification [30].

#### **5.3.1 Theory**

If the acoustic wavelength in a fluid, such as air, is assumed to be much larger than one dimension of the system of interest, that dimension need not be considered in calculations as pressure and velocity are assumed to be constant across it. The problem therefore is reduced in complexity by elimination of that variable. The application of this assumption to the acoustics of ducts means that if the diameter of a duct is small enough with respect to wavelength, plane wave propagation can be assumed down the duct, this gives rise to the high frequency limit imposed on impedance tubes. Above a given frequency the acoustic wavelength in air becomes comparable with the dimensions of the tube and hence propagation can no longer be considered only in the direction of the tube's length but also across its width so the plane wave simplification can not be accurately applied; a more complex propagation model would need to be considered not making a plane wave assumption.

If this low frequency assumption is taken further, and the wavelength becomes much larger than all of the dimensions of the device, although varying temporally, each acoustic variable can be considered constant in the all three directions of the spatial domain, i.e. pressure and velocity are constant across all of its dimensions at a given moment in time. If these conditions are applied, the equation of motion is greatly simplified, such that any spatial dependency is removed, reducing the problem to that of only a single degree of freedom variant only with time. When these conditions are assumed the components of the system can be considered as a lumped elements or lumped parameters. This is a common engineering technique and is used extensively in loudspeaker design and modelling [31, 32].

A major advantage of using a lumped element method is that it is very easy to draw a schematic representation of a system utilising analogies between mechanical, acoustical and electrical components; this is common practice for engineers and allows each section to be represented as an electrical, mechanical or acoustical diagram. Electrical circuits are commonly chosen as the schematic representation because electrical circuit theory is widely known and understood throughout many spheres of science and engineering. Drawing a schematic diagram means that the differential equations governing a given system can be easily determined and solved on inspection. This is relatively simple if the spatial variables are removed however if the spatial dimensions are re-introduced for smaller wavelengths or larger devices the differential equations become very complicated and it becomes profitable to revert to elementary acoustics and the solution of the wave equation again. As such there is a high frequency limit imposed on the use of lumped parameter models, which states that the highest frequency should have a wavelength greater than all the dimensions of the system being modelled [27].

#### 5.3.1.1 **Equivalent Circuits**

The premise behind the theory of equivalent circuits is to represent a physical situation, be it mechanical or acoustical, in the form of an electrical circuit. In order to successfully do this it is necessary to define analogies between electrical, mechanical and acoustical domains such that the equivalent circuits retain their integrity. The

following, briefly describes two commonly used analogies for the purpose of equivalent circuit analysis, these are the impedance and mobility analogues.

In terms of electrical oscillations (of great importance in the field of electroacoustics) there are three principle electronic components each one either storing or dissipating energy:

- Inductors  $L_E$ , store magnetic energy (flux)
- Capacitors  $C_E$ , store electrical energy (charge)
- Resistors  $R_E$ , dissipate energy

If the current is known, an expression for the potential difference across each component can be formed such that:

$$v = L_E \frac{di}{dt}, \quad v = \frac{\int i \cdot dt}{C_E}, \quad \text{and} \quad v = R_E i \quad (5.1)$$

Assuming a sinusoidal input current,  $i = i_0 e^{j\omega t}$  the impedance of these components can be determined as:

$$\begin{aligned} v_0 e^{j\omega t} &= i_0 e^{j\omega t} j\omega L & v_0 e^{j\omega t} &= \frac{i_0 e^{j\omega t}}{j\omega C} & Z &= \frac{v}{i} = R \\ Z &= \frac{v}{i} = j\omega L & Z &= \frac{v}{i} = \frac{1}{j\omega C} & & \end{aligned} \quad (5.2)$$

Analogous to these three electrical components of oscillation are three mechanical oscillatory components:

- Mass  $M_M$ , stores kinetic energy
- Compliance  $C_M$ , stores potential energy
- Frictional resistance (damping)  $R_M$ , dissipates energy

For the mechanical case, velocity  $u$  is the flow variable so can be thought of as analogous to electrical current and force  $F$  is the potential variable and can be thought of as analogous to voltage. In the same way as for the electrical components, if the velocity of each section in the mechanical components is known and assumed to be sinusoidal, the force across, and the impedance of the components can be determined by the following equations:

$$\text{From Newton's law of force } F_M = M_M \frac{du}{dt} \text{ and } Z_M = j\omega M_M$$

$$\text{From Hook's law } F_M = \frac{\int u \cdot dt}{C_M} \text{ and } Z_M = \frac{1}{j\omega C_M}$$

$$\text{From classical mechanics } F_M = R_M u \text{ and } Z_M = R_M$$

(5.3)

Aside from Newton's law of force which is universally valid, these are only first order approximations and therefore are more accurate when small displacements are considered, with larger displacements the system is no longer linear which complicates matters and lumped parameter analysis is no longer valid.

In both the electrical and mechanical cases, the components are assumed to be ideal, so that, an inductor has no capacitance or resistance and conversely a compliance has no mass *et cetera*. This is a useful first approximation and extra components can be added to a model to account for the fact that they are not in fact ideal, Rossi [27] provides a more extensive analysis this topic looking at the equivalent mass of an ideal compliance *et cetera*. In most situations the elements in the circuit can be considered as 'lumped' such that no mechanical or acoustical component exhibits any wave motion within the element.

As with mechanical values there are three acoustical quantities that pertain to the oscillatory electrical components such that:

- Acoustic mass or inertance  $M_A$ , stores kinetic energy
- Acoustic compliance  $C_A$ , stores potential energy
- viscous damping  $R_A$ , dissipates energy

In the acoustic case, volume velocity  $U$  is the flow variable (analogous to current) and pressure  $p$  is the potential variable (analogous to voltage). Therefore if the volume velocity through a component is known then it is possible to calculate the pressure by across the components given a sinusoidally oscillating volume velocity by:

$$p = M_A \frac{dU}{dt} \text{ therefore } Z_A = j\omega M_A$$

$$p = \frac{\int U \cdot dt}{C_A} \text{ therefore } Z_A = \frac{1}{j\omega C_A}$$

$$p = R_A U \text{ therefore } Z_A = R_A$$

(5.4)

Combining these analogies leads to the impedance analogue which can be summarised by Table 5.1:

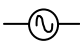
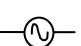

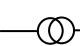
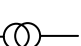
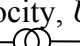
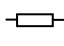


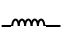


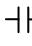
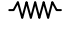

Impedance Analogue			
	Electrical	Mechanical	Acoustical
<b>Potential Variable</b>	Voltage, $e$ 	Force, $F_M$ 	Pressure, $p$ 
<b>Flow variable</b>	Current, $i$ 	Velocity, $u$ 	Volume velocity, $U (= u \times S)$ 
<b>Dissipative component</b>	Resistance, $R_E$ $Z_E = R_E$ 	Damping, $R_M$  $Z_M = R_M$	Acoustic damping, $R_A$  $Z_A = R_A$
<b>Kinetic storage component</b>	Inductance, $L_E$ $Z_E = j\omega L_E$ 	Mass, $M_M$  $Z_M = j\omega M_M$	Acoustic mass, $M_A$  $Z_A = j\omega M_A$
<b>Potential storage component</b>	Capacitance, $C_E$ $Z_E = 1/j\omega C_E$ 	Compliance, $C_M$ $Z_M = 1/j\omega C_M$ 	Acoustic compliance $C_A, Z_A = 1/j\omega C_A$ 

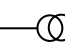
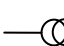
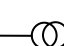
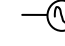
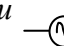

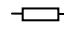


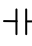
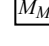

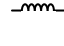
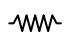

Table 5.1 Summary of the impedance analogue

This impedance analogue is very useful and can be used to model many practical scenarios. Using Kirchoff's current and voltage laws it simply a matter of whether to connect components in parallel or series. Another analogy also exists which makes use

of the reciprocity of electrical components that is to say that an inductor behaves to current how a capacitor behaves to voltage and vice versa, i.e.:

$$i = C_E \frac{de}{dt} \text{ and } e = L_E \frac{di}{dt} \quad (5.5)$$

This leads to another analogy which is the reciprocal of the impedance analogy and consequently called the mobility analogue, so that inductors become capacitors and vice versa and resistances become conductances (a reciprocal resistance). Any components that were connected in series will consequently need to be connected in parallel and any in parallel connected in series in order to obey Kirchoff's laws. This analogy can be seen as the direct opposite to the impedance analogue and can be surmised in the following in *Table 5.2*. Because they are complete opposites of each other, the results yielded by both analogies will be identical. The impedance analogue is more intuitive, however it is useful especially in the analysis of loudspeakers to use both impedance and mobility analogues as it makes combining the circuits somewhat easier as will be seen later:

<b>Mobility Analogue</b>			
	<b>Electrical</b>	<b>Mechanical</b>	<b>Acoustical</b>
<b>Potential Variable</b>	Current, $i$ 	Force, $F_M$ 	Pressure, $p$ 
<b>Flow variable</b>	Voltage, $e$ 	Velocity, $u$ 	Volume velocity, $U (= u \times S)$ 
<b>Dissipative component</b>	Conductance, $1/R_E$ $Z_E = 1/R_E$ 	Damping, $R_M$ $Z_M = 1/R_M$ 	Acoustic damping, $R_A$ $Z_A = 1/R_A$ 
<b>Kinetic storage component</b>	Capacitance, $L_E$ $Z_E = 1/j\omega L_E$ 	Mass, $M_M$ $Z_M = 1/j\omega M_M$ 	Acoustic mass, $M_A$ $Z_A = 1/j\omega M_A$ 
<b>Potential storage component</b>	Inductance, $C_E$ $Z_E = j\omega C_E$ 	Compliance, $C_M$ $Z_M = j\omega C_M$ 	Acoustic compliance $C_A, Z_A = j\omega C_A$ 

*Table 5.2* Summary of the mobility analogue

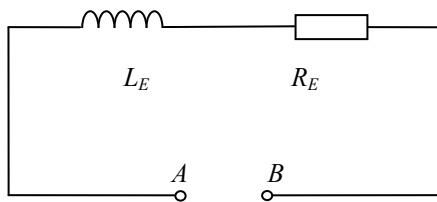


### 5.3.2 Analysis

Subsequent analysis shows how the absorber system can be modelled easily with the use of lumped elements and equivalent circuits. Analysing electrical, mechanical and acoustical sections in turn to derive individual equivalent circuits and then combining the three into a single circuit diagram allows the complex surface impedance of the absorber to be predicted and as such, calculation of the systems reflection factor and absorption coefficient.

#### 5.3.2.1 Electrical Section

Electrically, a loudspeaker consists simply of an alternating current through a coil of wire in the presence of a magnetic field, thus it can be considered as an inductor with inductance,  $L_E$  and associated resistance,  $R_E$ . In electrical terms the loudspeaker can be simplistically modelled by *Figure 5.1*:



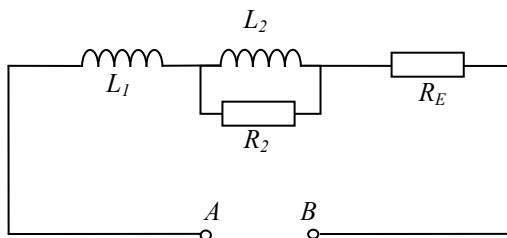
**Figure 5.1** Simple representation of the electrical section of a loudspeaker

The impedance of the above circuit is a combination of the resistive and reactive parts such that the electrical impedance is given by:

$$Z_E = j\omega L_E + R_E \quad (5.6)$$

In a loudspeaker the terminals,  $A$  and  $B$  would be connected to a sound source i.e. an AC voltage generator of some description. In the absorber system however the terminals can be either left open circuit, connected together or connected across a complex passive load impedance, this will alter the frequency response of the electrical circuit and will consequently change the impedance presented to the induced current, altering the mechanical properties of the system. This will be seen in greater detail in the next chapter.

In many loudspeaker applications the model of the electrical section shown in *Figure 5.1* is used and is adequate; in fact in many cases the inductance of the voice coil  $L_E$  is even ignored as it is predominantly a high frequency component, therefore, in order to make the modelling more simple it is often omitted from the circuit. In the next chapter small changes are made to this motor impedance with the addition of further electronic components, it is important therefore to insure that the base motor impedance is predicted to the highest degree of accuracy so the effect of the additional components can be quantified precisely. There are more complicated models available of a loudspeaker's motor impedance (electrical section) as demonstrated by Wright [33] who included additional variable resistance and inductance terms which allow the accurate prediction of impedance up to higher frequencies; other models take into account eddy currents within the voice coil [34]. The model chosen for this application however comes from the MLSSA SPO manual [26] ] where the motor impedance is represented such that the voice coil resistance,  $R_E$  is in series with an inductance modelled as an inductor,  $L_1$  in series with a lossy inductance  $L_2||R_2$ . In this case the circuit becomes as *Figure 5.2*.



*Figure 5.2* More complicated representation of the electrical section of a loudspeaker

This model is more accurate at higher frequencies, it was chosen for this application because it is the model used by the MLSSA SPO module to obtain the Thiele/Small parameters of loudspeakers (see section 5.3.3).

### 5.3.2.2 Mechanical Section

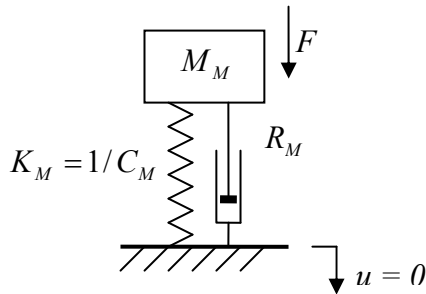
Mechanically a loudspeaker is simply a diaphragm (a paper cone) which is set into motion by an electromotive force. There is also a spring in the system consisting of the spider and the surround of the loudspeaker bringing the cone back to its position of

equilibrium each time it is displaced. The spider works at the apex of the cone and the surround on the outside of the cone ensuring equal force is applied to all areas of the cone with no phase lag of the combined restoring force. The diaphragm of a loudspeaker is conical in a shape to increase its stiffness in the plane normal to the intended motion; this ensures that it moves backwards and forwards as a piston. That the diaphragm moves with pistonic oscillation is an important assumption to make as it eliminates the need to model complex bending waves on the diaphragm that appear at higher frequencies otherwise known as ‘cone break up’. Attempting to model a loudspeaker using lumped parameter techniques at higher frequencies will lead to spurious results as bending waves alter both the moving mass and the compliance of the diaphragm making it a nonlinear system. For lower frequency radiation however the pistonic assumption is valid and enables accurate predictions.

A magnetic field is generated by a large permanent magnet which is held in place by a chassis so as not to put a load on the diaphragm. As a consequence of this magnetic field, the induced movement of the cone is governed in frequency and magnitude by the frequency and strength of the alternating current that is applied across the terminals. The absorber system uses the loudspeaker in reverse to induce a current in the voice coil given oscillation of the diaphragm in sympathy with an acoustic pressure. As with a standard membrane absorber the cone will generate a particle velocity in the cabinet which is then absorbed by porous material. The absorber will have a resonant frequency inherently controlled by the moving mass of the diaphragm and the stiffness of the spring (both the mechanical suspension compliance and the compliance of the air volume within the cabinet). This enables the resonant frequency to be altered by changing these parameters, however this is awkward as it involves rebuilding the entire absorber using different materials and geometry, and this is obviously rather impractical. It is possible however to use the electrical section of the absorber to change the resonance in the mechanical domain. The induced current will be impeded by the electrical components  $L_1$ ,  $L_2$ ,  $R_2$ ,  $R_E$  and those connected across terminals  $A$  and  $B$  as seen from *Figure 5.2*. These components have a frequency dependence of their own, thus the electrical impedance will be larger at some frequencies than at others enabling the induced current to flow more easily at some frequencies. Mechanically the system will oscillate with greater amplitude when the impedance to the induced current is at a

minimum and as such the electrical section will have ramifications on the resonance properties of the entire system.

Considering just the mechanical section of the loudspeaker it can be seen that with the diaphragm moving pistonicly, on the combined compliance it can be represented simply as a mass on a spring as in *Figure 5.3*:



**Figure 5.3** Mechanical representation of a loudspeaker

The mass  $M_M$  moves on a spring with stiffness  $K_M$  and compliance  $C_M$ , there is also some inherent damping in the mechanical system  $R_M$  which comprises of losses within the mounting and suspension of the diaphragm. The above system can be easily solved using differential equations, such that the equation of motion becomes:

$$F = M_M \frac{du}{dt} + R_M \dot{u} + K_M \int u \cdot dt \quad (5.7)$$

Assuming sinusoidal oscillation,  $F = F_0 e^{j\omega t}$  and  $u = u_0 e^{j\omega t}$

$$F_0 e^{j\omega t} = j\omega M_M u_0 e^{j\omega t} + R_M u_0 e^{j\omega t} + \frac{1}{j\omega C_M} u_0 e^{j\omega t}$$

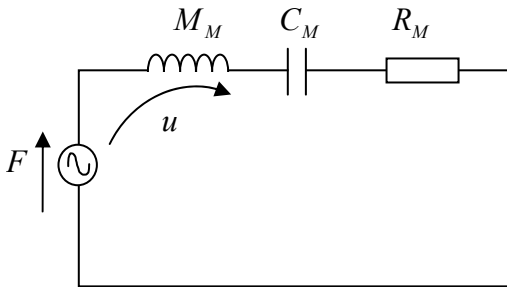
$$F = j\omega M_M u + R_M u + \frac{1}{j\omega C_M} u \quad (5.8)$$

Mechanical impedance can be written as  $Z_M = F/u$  therefore the total mechanical impedance of the above system is:

$$Z_M = j\omega M_M + R_M + \frac{1}{j\omega C_M}$$

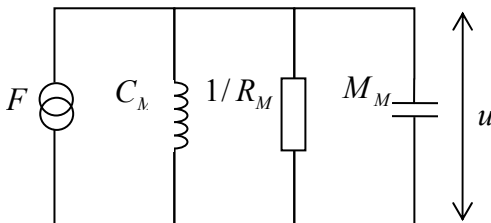
(5.9)

This is the expected result which can also be obtained by modelling the scenario with the impedance analogue leading to the equivalent circuit shown in *Figure 5.4*. This impedance is in the same format as an electrical impedance with an inductor a resistor and a capacitor.



**Figure 5.4** Impedance analogue circuit of the mechanical section of a loudspeaker

The same mechanical system can be modelled with the mobility analogue as the reciprocal of *Figure 5.4* such that the circuit becomes as *Figure 5.5*:



**Figure 5.5** Mobility analogue circuit of the mechanical section of a loudspeaker

The impedance of this circuit can be determined as follows:

$$\frac{1}{Z_{Tot}} = \frac{1}{Z_1} + \frac{1}{Z_2} \dots + \frac{1}{Z_n}$$

$$\frac{1}{Z_{Tot}} = \frac{1}{j\omega C_M} + j\omega M_M + R_M$$

(5.10)

Note that this admittance/mobility in *Figure 5.5* is the same as the impedance of the circuit in *Figure 5.4*. One circuit therefore is said to be the ‘dual’ of the other. Both circuits can be used to determine the velocity and the force and yield the same results.

The mechanical system will resonate when the imaginary part becomes zero therefore the resonant frequency can be calculated using equation 5.11:

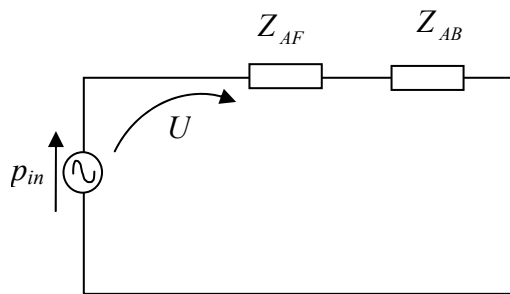
$$j\omega M_M + \frac{1}{j\omega C_M} = 0$$

$$\omega = \frac{1}{\sqrt{M_M C_M}}$$
(5.11)

Resistive losses will affect only the Q-factor of the resonant curve.

### 5.3.2.3 Acoustical Section

For the acoustical section it is assumed that the incident acoustic wave (alternating pressure source) causes the same volume velocity at both the front and back of the diaphragm each providing a complex impedance load as such the circuit can be represented in with the impedance analogue by *Figure 5.6*.

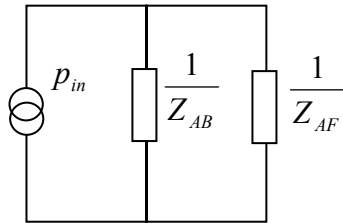


**Figure 5.6** Impedance analogue circuit of the acoustical section of a loudspeaker

$Z_{AF}$  and  $Z_{AB}$  are the impedance at the front and back of the diaphragm respectively. The impedance at the back of the diaphragm is the easier of the two to determine; it consists predominantly of the compliant air load of the cabinet,  $C_A$  and the resistive damping provided by the porous absorbent,  $R_A$ .  $Z_{AF}$  is the radiation impedance as a result of the air load in front of the absorber and it depends on what space the absorber

‘radiates’ into. When in free space the impedance at the front of the diaphragm is a combination of an acoustic mass term and a resistive air load on the diaphragm given by the radiation impedance of a baffled piston as in equation 5.19.  $Z_{AF}$  is less complicated if the absorber radiates in tube with plane wave propagation as is modelled in subsequent sections for comparison with impedance tube tests. In this case the mass term disappears and the radiation impedance can be given by equation 5.20. Greater detail will be paid to these terms in section 5.3.3.

The mobility analogue can also be used to represent the system as an electrical circuit. Pressure becomes the flow variable (current), volume velocity the potential variable (voltage).

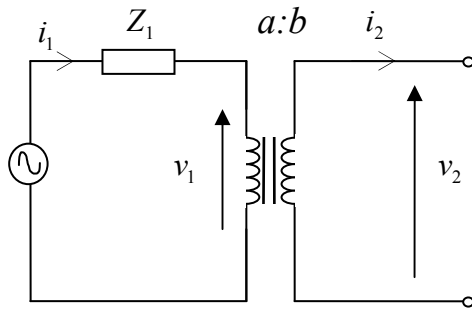


**Figure 5.7** Mobility analogue circuit of the acoustical section of loudspeaker used as a membrane absorber

#### 5.3.2.4 Combining the Sections

Once all of the sections have been individually derived it is important to link them together correctly, this is done using ideal transformers forming an electrical link between the circuits enabling each section to be written in the same units so the overall impedance of the system can be determined from a combined circuit of all three sections.

Ideal transformers are electrical transformers where there is assumed to be no losses in the coils, i.e. they have negligible resistance and inductance such that all power is conserved. Therefore for the transformer in *Figure 5.8*  $v_2a = v_1b$  and  $i_1a = i_2b$ .



**Figure 5.8** Idealised transformer

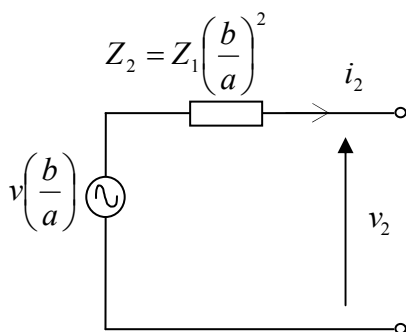
In order to calculate the output voltage,  $v_2$  when multiplying out the transformer it is simply a matter of multiplying the input voltage,  $v_1$  by the turns ratio ( $a/b$ ) and to determine the current in the secondary circuit, the input current is divided by this turns ratio. With this in mind the equivalent impedance,  $Z_2$  in *Figure 5.9* can also be determined when multiplying out the transformer to form a single circuit such that:

$$Z_1 = \frac{v_1}{i_1} = \frac{v_2 \left(\frac{a}{b}\right)}{i_2 \left(\frac{b}{a}\right)} = \frac{v_2}{i_2} \cdot \left(\frac{a}{b}\right)^2$$

$$Z_2 = Z_1 \cdot \left(\frac{a}{b}\right)^2$$

(5.12)

The simplified circuit can then be written as *Figure 5.9*:



**Figure 5.9** Simplified idealised transformer

Looking from the position of  $v_2$  *Figure 5.8* and *Figure 5.9* are electrically equivalent.



When applying this transformer theory to the absorber problem, converting the three circuits into one, it is important to maintain congruence in the circuits, that is to say the circuits must be converted so that the units are all in the same domain. For example it is possible to convert all of the sections into either the electrical, mechanical or the acoustic units. For the purposes of this problem it is the acoustical domain that is of interest so circuits will be combined accordingly. In order to convert all of the circuits into the acoustical domain the mechanical and electrical sections can first be combined to produce a single circuit with mechanical units and then this circuit combined with the acoustical circuit to produce just one circuit in the acoustic domain.

To successfully multiply out the transformers such that any electrical terms are converted to mechanical terms, the correct turns ratio must be chosen for the coils of the transformer. In order to convert an electrical term into a mechanical term Faradays laws are used as equations 5.13 and 5.14.

$$F = Bli \tag{5.13}$$

$$v = Blu \tag{5.14}$$

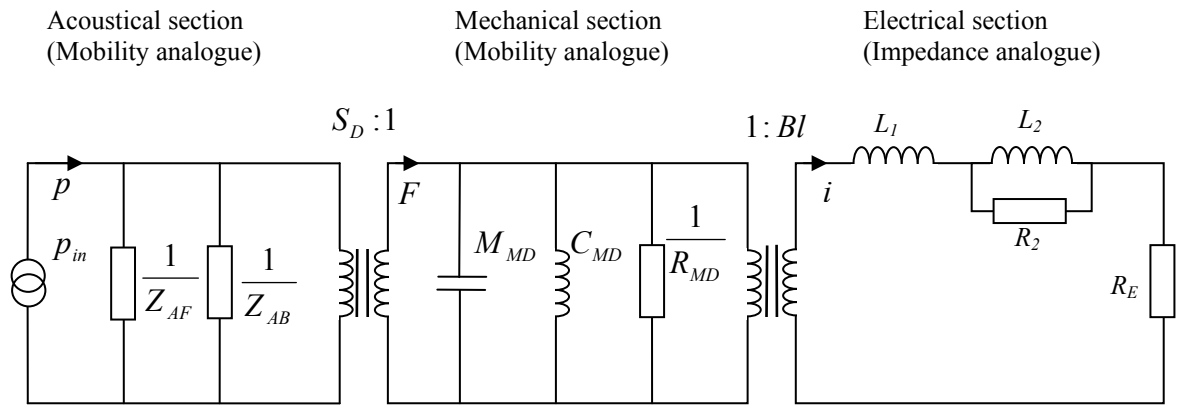
where  $i$  is the current flowing through the coil,  $B$  is the magnetic flux density of the magnet measured in Tesla's,  $l$  is the length of the coil,  $u$  is the velocity of the coil and  $v$  is the voltage across the coil. The common link between these formulae is the force factor ( $Bl$ ). As such this can be used as the turns ratio so that a voltage can become a force and a current can become a velocity, this means the mechanical section needs to be represented by the mobility analogue as in *Figure 5.5*.

The mechanical and acoustical domains can be linked by using the equations:

$$p = \frac{F}{S_D}, \text{ and } U = uS_D \tag{5.15}$$

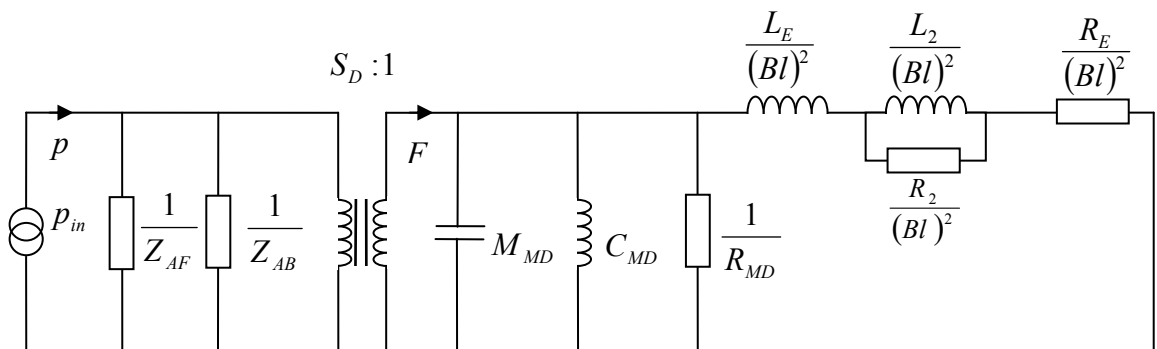
The common term here is  $S_D$  which is used as the turns ratio of the transformer for the conversion, therefore what was a force in mechanical units will become a pressure in

the acoustic section and what was a velocity in the mechanical section will now become a volume velocity. As such the acoustic section needs also to be modelled with the mobility analogue to prevent an incongruity of values. The three sections linked with the transformers then becomes as per *Figure 5.10*:



**Figure 5.10** Equivalent circuit linking electrical, mechanical and acoustical sections with transformers

The transformer linking the mechanical and the electrical sections is removed using the rules for idealised transformers, dividing impedances by the square of the turns ratio ( $Bl/1$ ) thus the circuit becomes:

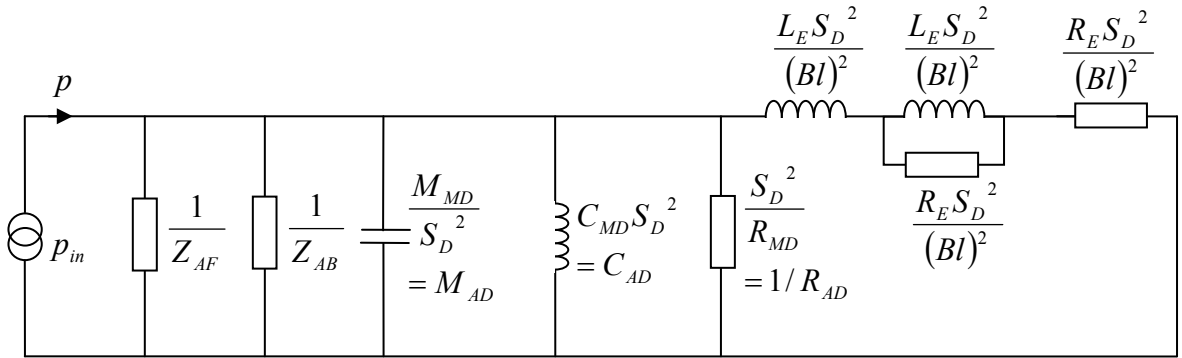


**Figure 5.11** Equivalent circuit of membrane absorber with electrical and mechanical sections combined

What was a current in the electrical section has now become a force in the mechanical domain from equation 5.13 and what was a voltage has become a velocity from equation 5.14. Thus the right hand side circuit consists now entirely of components with mechanical units. The mechano-acoustical transformer is now removed by multiplying all the impedances by the square of the turns ratio ( $1/S_D$ ). It is the impedance that is multiplied out rather than the component value hence:

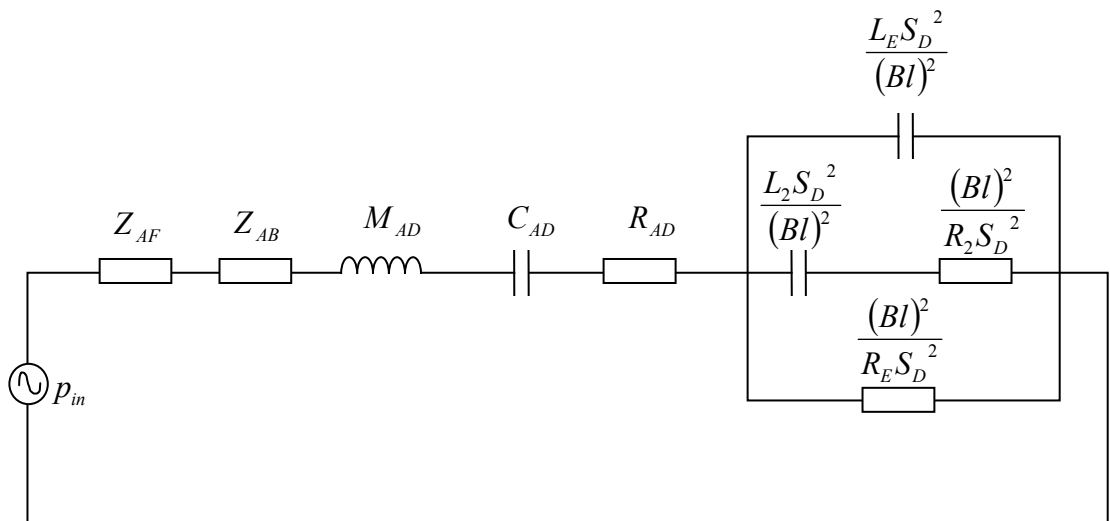
$$\frac{1}{j\omega M_{MD}} \times S_D^2 = \frac{1}{j\omega \left( \frac{M_{MD}}{S_D^2} \right)} \text{ so the component value is } \frac{M_{MD}}{S_D^2}$$

(5.16)



**Figure 5.12** Equivalent circuit of membrane absorber with electrical, mechanical and acoustical sections combined

The circuit in *Figure 5.12* can be directly solved to determine the impedance of the absorber system however it is easier to put the circuit into the impedance analogue by taking its dual and to rename some of the components such that it is easier to define their physical values. The components are renamed as they are now in acoustical units using the relationship that acoustical impedance can be determined by dividing the mechanical impedance by a factor of area squared (the operation performed when the transformer was multiplied out). Taking the dual of the circuit gives:



**Figure 5.13** Equivalent circuit of membrane absorber in impedance analogue

This is the full equivalent circuit in the impedance analogue for the loudspeaker absorber system upon which all subsequent analysis is based.

### 5.3.3 Defining the Parameters

In order to calculate the impedance of this circuit it is important that the component values can be determined. These can be obtained using direct theory and also by measuring the driver's Thiele/Small signal parameters [31, 32]. The parameters are also often referred to as small signal parameters because they are physical constants pertaining to a loudspeaker when operating linearly i.e. when a small signal is applied rather than a large signal which would cause non-linear behaviour. Measuring the Thiele/Small parameters of a loudspeaker can be done in several ways [35, 36, 37].

The method chosen here was the added mass method. With this method, weights are added to the diaphragm such that the additional moving mass decreases the driver's resonant frequency,  $f_s$  by about 20%. In the added mass technique  $M_{MS}$  is found first from equation 5.17:

$$M_{MS} = \frac{M_{ADDED}}{\left(\frac{f_s}{f_s'}\right)^2 - 1} \quad (5.17)$$

Where  $M_{ADDED}$  is the added mass,  $f_s$  is the drivers' resonant frequency and  $f_s'$  is the driver's resonant frequency with the additional mass. Using this value of  $M_{MS}$  the free-air mechanical compliance of the driver can be obtained from:

$$C_{MS} = \frac{1}{(2\pi f_s)^2 M_{MS}} \quad (5.18)$$

Other parameters can be obtained from performing electrical impedance tests on the driver. This procedure was done automatically using a maximum length sequence signal analyser (MLSSA). The parameters that were obtained were:

$M_{MS} = 28.152\text{g}$  , the mechanical moving mass of the driver with an air load

$C_{MS} = 385.276\mu\text{mN}$  , the mechanical compliance of the driver

$R_E = 12.415\Omega$  , the DC electrical resistance of the driver voice coil

$R_2 = 5.02\Omega$  , the second equivalent resistance of voice coil

$L_1 = 0.907\text{mH}$  , the inductance of the equivalent lossless inductor

$L_2 = 1.595\text{mH}$  , the inductance of the equivalent lossy inductor

$R_{ES} = 360.575\Omega$  , the mechanical losses of the diaphragm in electrical units

$Bl = 20.169\text{Tm}$  , the force factor of the driver

$S_D = 0.05768\text{m}^2$  , the area of the diaphragm

The subscript notation follows the rules for nomenclature as defined in Appendix I.

The acoustic impedance at the front and back of the diaphragm, given by  $Z_{AF}$  and  $Z_{AB}$  respectively, can be expanded in order to determine their values. The impedance at the front is the radiation impedance; this is a combination of the complex air load on the driver consisting of a reactive part (mass loading) and a resistive part (damping). Assuming piston movement of the diaphragm in an infinite baffle, the radiation impedance of the diaphragm at low frequencies ( $ka < 1$ ) can be written as [15]:

$$Z_{AF} = R_{AF} + j\omega M_{AF} = \frac{\rho_0 c k^2}{2\pi} + j\omega \frac{8\rho_0}{3\pi^2 a} \quad (5.19)$$

This would be the radiation impedance if the driver were to be placed in  $2\pi$  space, i.e. used within a room. However in order to compare predictions with measurements made in the impedance tube the radiation impedance is changed such that it more closely represents this plane wave case. The radiation impedance of the piston can be determined by considering a plane wave incident to a rigid surface. For such a case the ratio of pressure to particle velocity is given as  $\rho_0 c$  such that the acoustic impedance is given as:

$$Z_A = \frac{P}{U} = \frac{\rho_0 c}{S} \quad (5.20)$$

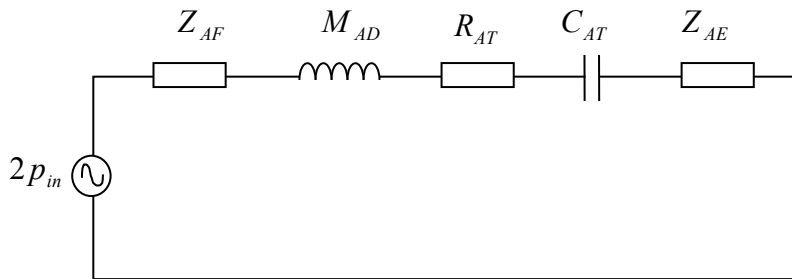
As pressure is scalar the total pressure when a plane wave is reflected from a plane surface is equal to  $2p_i$  therefore in the analogue the plane wave can be represented by a voltage generator of strength  $2p_i$  with a radiation impedance in front of the piston given by equation 5.20.

The impedance at the back of the diaphragm is a combination of the compliant load of the sealed volume of air in the cabinet,  $C_{AB}$  and the resistive losses due to the porous absorbent in the cabinet  $R_{AB}$ . The compliance of a sealed volume can be written as:

$$C_{AB} = \frac{V_B}{\rho_0 c^2} \quad (5.21)$$

where  $V_B$  is the volume of the box. The resistive losses can be determined by an acoustic model such as the Delany and Bazley empirical model. Although the Delany and Bazley model is inaccurate at very low frequencies it is sufficient for the purposes of estimating the value of  $R_{AF}$  using equations 2.11, 2.12 and 2.13.

From these parameters all of the component values in the circuit can be determined and the total impedance found. The circuit in *Figure 5.13* can be simplified as shown in *Figure 5.14*:



**Figure 5.14** Simplified equivalent circuit of membrane absorber

Where:

$$M_{AD} = \frac{M_{MS}}{S_D^2} \quad (5.22)$$

$$R_{AT} = R_{AD} + R_{AB} = \frac{R_{MS}}{S_D^2} + R_{AB} \quad (5.23)$$

Where  $R_{AD}$  is the damping of the diaphragm in acoustical units and  $R_{MS} = (Bl)^2 / R_{ES}$  :

$$C_{AT} = \frac{C_{AD}C_{AB}}{C_{AD} + C_{AB}} \quad (5.24)$$

$C_{AD}$  is the acoustic compliance of the diaphragm, calculated from the mechanical compliance of the diaphragm with an air load,  $C_{MS}$  so that:

$$C_{AD} = C_{MS}S_D^2 \quad (5.25)$$

The acoustic impedance as a result of the electrical section,  $Z_{AE}$  is the parallel combination of impedance given by equation 5.26:

$$Z_{AE} = \left[ \frac{1}{z_1} + \frac{1}{z_2} + \frac{1}{z_3} \right]^{-1}$$

Where  $z_1 = \frac{1}{j\omega \left( \frac{L_E S_D^2}{(Bl)^2} \right)}$ ,  $z_2 = \frac{L_2 S_D^2}{(Bl)^2} + \frac{(Bl)^2}{R_2 S_D^2}$  and  $z_3 = \frac{(Bl)^2}{R_E S_D^2}$

$$(5.26)$$

#### 5.3.4 Calculating the Absorption of the System

Once the final equivalent circuit has been formed it is a simple matter to determine the specific acoustic impedance of the system by solving the circuit using basic electronics theory. From this impedance the reflection factor and the acoustic absorption can be found using equations 2.7 and 2.4 respectively.

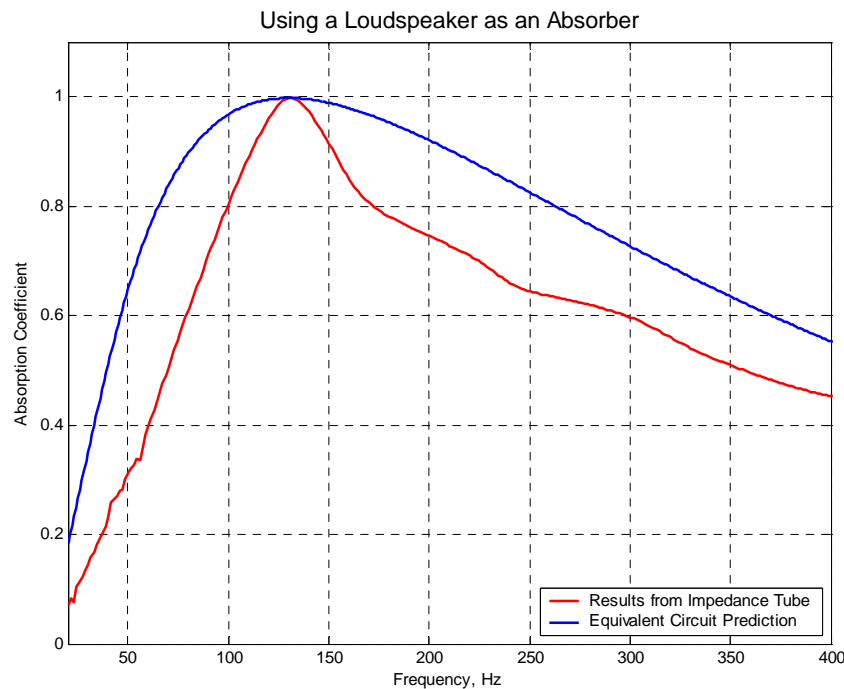
The combined acoustic impedance of the circuit is found by equation 5.27:

$$Z_{TOT} = j\omega M_{AD} + \frac{1}{j\omega C_{AT}} + R_{AT} + Z_{AF} + Z_{AE} \quad (5.27)$$

Multiplying this by a factor of the diaphragm area gives the specific acoustic impedance of the system from which the absorption can be obtained.

#### 5.4 Implementing the Model

The equivalent circuit model was implemented using MATLAB to plot the predicted absorption versus frequency of the driver. *Figure 5.15* shows the predicted and measured absorption on the same axes. The code used to generate the results can be found in Appendix J.



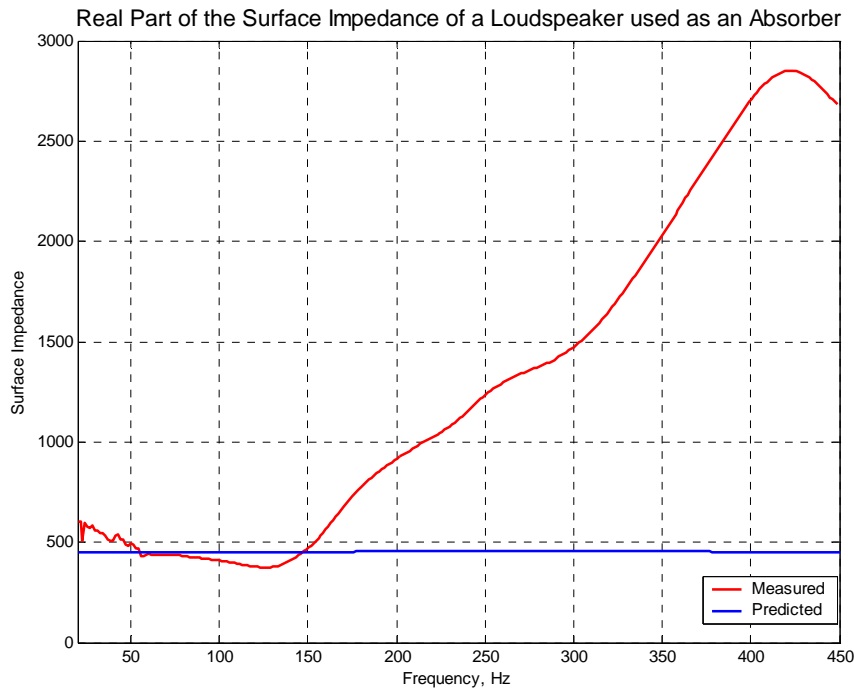
**Figure 5.15** Comparison of equivalent circuit model with impedance tube measurements

##### 5.4.1 Discussion

Good correlation between measurement and prediction is shown in terms of absorption magnitude and resonant frequency. The equivalent circuit model does however predict a broader Q-factor of absorption than measurements show. This is due the limitations of the lumped element modelling technique and results in difficulty in accurately predicting the surface impedance of the system for all frequencies. Looking at the real

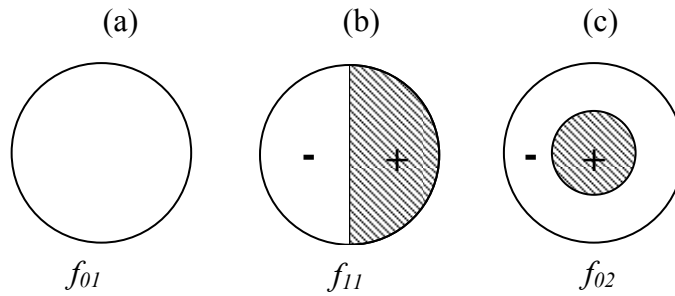


part of the impedance (shown in *Figure 5.16*) for both the measured and the modelled cases reveals that there is a dramatic increase in the real part of the measured surface impedance at higher frequencies which is not present in the predicted data.



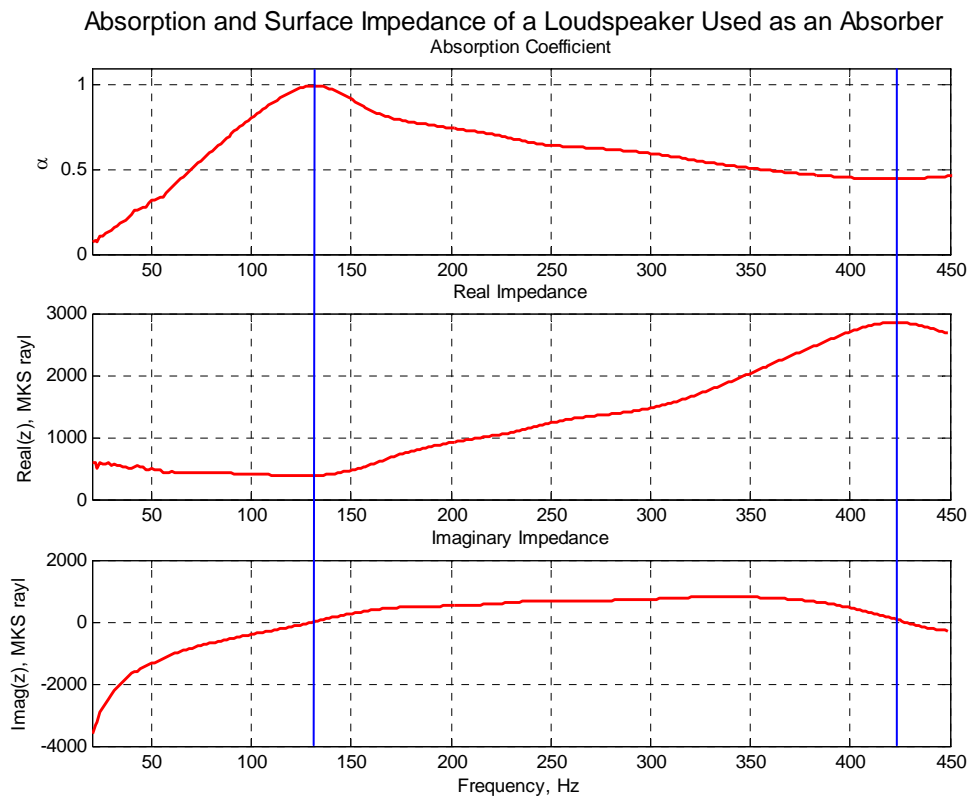
**Figure 5.16** Real part of surface impedance from both predicted and measured data

Accurate prediction of the losses in the system are shown at low frequency but the accuracy decreases as the frequency increases, this explains why the predicted Q-factor of the resonant curve is broader than the measured value. With the real part of the measured impedance tending sharply away from characteristic impedance the system reaches maximum absorption over only a narrow bandwidth which is contrasted with the prediction where the real component of the impedance remains roughly equal to characteristic impedance for the entire frequency range. The inaccuracy in the prediction model is the result of secondary resonances of the driver diaphragm that cannot be modelled using the lumped element method as it only predicts the fundamental resonance of systems. The first three modes of a circular plate can be given as *Figure 5.17* [38].



**Figure 5.17** First three vibrational modes of a circular plate

The second modal frequency given by  $f_{11}$  is a resonant mode but will not generate any absorption as there is cancellation on the diaphragm i.e. the diaphragm is ‘pushing’ and ‘pulling’ the same amount of air, consequently there is no resultant transmission of energy and hence no absorption. It would therefore be expected that the imaginary part of the surface impedance would exhibit a secondary point of zero crossing at this modal frequency but which would show insignificant absorption, looking at *Figure 5.18* this becomes clear. The cancellation at this modal frequency causes the real part of the surface impedance to increase preventing efficient transmission, resulting in minimum absorption as shown by *Figure 5.18*:



**Figure 5.18** Multi-plot of absorption and surface impedance showing the first two resonant modes of the loudspeaker

The blue lines on the *Figure 5.18* show where the imaginary part of the surface impedance goes to zero, illustrating the first two resonances of the diaphragm. It can be seen from the figure that at the second of these modes (corresponding to *Figure 5.17b*) there is negligible absorption as the real part of the surface impedance has reached a maximum and much larger than characteristic. Thus the inability of the model to predict secondary and tertiary resonances of the driver means that the final predicted absorption curve exhibits increased Q-factors when compared to the measured data. As a result there will be inaccuracies in the predictions made by the model but the behavioural characteristics of the fundamental mode in terms of frequency and magnitude of absorption will be accurate. Thus the model can be used to obtain predictions of further scenarios as modelled in chapter 6. It is further shown in chapter 6 that the model accurately predicts the trends in changing resonant characteristics introduced by additional electronic loads connected to the terminals of the driver as shown in *Figure 6.4* and *Figure 6.11*.

## **5.5 Conclusion**

Using a loudspeaker as a membrane absorber has been shown to produce high absorption coefficients at low frequency. The system behaves as a membrane absorber and could prove to be useful for practical studio applications by using redundant loudspeakers to absorb unwanted modal components within a room.

The loudspeaker absorber system has been modelled using electroacoustic theory and a lumped element model. The prediction of acoustic absorption matched up well with the measured values obtained from impedance tube tests. It was noted that the lumped element model does not allow for the prediction of the system's higher order resonances, causing inaccuracy in the prediction of the surface impedance at higher frequencies, resulting in the model predicting broader Q-factors than the measured data shows. The model does however predict accurately the frequency and magnitude of resonance and can be used as a first approximation of the absorber's behaviour especially with a changing electronic load impedance as shown in chapter 6.

The next section of work outlines how a passive electronic load on the driver can be used to reduce the resonant frequency and Q-factor of the loudspeaker absorber system. The equivalent circuit model presented in this chapter will be extended to model such changes in the motor impedance of the loudspeaker.

## **6. CHANGING THE RESONANT CHARACTERISTICS OF A LOUDSPEAKER-ABSORBER USING PASSIVE ELECTRONICS**

### **6.1 Introduction**

The previous chapter outlined the basic principles of the modelling and use of a loudspeaker used, in reverse, as an acoustic absorber. Sound incident to the diaphragm of the loudspeaker, forces it into oscillation in sympathy to the frequency of the incident wave causing a particle flow in the cabinet which is absorbed by porous material. The system, as expected, was shown to have a distinct resonant peak, the frequency and magnitude of which was controlled by the mechanical, acoustical and the electrical components of the system. This was brought together in the form of a lumped parameter

model which enabled prediction of the overall acoustic impedance of the system from an equivalent circuit, which in turn was used to determine the complex reflection factor and hence the normal incidence absorption coefficient. This model was then compared to tests performed in an impedance tube and was shown to accurately predict the frequency and magnitude of the system's resonance.

In the current chapter, the principles of the previous chapter are built upon such that parameters concerning the system are changed in order to produce an absorber with variable resonance characteristics. For a standard membrane absorber it is possible, if not practical, to alter the mechanical and acoustical compliance, mass and damping terms within the system to change its resonant characteristics. This is often very impractical as it means altering physical properties such as the volume/depth of the cabinet or the material of the membrane. These changes demand a complete reconstruction of the absorber so are not only time consuming but are also financially costly. Using a loudspeaker as an absorber can provide a solution to this problem as there is the addition of an electrical domain in the system. Changing this electrical section using variable components enables the combined acoustic impedance of the system to be altered. The real part of the impedance, which determines the magnitude and the Q-factor of absorption, can be altered by the addition of resistive components. The imaginary part, which dictates the frequency of the resonance, can be altered by the inclusion of additional reactive components.

Altering acoustical properties of resonant systems with the use of electronic components is not a new idea; it has been applied to many areas including design of loudspeakers with a better low frequency response [29]. In this case Stahl used electronic components connected to an amplifier thereby changing the impedance load as seen by the loudspeaker, Stahl noted that this caused the fundamental resonance to be altered and enabled tuning to produce a better low frequency response. Stahl's paper also demonstrated a lumped element model to back up laboratory tests. This application was focused on the radiation of sound but the theory of changing an electronic load to alter an acoustic system has been applied also to the absorption of sound in the field of aeroacoustics [39]. In this case a Helmholtz absorber was presented with a piezoelectric backplate, the impedance of which could be varied by the addition of resistive and reactive electronic components such that the resonant frequency and damping were

altered. Results showed a shift in resonant frequency of up to 20% with the inclusion of capacitive and inductive components. Resistive components could also be added and were shown to alter the Q-factor of the resonance by the increase in damping. The application for this study was in engine liners for aircraft where the frequency of noise from the engine depends on the velocity of the aircraft therefore an absorber with variable characteristics is desirable.

Using loudspeakers as absorbing systems has also been used extensively in room acoustics with active absorption systems [40, 41] these systems use powered electronic circuits and loudspeakers to cancel out incident sound by radiating a phase inverted version of that sound which destructively interferes, absorbing the incident wave. It is also possible to combine active and passive absorption techniques for room acoustic applications [42]; this patented bass trap uses active control to tune a loudspeaker such that it will passively absorb acoustic energy at its resonant frequency, Kashani and Wischmeyer presented results displaying significant attenuation in a low frequency band. The system allows two room modes to be absorbed simultaneously using this active tuning. A further example of combining active and passive techniques is in the field of space and rocket technology, where noise in the nose cone of a launch vehicle can get to such large levels (exceeding 140dB) that damage can be inflicted on the vehicle. Kemp and Clark [43] presented a technique combining a passive and active control approach using an active input (an accelerometer on a loudspeaker) to actively change the resonance characteristics of a loudspeaker that was used passively to absorb the noise in the fairing (nose cone), they demonstrated peak reductions in excess of 12dB using this technique.

Both of the techniques mentioned above, using loudspeakers in the absorption of sound use an active approach of tuning absorbers; however the absorber system presented here does not utilise any active control but achieves high absorption coefficients over a range of two and a half octaves using only passive techniques. As such this technique is an extension of other methods available. In this work the resonant frequency can be altered to allow the absorber to be transferred from room to room and retuned to match the fundamental mode of that room. The magnitude and Q-factor of the absorption curve can also be altered with the aim of smoothing out the frequency response. Of primary interest is the effect of a single load resistance or capacitance, these will therefore be

described first. However the complex load impedance connected to the terminals of the loudspeaker could potentially contain any combination of resistive and reactive components to produce the optimum resonant characteristics for a given application and more complex arrangements will hence be analysed in subsequent sections.

Changing the resistive element of the impedance presented to the terminals *A* and *B* of the loudspeaker used as an absorber was analysed first.

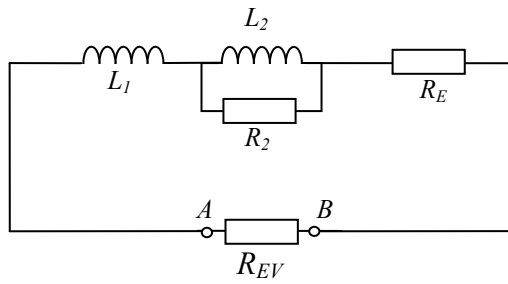
## **6.2 Changing the Load Resistance**

It is useful in applications to be able to determine the Q-factor of the absorption provided by a membrane absorber, the advantage can be seen in two ways. Firstly if the Q-factor is decreased it enables an increased bandwidth of absorption, something highly sought after in room acoustics, to result in a room with a flatter response with respect to frequency over a wider bandwidth. Secondly if the Q-factor could be increased it allows more selectivity with the frequencies that the system could absorb, such that if there was a problem with increased modal excitation at a discrete frequency it could be selectively absorbed without effecting neighbouring frequencies. Varying the load resistance will be elucidated in the subsequent section altering the Q of the resonance by a degree of 34% allowing for the user to select the Q-factor within certain bounds for the application of choice. There is also the possibility of applying a negative resistance across the terminals to decrease the Q-factor still further but this would require an additional power source and falls outside the scope of this project.

### **6.2.1 Theory and Prediction**

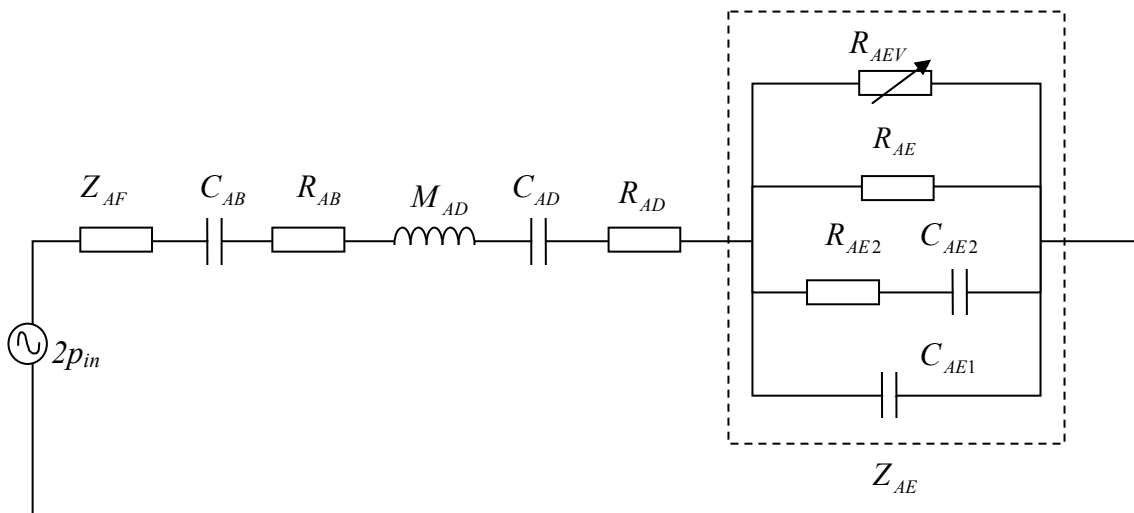
The lumped element model derived in the previous chapter was extended here to allow the modelling of additional passive electronic components in the electrical section of the analogue. With the additional variable resistance,  $R_{EV}$ , the electrical section of the equivalent circuit as modelled with the impedance analogue then becomes as *Figure 6.1*:





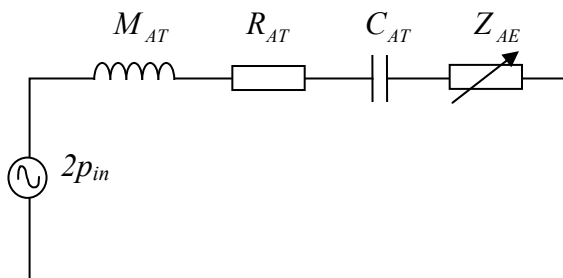
**Figure 6.1** Electrical section of the absorber equivalent circuit with an additional variable resistor across terminals *A* and *B*.

When this is combined with the mechanical and acoustical sections in the same way as demonstrated in chapter five and the dual of the circuit taken the final circuit becomes as *Figure 6.2*:



**Figure 6.2** Full equivalent circuit of absorber with additional variable resistor across terminals

Simplifying this circuit it can be written as:



**Figure 6.3** Simplified equivalent circuit of absorber

The impedance of the electrical section in acoustical units is given by  $Z_{AE}$  the expression for which is given by equation 6.1:

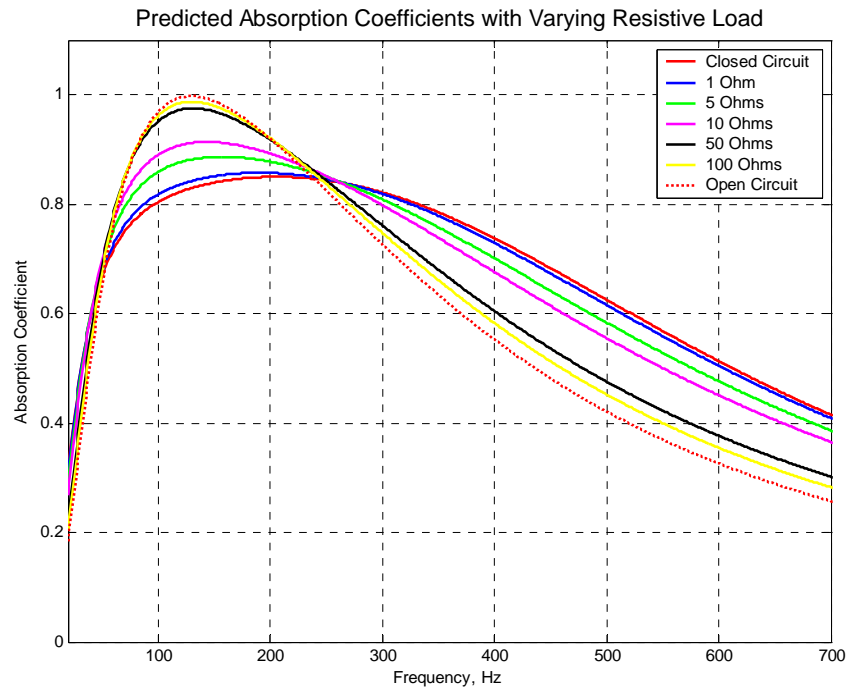
$$Z_{AE} = \left[ \frac{R_{AE} + R_{AEV}}{R_{AE} R_{AEV}} + \frac{\omega C_{AE2}}{j + \omega C_{AE2} R_{AE2}} + j\omega C_{AE1} \right]^{-1} \quad (6.1)$$

where;

$$\begin{aligned} R_{AEV} &= \frac{(Bl)^2}{R_{EV} S_D^2}, & R_{AE} &= \frac{(Bl)^2}{R_E S_D^2}, \\ R_{AE2} &= \frac{(Bl)^2}{R_2 S_D^2}, & C_{AE1} &= \frac{L_1 S_D^2}{(Bl)^2}, \\ \text{and} & & C_{AE2} &= \frac{L_2 S_D^2}{(Bl)^2} \end{aligned} \quad (6.2)$$

The variable resistance,  $R_{EV}$  changes the value of  $R_{AEV}$  by a factor of its reciprocal, such that an increase in  $R_{EV}$  reduces the value of  $R_{AEV}$ .

This extension to the original model demonstrated in chapter 5 yields the following absorption coefficient graph for varying the load resistance on the driver:



**Figure 6.4** Changes in absorption curves with a variable resistor connected across loudspeaker terminals

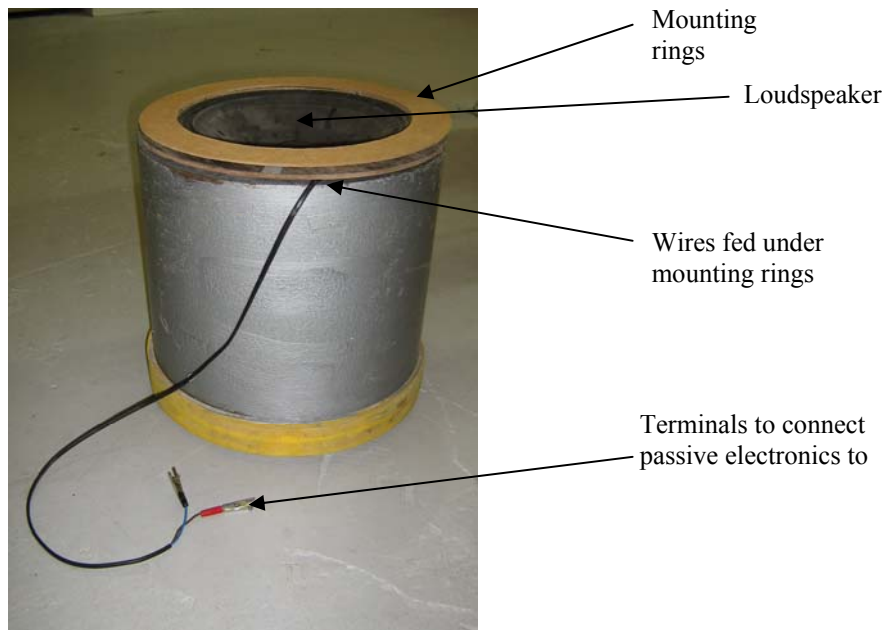
This prediction shows that the Q-factor of the absorption curve rises with an increase in load resistance; this is counter to intuition which states that additional resistance adds damping to the circuit and should therefore reduce the Q-factor rather than increase it. The reason for this is that the final analogue is written in the impedance analogue such that electrical resistances actually become conductances, so an increase in the load resistance actually increases the conductance in acoustical units.

The variations in Q-factor are governed by the open and closed circuit limiting conditions. The closed circuit offers the minimum load resistance and the open circuit case offers the highest possible load resistance, thus these conditions define the minimum and maximum Q-factors obtainable with standard linear electrical resistors.

### 6.2.2 Measurements

Measurements were made using the specially constructed impedance tube in the same manner as in chapter 5. The electrical load resistance applied to the terminals of the driver was altered for each measurement using a standard variable resistance box with a maximum error of 0.1% verified with a digital multi-meter. In order to connect the

resistance box to the terminals of the driver, wires had to be fed from the driver under the mounting rings shown in *Figure 6.5*:

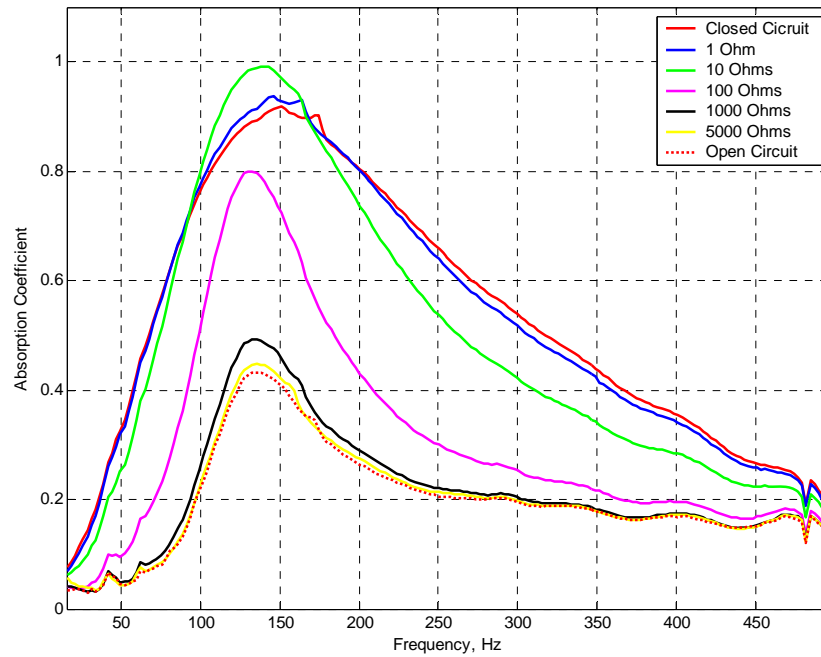


**Figure 6.5** Mounting of loudspeaker in large sample holder for impedance tube testing

Care had to be taken to avoid any leaks between the mounting rings and the top of the sample holder so as to prevent spurious results. This was achieved by using Blu-tak to block any gaps.

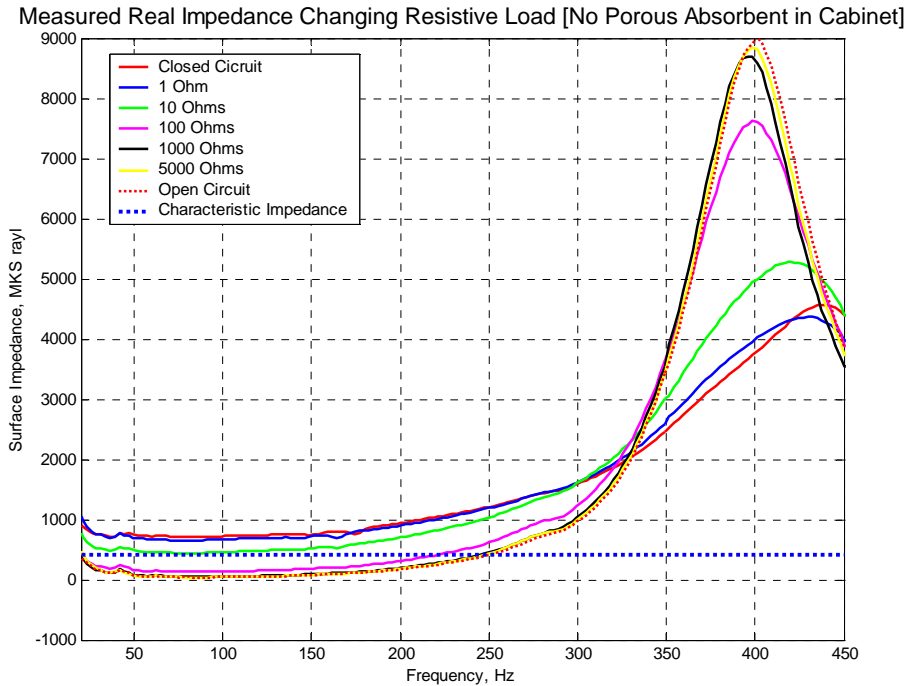
Initial measurements were made with no porous absorbent in the sample holder; this was done so that the Q-factor would be higher in order that the effect of the changing resistance could be more clearly discernable. On subsequent analysis it was found that these measurements did not match up well with predictions. The absorption coefficient curves that were obtained are seen in *Figure 6.6*:

Measured Absorption Coefficient Changing Resistive Load [No Porous Absorbent in Cabinet]



**Figure 6.6** Measurements made on absorber in impedance tube changing resistive load on loudspeaker terminals

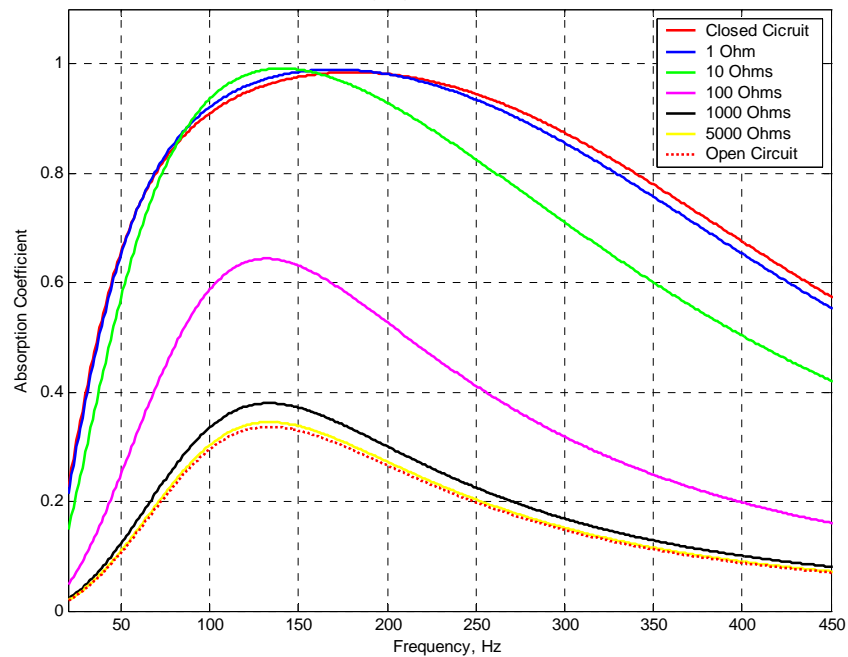
It is seen from *Figure 6.6* that the trend does not behave as predicted in *Figure 6.4*. In *Figure 6.4* an increase in resistive load leads to an increase in Q-factor and consequently higher absorption coefficients, this trend is reversed in *Figure 6.6* when there is no porous absorbent backing to the loudspeaker, thus the measurements behave in the opposite manner to the predictions. The answer to this quandary of the incongruity between measurements and prediction can be found on inspection of the real part of the surface impedance as shown in *Figure 6.7*.



**Figure 6.7** Real part of the measured surface impedance of absorber with a variable resistive load without porous absorption in the cabinet

It can be seen from *Figure 6.7* that around the resonant frequency ( $\sim 135$  Hz) an increase in resistive load causes a decrease in the real part of the surface impedance. Initially for resistances from the closed circuit case to the 10 Ohm case the real part gets progressively nearer to the characteristic impedance of air (given by the dotted blue line) and hence the trend is an increase in absorption with an increase in resistance. After the 10 Ohm load resistance the trend in the real part of the impedance tends away from characteristic impedance with an increase in resistance which explains the reverse in trend such that an increase in resistance causes a decrease in absorption. The prediction model was changed to account for this decrease in real impedance by removing the porous absorbent in the cabinet. The predicted absorption coefficient for this case shows better agreement with measurements.

Predicted Absorption Coefficient Changing Resistive Load [No Porous Absorbent in Cabinet]

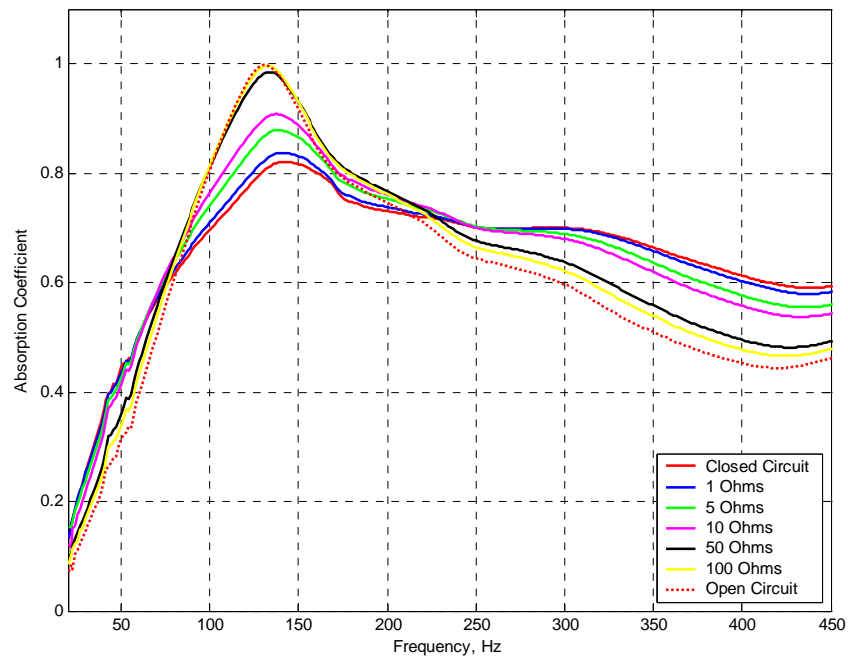


**Figure 6.8** Predicted absorption coefficient changing the resistive load on the absorber without porous absorption in cabinet.

When the model is amended such that there is no porous absorbent in the cabinet (sample holder) and the real part of the impedance decreased, the trend matches up more favourably with measurements exhibiting an increase in Q-factor with increasing resistance. When the porous absorbent is included in the cabinet the overall real part of the surface impedance rises above characteristic impedance such that with each increase in resistance the value of the real part gets further from characteristic impedance hence tends away from maximum absorption and a decrease in Q-factor.

To demonstrate this effect, measurements were repeated with porous absorbent in the cabinet. Results were again plotted with respect to frequency and yielded the graph in *Figure 6.9*.

Measured Absorption for Different Resistive Loads [With Porous Absorbent in Cabinet]



**Figure 6.9** Measured absorption coefficient of absorber with variable resistive load with porous absorption in the cabinet

This measurement shows good agreement with the predicted values plotted in *Figure 6.4* confirming the validity of the model. Graphs with both the measured and predicted results plotted on the same axes for each individual resistive load can be found in Appendix K. The model, as mentioned in section 5.4.1, tends to slightly over predict the Q-factor of the resonance but as will be seen in section 6.5.2 the trend of how the Q-factor changes with increasing resistive loads is accurately predicted.

There is a slight shift in resonant frequency that is shown in both the measured and the predicted data, the resonant frequency decreasing slightly with the additional resistive load. The reason for this shift is found when analysing the combined complex impedance of the electrical section  $Z_{AEV}$ . Expanding equation 6.1 shows that  $R_{AEV}$  becomes a factor of the  $\omega C_{AE1}$  and  $\omega C_{AE2}$  therefore changing the resistive load will have an effect on the magnitude of the reactive parts and consequently on the resonant frequency of the system. This effect is small when compared with the fundamental resonance frequency with the closed circuit case; the shift is from 142 to 132Hz a shift of just 7%. Greater shifts in resonant frequency can be obtained if a capacitor is introduced into the circuit as seen in section 6.2.3.



### 6.2.3 Summary

Changing the resistive load has been shown to have different effects on the Q-factor of the resonant peak of absorption in the loudspeaker absorber system. The effect depends on the initial magnitude of the real part of the surface impedance. It has been shown that if the real impedance is above characteristic impedance for the closed circuit case then the trend is an increase in Q-factor and absorption with an increase in resistance as with each addition of resistance the real surface impedance of the system gets progressively closer to characteristic impedance of air and hence maximum absorption at resonance. The trend is reversed if the real part is initially below characteristic impedance for the closed circuit case, as with each addition of resistance the value at resonance tends away from characteristic impedance resulting in a decrease in absorption and Q-factor with increase in resistance.

When designing a resonant absorber of this type it will be useful to change the Q-factor of the resonance to selectively absorb discrete frequencies to a certain degree to achieve the flattest possible room response with respect to frequency. Section 6.5 will outline some useful equations and graphs that could be used to determine what resistive value should be used to achieve a given Q-factor for a specific driver.

## 6.3 Changing the Capacitive Load

As well as adding a variable resistor to the terminals of the loudspeaker it is possible also to include the addition of reactive components, in this section a variable capacitor was included in the circuit. The desired outcome of this was the lowering of the system's resonant frequency. Experiments were performed in the impedance tube and the scenario modelled using the standard equivalent circuit approach as in previous sections. Measurements showed that shifts in resonant frequency of up to 39% were possible with the addition of a single capacitor.

### 6.3.1 Theory and Prediction

Adding a capacitor into the circuit in *Figure 5.13* leads to the equivalent circuit shown in *Figure 6.10* from which predictions of how the absorber system will behave with changing load capacitance can be made. Thus the new circuit becomes:

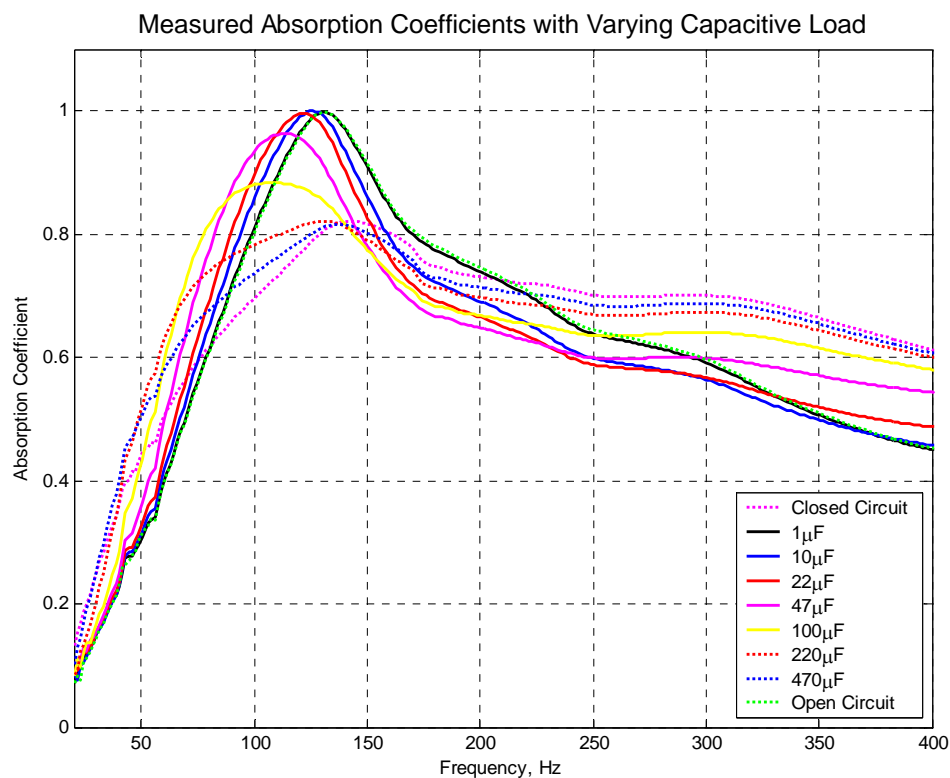


**Figure 6.11** Predicted absorption curves with a variable capacitor connected to loudspeaker terminals

The graph shows a decrease in resonant frequency with an increase in capacitive load. Results from the equivalent circuit model suggest that there is an optimum capacitance where by increasing the capacitance further will begin to increase the resonant frequency until once again it resonates at the same frequency as the closed circuit case. The model predicts a resonant frequency shift of some 51% with the system resonating at 174Hz for the closed circuit case and 85Hz with a 220 $\mu$ F load capacitance.

### 6.3.2 Measurements

Measurements were once again performed in the low frequency impedance tube. The results were made with porous absorbent material in the cabinet as this is the most important case if the absorber were to be used in a practical setting. Standard electrical component capacitors were used in the measurements with capacities ranging from 1-470 $\mu$ F. Results yielded the following *Figure 6.12*.



**Figure 6.12** Measured absorption curves, changing the load capacitance connected across loudspeaker terminals

Results from the measurements show a similar trend to the predictions such that an increase in capacitive load leads to a decrease in the system's resonant frequency. The lowest frequency was found with a capacitance of 100  $\mu\text{F}$ . The prediction model and the measurements show that if the capacitance is increased too much then resonant frequency increases again. The high frequency limit is given by the closed circuit condition. The measured results show a resonant frequency shift from 172Hz to 105Hz which corresponds to a shift of 39% which is slightly less than predicted due to limitations in the lumped element method of analysis mentioned in section 5.4.1.

### 6.3.3 Discussion

Results show that with the addition of the reactive component there appears to still be some resistive losses added into the system manifesting as a reduction in the Q-factor of the resonance peak. This is due to the construction of the circuit, namely the fact that the components are connected to the voice coil in series. Looking at the equivalent circuit of the absorber, it is seen that in the final analogue circuit, what was electrically in series becomes in parallel in the final model. Combining the complex impedances in parallel means that the resistive components have impact on the frequency and that reactive components have an impact on resistive losses, such that the resistive components become multipliers of frequency dependent terms and capacitors become multipliers of resistive terms. This means that when trying more complex scenarios such as adding additional resistive components to achieve high absorption at the lowest possible frequency, a trade off has to be made. As more resistance is added the resonant frequency can be shifted less by the reactive component as the resistive component becomes the dominant term in controlling the motor impedance.

### 6.3.4 Summary

By adding a capacitive load to the terminals of the driver it has been shown that it is possible to achieve a resonant frequency shift of 39%. A maximum value of capacitance was found, a value above which would begin to increase the resonant frequency again. The optimum capacitance in the model was 220 $\mu\text{F}$  where as in measurements was 100 $\mu\text{F}$ . This value is subject to change given a specific driver; this is the topic of section 6.5.1. Increasing the capacitance, as well as lowering the resonant frequency, also

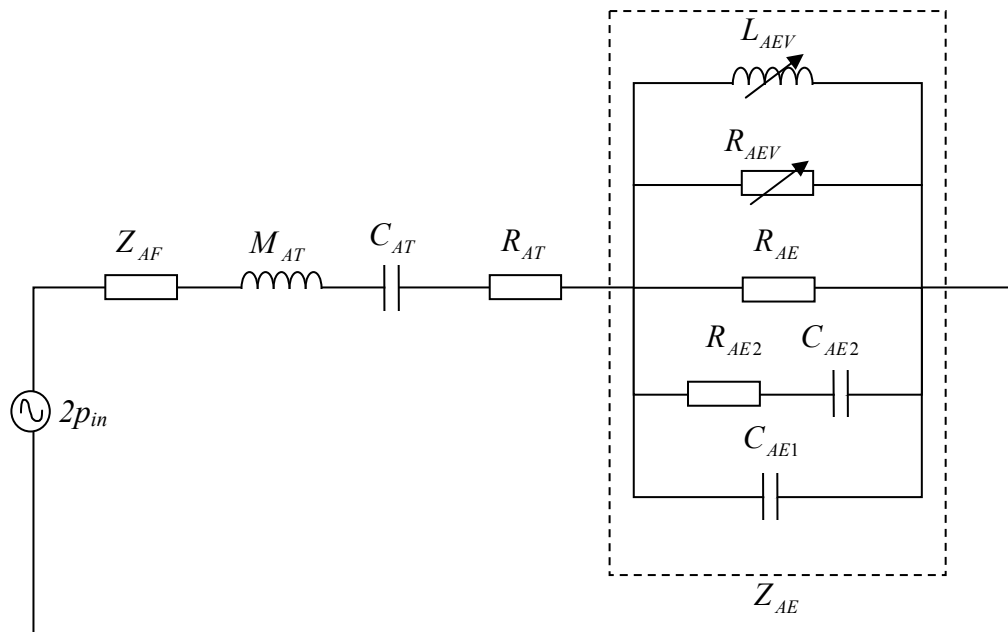
increases the Q-factor of the resonance curve thus there is a trade off between obtaining the lowest possible frequency of a given system and obtaining maximum absorption.

#### **6.4 Modelling Other Scenarios**

So far it has been shown that by adding a variable resistance or capacitance into the circuit the loudspeaker absorber can be tuned to exhibit different resonant characteristics such that the Q-factor and the resonant frequency can be altered. A variable resistor and capacitor constitute the simplest cases of adding both singular resistive and reactive components. In this next section further scenarios are modelled using the equivalent circuit model. Being able to change the resonant frequency of the system is very useful but it is to the detriment of absorption magnitude at resonance. More complicated combinations of electronic components could present an optimum situation where the lowest resonant frequency could be achieved but yet exhibit maximum absorption. Several combinations of additional electronic components are modelled in this section; firstly, resistors and capacitors in series and in parallel, secondly, the addition of an inductive component and thirdly, the combination of capacitive and inductive elements both in series and in parallel.

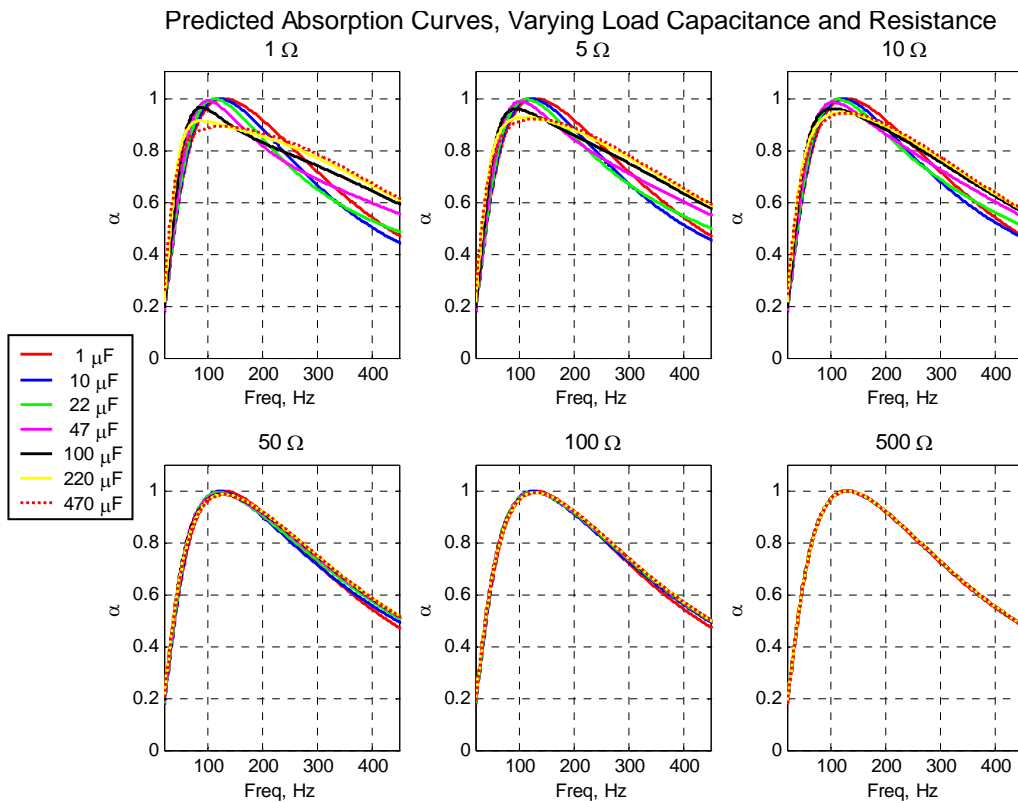
##### **6.4.1 Resistors and Capacitors in Series**

In order to see if there is a greater degree of tunability available with the loudspeaker absorber system it was seen what would happen if a variable resistor was placed with a variable capacitor in series, in the final equivalent circuit these appear as a variable inductor and conductance in parallel with the other motor impedance terms, the equivalent in this case is given by *Figure 6.13*:



**Figure 6.13** Equivalent circuit modelling a variable resistor in series with a variable capacitor connected to the terminals of the loudspeaker

It was hoped that the addition of the extra variable resistor in series with the variable capacitor would allow the system to resonate at the lowest possible frequency, as governed by the capacitor whilst having the maximum absorption coefficient at resonance, governed by the variable resistor. This turned out not to be the case as was seen when plotting the absorption coefficient versus frequency for varying capacitive and resistive loads. A multi-plot demonstrating how the trend in absorption changes with differing combinations of resistive and capacitive loads in series is shown in *Figure 6.14*.

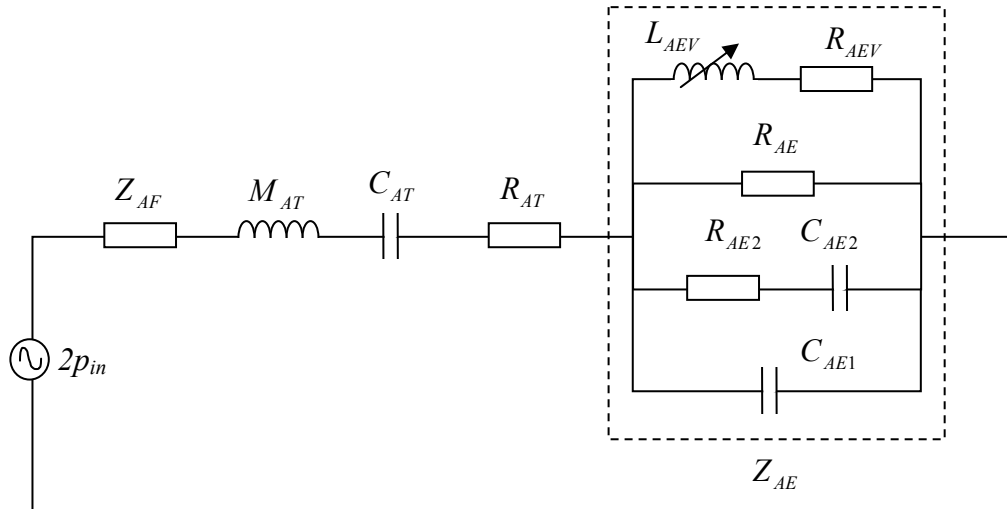


**Figure 6.14** Multi-plot showing changes in the trend of absorption for different combinations of resistors in series with capacitors

It can be seen from *Figure 6.14*, that a change in load resistance on the driver suppresses the effect of the change in capacitance to increasing amounts with an increase in resistance. Thus using a capacitor and resistor in series does not have the desired effect of lowest frequency absorption with maximum absorption coefficient. To discern the reason for it is helpful to look at the equivalent circuit in *Figure 6.13*. As the value of  $R_{EV}$  increases  $R_{AEV}$  decreases according to equation 6.2, thus current will flow more easily through that branch of the circuit. Consequently as  $R_{AEV}$  decreases, less current flows through  $L_{AEV}$  and the circuit tends towards the case with no variable capacitance at all, i.e. the equivalent circuit becomes as *Figure 6.2*. As the resistance is then very high it tends towards the open circuit case as results show in *Figure 6.14*. Therefore with a higher load resistance the change in load capacitance makes continually less difference to the resonant characteristics of the system. Consequently the simple series connection of a single resistor and capacitor does not constitute a useful case when aiming to increase the adaptability of the resonant absorber.

### 6.4.2 Resistors and Capacitors in Parallel

The combination of the variable resistance and capacitance can also be connected in parallel to the terminals such that in the final equivalent circuit they become a variable inductor in series with a conductance, the new equivalent circuit that defines the oscillation of the system becomes:



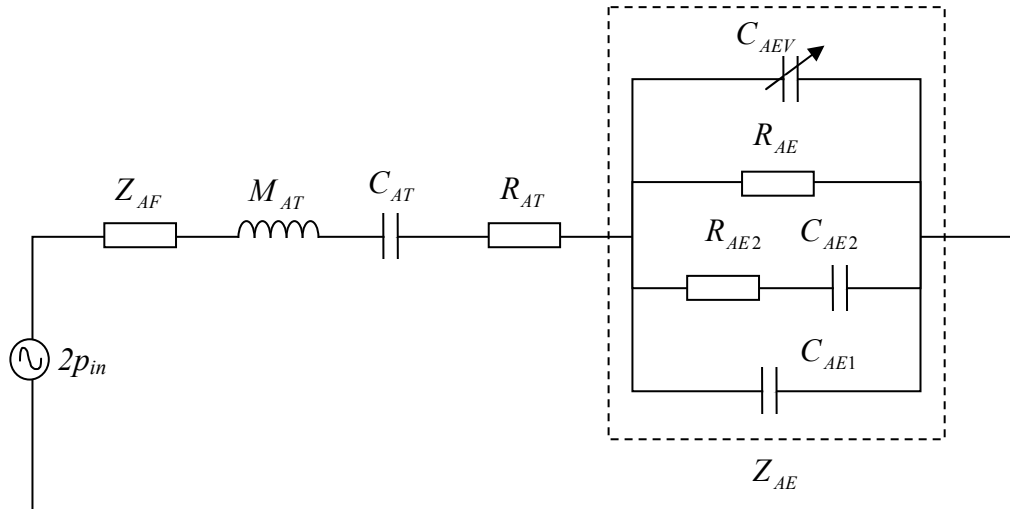
**Figure 6.15** Equivalent circuit modelling a variable capacitor in parallel with a variable resistor connected to the terminals of the loudspeaker

The effect of connecting a variable capacitor in parallel with a variable resistor will be the opposite of connecting the two in series. Increasing the resistive load,  $R_{EV}$  will decrease  $R_{AEV}$  causing more current to flow through the  $L_{AEV}$ . Thus as  $R_{EV}$  increases the effect of the variable capacitor increases, this can be seen from the multi-plot in Appendix L. Results show that for the minimum resistive load the circuit tends towards the open circuit case and with a maximum resistive load it tends towards the simple case of only a capacitor connected across the terminals, thus this combination behaves, as expected, in the opposite manner to the previous example of a variable resistor and capacitor in series. For the case of the components in series; increasing the value of resistance suppresses the effect of the capacitor in the circuit and conversely increasing the value of the capacitance suppresses the effect of the resistor. For the parallel circuit the opposite is true therefore it becomes apparent that it is not possible to obtain the lowest resonant frequency with maximum absorption using solely resistors and capacitors hence the next section models the addition of a variable inductor to increase the degree of freedom of the circuit.



### 6.4.3 Applying an Variable Inductor

If a variable inductor is added in series into the circuit it manifests itself as a variable capacitor in parallel with the voice coil impedance terms in addition to the final equivalent circuit *Figure 5.15*. The circuit that defines this condition then becomes as *Figure 6.16*:

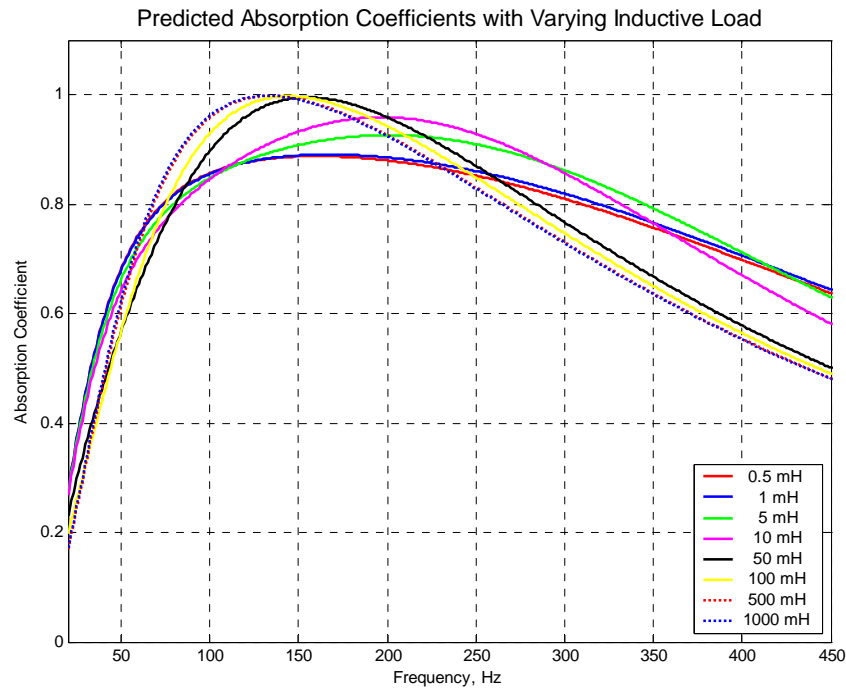


**Figure 6.16** Equivalent circuit modelling a variable inductor connected to the terminals of the loudspeaker

Where

$$C_{AEV} = \frac{L_{EV} S_D^2}{(Bl)^2}, \quad Z_{C_{AEV}} = \frac{1}{j\omega C_{AEV}} \quad (6.4)$$

Plotting the predicted absorption from this equivalent circuit yields *Figure 6.17*.

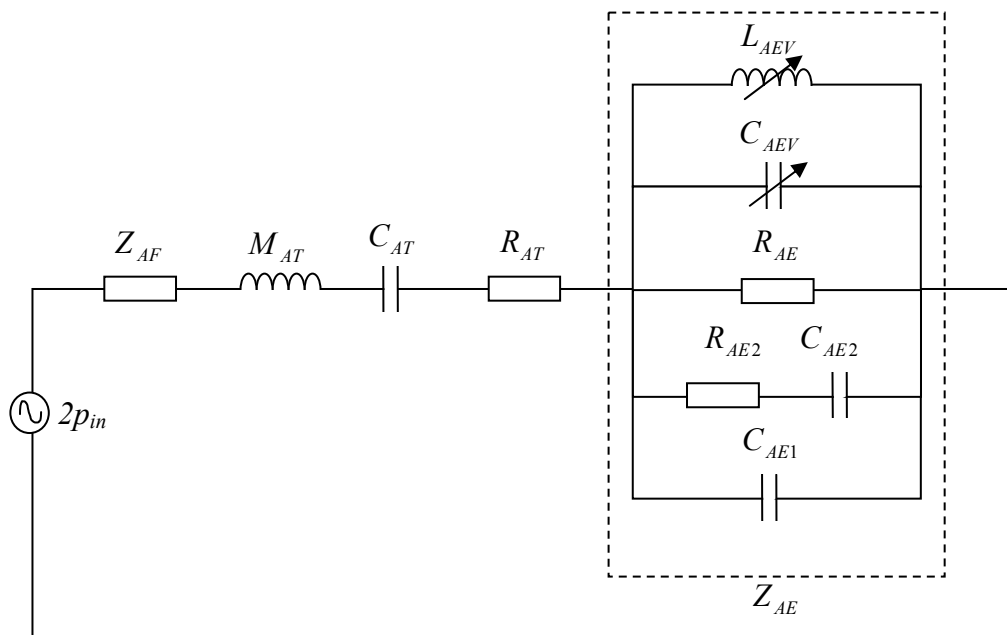


**Figure 6.17** Absorption curves changing inductive load on loudspeaker

When the load inductance  $L_{AEV}$  is small the impedance of  $C_{AEV}$  becomes very large according to equation 6.4, it can therefore be ignored for subsequent circuit analysis. Consequently current only flows through the other three parallel branches thus the circuit can be approximated by the closed circuit case with no additional passive electronics. Conversely if  $L_{AEV}$  is large the impedance of  $C_{AEV}$  becomes very small resulting in very little flow through the voice coil terms  $C_{AE1}$ ,  $C_{AE2}$ ,  $R_{AE2}$  and  $R_{AE}$ . In this case  $Z_{AE}$  tends to zero thus the circuit approximates to the open circuit case such that the motor impedance has no effect on the resonant characteristics of the absorber. These situations govern the limits of the setup. *Figure 6.17* demonstrates that with large inductances the circuit behaves as the closed circuit case and with small inductances as the open circuit case, intermediate inductance values cause frequency shifts in between these values in a similar way to using a capacitor. It is also possible obtain a higher resonant frequency than governed by the closed circuit condition where using a 10mH inductor causes a resonant frequency of 197Hz with an absorption coefficient of 0.96. The use of an inductor connected to the terminals of the loudspeaker consequently enables higher resonant frequencies but still achieving high absorption coefficients, it could therefore be profitable to combine more than one reactive component in order to achieve a wider bandwidth of absorption.

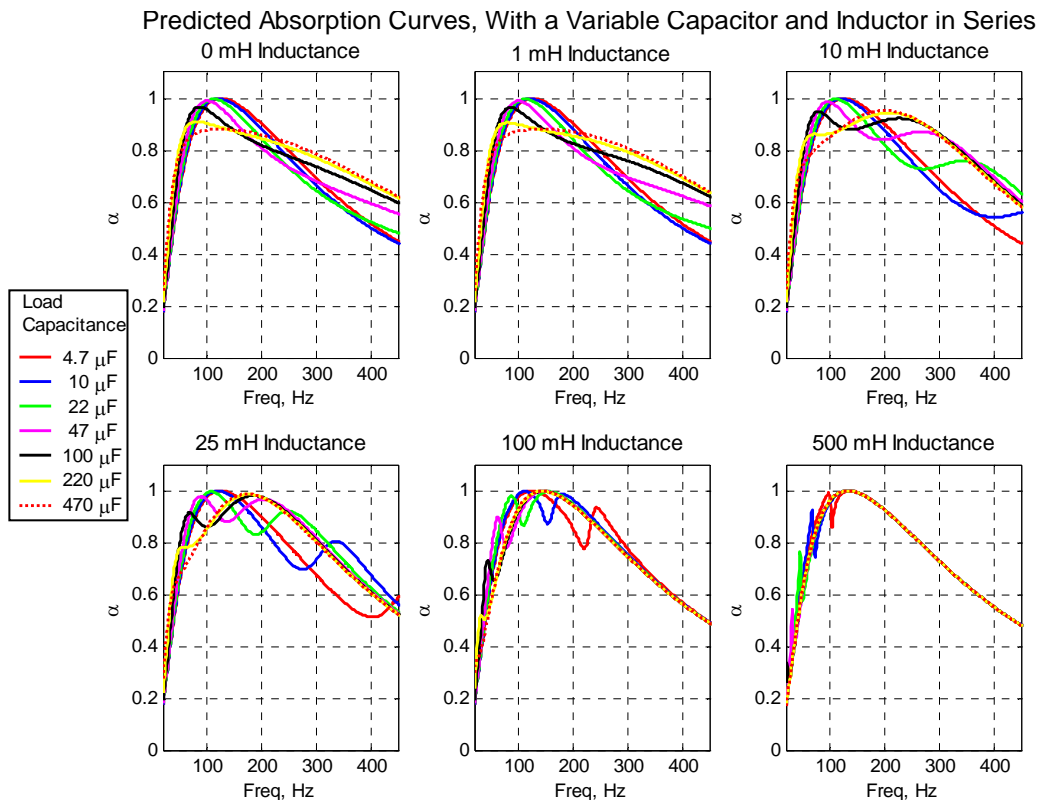
#### 6.4.4 A Variable Inductor and Capacitor in Series

In this section a variable inductor was modelled as connected in series with a variable capacitor, the equivalent circuit for this scenario is given by *Figure 6.18*. Utilising an inductor and a capacitor it was hoped that the advantages of both types of component could be exploited, the capacitor enabling lower frequency limits and the inductor enabling higher frequency limits, thus increasing the range of resonant frequencies.



**Figure 6.18** Equivalent circuit modelling a variable inductor in series with a variable capacitor connected to the terminals of the loudspeaker

With two reactive components in the circuit it is expected to have two resonances governed by the component values, as the passive electronic load now has an additional degree of freedom. *Figure 6.19* shows that this is the case with two resonant peaks when using a variable inductor in series with a variable capacitor. Using a large enough inductor means that the two resonant peaks occur in a similar frequency band such that the inductor enhances the low frequency effect of the capacitor. This additional degree of freedom provided by the inductor means that an increased range of frequencies can be obtained.

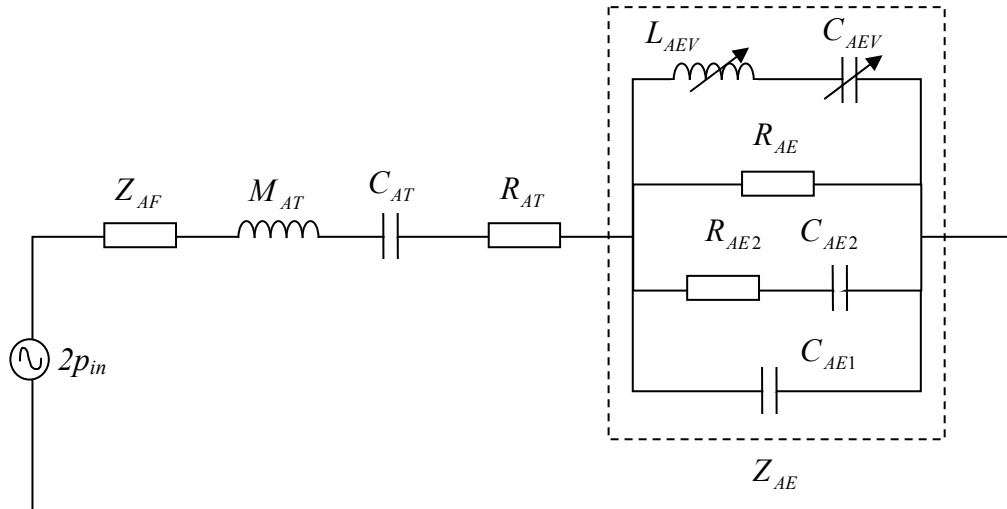


**Figure 6.19** Multi-plot of absorption trends with a variable inductive and capacitive load connected in series

*Figure 6.19* can be easily explained using the equivalent circuit in *Figure 6.18*. As  $L_{EV}$  is increased, the impedance of  $C_{AEV}$  decreases according to equation 6.4. If  $L_{EV}$  is increased still further the impedance of  $C_{AEV}$  approximates to that of a short circuit and the equivalent can be given by *Figure 5.15* which defines the terminals on the loudspeaker left open. In this case both the motor impedance terms and the variable capacitor have no effect on the resonant frequency of the system. With a small value of inductance the secondary resonant peak appears at a higher frequency not of interest in this application, however if the value of the inductor is increased, the advantages of using a variable inductor in series with variable capacitor can be seen. This series combination could be very useful as it enables a large bandwidth of absorption to be obtained, this can be seen especially clearly with a 10mH inductor in series with a 220 $\mu$ F capacitor. The resonance of the inductor is within very close proximity to the resonance as a result of the capacitor such that the final curve is a combination of these two, leading to a large bandwidth of absorption. This results in over 2.5 octaves (from 50-335Hz) of absorption coefficients above 0.8.

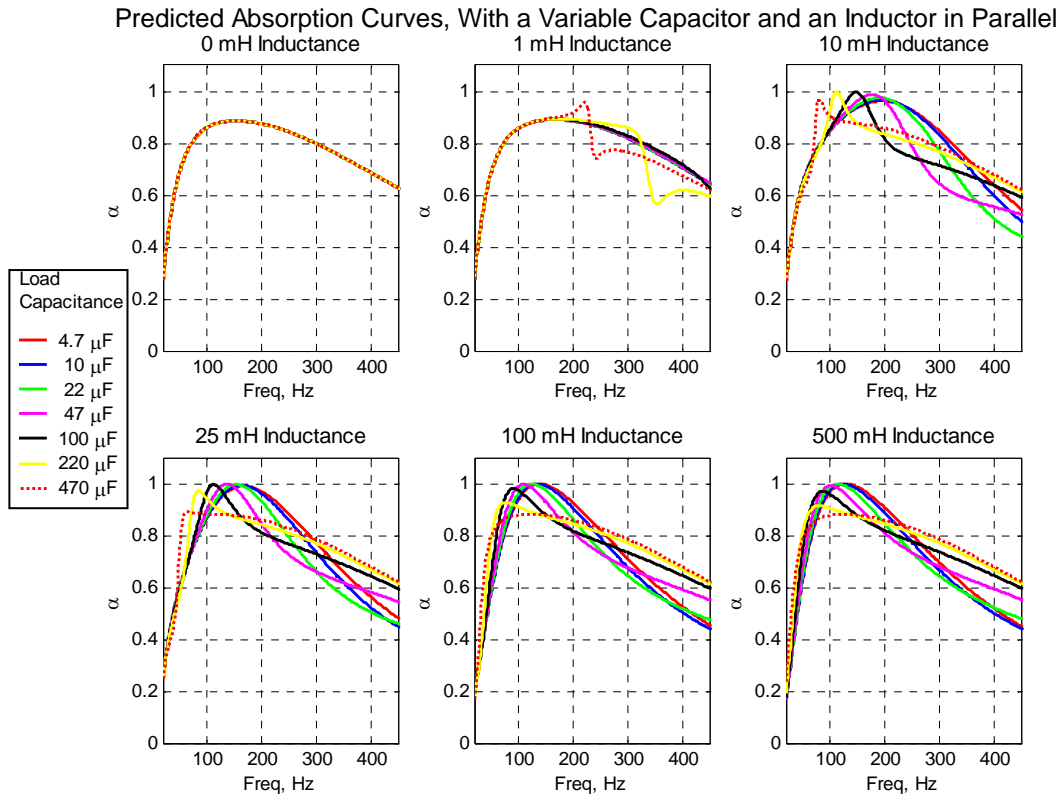
#### 6.4.5 A Variable Inductor and Capacitor in Parallel

A variable inductor in parallel with a variable capacitor can also be added as a passive impedance load to the driver, the equivalent circuit then becomes as *Figure 6.20*. Modelling a variable inductor and capacitor in parallel it was hoped it was possible to increase still further the tunability of the absorber system:



**Figure 6.20** Equivalent circuit modelling a variable capacitor in parallel with a variable inductor connected to the terminals of the loudspeaker

In this case, when  $L_{EV}$  is decreased the impedance of  $C_{AEV}$  increases, consequently less current flows through that branch of the circuit. When  $L_{EV}$  is zero this branch becomes tantamount to an open circuit according to equation 6.4 thereby,  $Z_{AE}$  is governed only by the original motor impedance terms. This corresponds to the situation when the loudspeaker terminals are connected together. When  $L_{EV}$  is increased, the impedance of  $C_{AEV}$  becomes negligible and the impedance is controlled by  $C_{EV}$  such that the equivalent circuit approximates the simple case of a capacitor connected across the terminals as given by *Figure 6.21*.



**Figure 6.21** Multi-plot showing predicted absorption trends with a variable inductor and capacitor connected in parallel to the terminals of the loudspeaker

Results show that by using a capacitor in parallel with an inductor enables a lower resonant frequency than simply using a capacitor on its own. The optimally low resonant frequency is seen when a 25mH inductor is connected in parallel with a 470 $\mu$ F capacitor, this demonstrates a resonant frequency of 65Hz, with an absorption coefficient in excess of 0.85. The maximum resonant frequency obtained using this technique is 223Hz, this corresponds to a maximum resonant frequency shift of 70%.

Using a capacitor in parallel with an inductor has been seen to provide a very significant shift in resonant frequency and as such could be very useful in the creation of a versatile membrane absorber for room acoustic applications.

#### 6.4.6 Summary

Section 6.4 has demonstrated several complex electrical impedance loads that could be connected to the terminals of the loudspeaker-absorber to increase its adaptability. Four special cases can hence be outlined with distinct advantages in the absorption of sound.

Firstly, simply adding a capacitor to the terminals has the effect of lowering the system's overall resonant frequency. This resonant frequency can then be reduced and indeed increased further by the addition of an inductor in parallel, increasing the degree of freedom of the system and allowing for a greater range of resonant frequencies to be obtained. Thirdly connecting a resistor across the terminals of the loudspeaker alters the Q-factor of the resonance, a decrease in resistive load increasing the Q-factor. This is important as it defines how much acoustic energy the absorber will absorb at the chosen frequency. The final important case is that of an inductor connected in series with a capacitor, this is an important case as it results in a broad bandwidth of absorption, something keenly sort after by the room acoustician.

Further scenario's of electronic load impedances could also be modelled using more than two reactive and resistive components to create more complex resistive loads thus optimising the absorber for the required task but of primary concern here is the simple case of up to two reactive and resistive components shown in the four important scenario's above.

### **6.5 Optimising the Passive Electronic Load for a Given Set of Driver Parameters**

In order to be able to fine tune the absorber system such that it achieves maximum absorption at a set resonant frequency or with a specified Q-factor it is important to ascertain what component values must be used in order to achieve the desired results. This section outlines methods of determining capacitance and resistance values to be able to achieve specific resonant frequencies and Q-factor's based on a single component load. This is the first step towards an automated system which could adaptively change the passive electronic load presented to the driver given a certain input frequency spectrum. A microphone could be used to determine the fundamental frequency incident to the driver or that is problematic in a room and some intelligent hardware could change a combination of electronic components connected to the terminals accordingly, such that the absorption characteristics were optimum for that room. On a more simplistic level, if this design of membrane absorber were to be marketed it would be important to know what capacitance, inductance or resistance was needed to shift the resonant frequency or Q-factor to avoid iterations in design of the absorber.

### 6.5.1 Determining the Capacitance Needed for a Certain Resonant Frequency

Finding the capacitance value needed for a given resonant frequency can be done by using equations determined from the equivalent circuit analysis. Forming an equation for when the imaginary part of the surface impedance equals zero, namely when the system resonates, allows a graph to be plotted of resonant frequency versus capacitance such that the optimum capacitance can be determined for a desired resonant frequency.

For the simple case of an electrical circuit with an inductor, capacitor and resistor (an LCR circuit) in series or in parallel such as is represented by the open circuit condition it is a simple matter to determine the resonant frequency of the system by setting the imaginary part to zero such that:

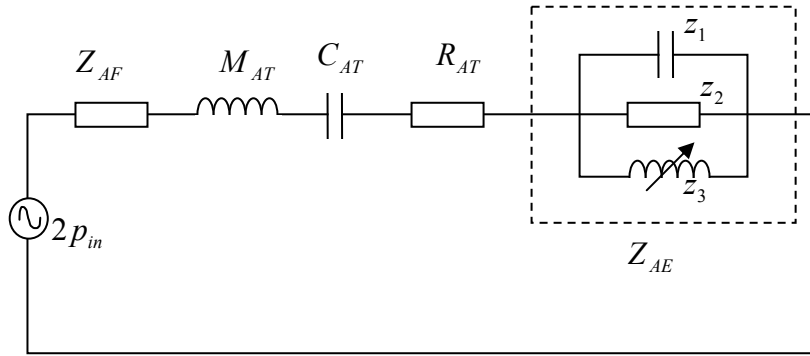
$$j\omega_{res}M_{AT} = -\frac{1}{j\omega_{res}C_{AT}}$$

$$\omega_{res} = \frac{1}{\sqrt{M_{AT}C_{AT}}}$$
(6.5)

As such it is not difficult to determine the capacitance value needed to result in a given resonant frequency. For the equivalent circuit in *Figure 6.10* it is a slightly more complicated problem. The parallel LCR circuit making up the complex impedance  $Z_{AE}$ , in series with the other impedances means that more attention needs to be paid to the problem.

Using a simplified formulation of the motor impedance valid for low frequencies but less accurate for higher frequencies, *Figure 6.10* can be written in the form of *Figure 6.22* so that  $Z_{AE}$  become the parallel addition of three complex impedances,  $z_1$ ,  $z_2$  and  $z_3$ , the circuit then becomes:





**Figure 6.22** Equivalent circuit of absorber system with simplified motor impedance terms and variable capacitor connected to terminals

Where,

$$z_1 = \frac{1}{j\omega \left( \frac{L_E S_D^2}{(Bl)^2} \right)} = \frac{1}{j\omega C}, \quad z_2 = \frac{(Bl)^2}{R_E S_D^2} = R, \quad z_3 = j\omega \left( \frac{C_E (Bl)^2}{S_D^2} \right) = j\omega L \quad (6.6)$$

And

$$Z_{AE} = \left( j\omega C + \frac{1}{R} + \frac{1}{j\omega L} \right)^{-1} = \frac{j\omega LR}{R - \omega^2 LCR + j\omega L} \quad (6.7)$$

Multiplying top and bottom by complex conjugate,  $R - \omega^2 LCR - j\omega L$

Gives:

$$Z_{AE} = \frac{j(\omega LR^2 - \omega^3 L^2 CR^2) + \omega^2 L^2 R}{R^2(1 - 2\omega^2 LC + \omega^4 L^2 C^2) + \omega^2 L^2} \quad (6.8)$$

So taking just the imaginary part of  $Z_{AE}$

$$\text{Im}(Z_{AE}) = \frac{\omega LR^2 - \omega^3 L^2 CR^2}{R^2(1 - 2\omega^2 LC + \omega^4 L^2 C^2) + \omega^2 L^2} \quad (6.9)$$

Therefore the imaginary parts of the entire system can be given as:

$$\text{Im}(Z_{tot}) = \frac{\omega^2 M_{AT} C_{AT} - 1}{\omega C_{AT}} + \frac{\omega L R^2 - \omega^3 L^2 C R^2}{R^2(1 - 2\omega^2 L C + \omega^4 L^2 C^2) + \omega^2 L^2} \quad (6.10)$$

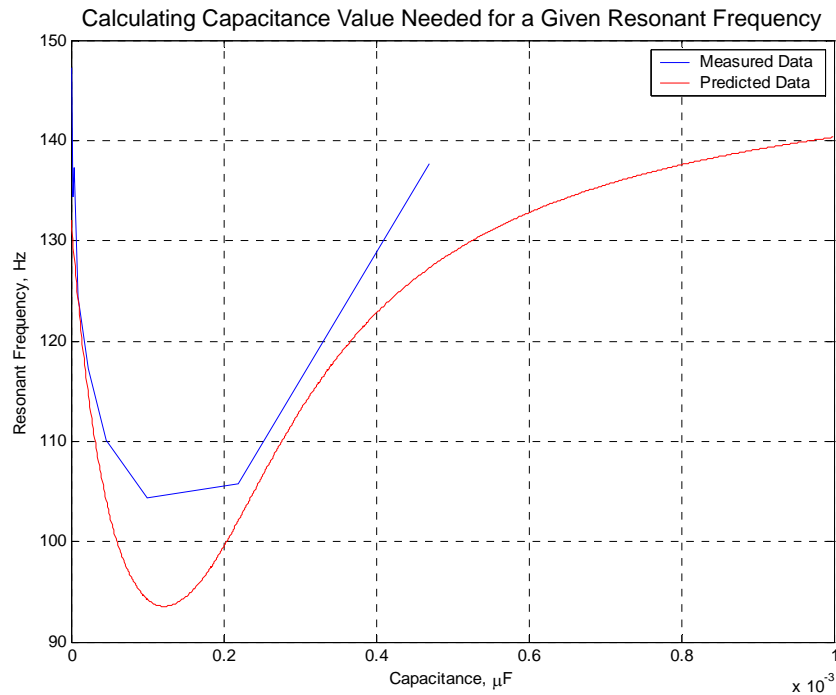
The system resonates when the imaginary component is zero such that:

$$\begin{aligned} \frac{\omega_{res}^2 M_{AT} C_{AT} - 1}{\omega_{res} C_{AT}} &= - \frac{\omega_{res} L R^2 - \omega_{res}^3 L^2 C R^2}{R^2(1 - 2\omega_{res}^2 L C + \omega_{res}^4 L^2 C^2) + \omega_{res}^2 L^2} \\ \therefore (\omega_{res}^2 M_{AT} C_{AT} - 1) (R^2(1 - 2\omega_{res}^2 L C + \omega_{res}^4 L^2 C^2) + \omega_{res}^2 L^2) &= (\omega_{res}^3 L^2 C R^2 - \omega_{res} L R^2) (\omega_{res} C_{AT}) \end{aligned} \quad (6.11)$$

Expanding this gives a quadratic in L so that:

$$\begin{aligned} L^2 (\omega_{res}^6 M_{AT} C_{AT} C^2 R^2 - \omega_{res}^4 (C_{AT} C R^2 + M_{AT} C_{AT} - R^2 C^2) - \omega_{res}^2) + \dots \\ L (\omega_{res}^4 (-2M_{AT} C_{AT} R^2 C) - \omega_{res}^2 (2R^2 C + C_{AT} R^2)) + \dots \\ R^2 (\omega_{res}^2 M_{AT} C_{AT} - 1) = 0 \end{aligned} \quad (6.12)$$

Finding the roots of this equation allows  $L$  to be determined for a given resonant frequency,  $\omega_{res}$ . The capacitance value needed can then be determined from equation 6.6. Plotting how the resonant frequency changes with capacitance yields the following graph shown in *Figure 6.23*:



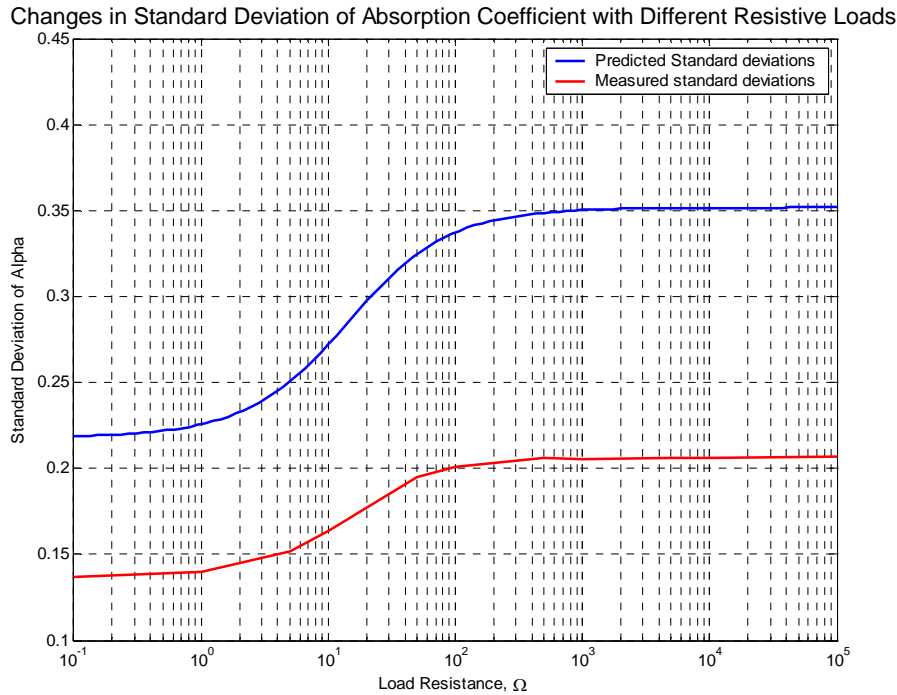
**Figure 6.23** Resonant frequency versus capacitance value to determine the component value needed for a given resonant frequency

Comparing the measured and predicted curves it is seen that the trend of behaviour of the absorber with changing capacitance is accurately predicted by the equivalent circuit model. The curve shows that the system initially resonates at the condition governed by the open circuit case with zero capacitance. As the capacitive load increases the resonant frequency decreases correspondingly. As the capacitive load increases still further, the impedance decreases and the circuit tends towards the closed circuit condition and consequently the resonant frequency rises again as the capacitor has less effect and resonance is controlled by the other motor impedance terms. An optimum capacitance value for the lowest resonant frequency can be found by computing the turning point of the above curve.

### 6.5.2 Determining How the Q-factor Changes With Resistance

Determining the Q-factor achieved by the addition of a specific value of resistance is not as simple on first sight as determining the capacitance needed for specific resonant frequencies. In order to find the Q-factor the 3dB down points need to be known either side of the resonant peak, this not so straight forward to express mathematically therefore a different method of determining the Q-factor of the resonance was used.

This was to determine the standard deviation of the absorption curve as shown in *Figure 6.24*.

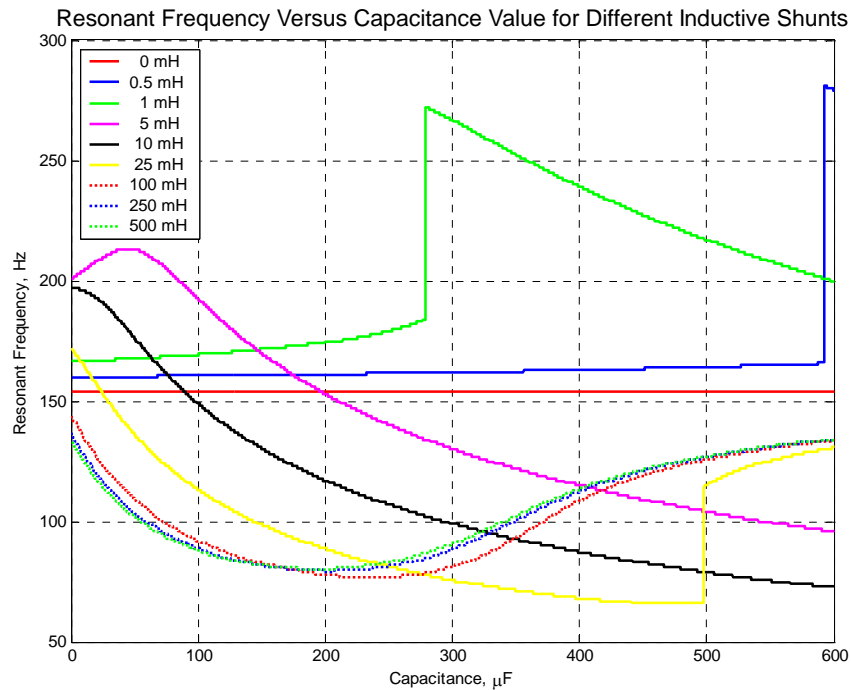


**Figure 6.24** Standard deviation changes in absorption curve for different load resistances on loudspeaker terminals, a comparison between measurement and prediction

Results show a similar trend in prediction and model of change in standard deviation with resistive loads on the loudspeaker. There is an offset between the measurements and prediction which, as outlined in section 5.4.1, is a result of limitations in the lumped parameter model such that it cannot predict resonances above the fundamental resonance, resulting in the model predicting broader Q-factors. The trend of behaviour is however accurately predicted, enabling the model to be used to adjudicate change in Q-factors. The prediction shows a change in absorption standard deviation of 38% and the measurement of 34%.

### 6.5.3 Determining the Optimum Shunt Inductance of a Capacitor

Defining an equation to determine the optimum combination of inductance and capacitance is quite involved but can be achieved by a simple graph of resonant frequency versus capacitance with different inductive shunts, done in MATLAB, demonstrating the lowest frequency obtainable using an inductor in parallel with a capacitor.



**Figure 6.25** Resonant frequencies of absorber with varying capacitance and inductance in parallel connected to the loudspeaker terminals

*Figure 6.25* demonstrates that an optimally low resonant frequency can be obtained using a 25mH inductor in parallel with a 470 $\mu$ F capacitor. It also shows that it is possible to achieve a high frequency limit for the fundamental resonant frequency, which is below 250 Hz. This is achieved using 5mH inductor in parallel with a 47 $\mu$ F capacitor.

## 6.6 Conclusion

This chapter has outlined the principles, measurement and modelling of changing a passive electronic load to a loudspeaker absorber system. Results demonstrate that the addition of a variable resistor enables a change in standard deviation of absorption of 34%. This would be suitable for a situation where maximum absorption would not be ideal, for example if the problem was not too severe or if a wider bandwidth is more highly sought after than maximum absorption.

The addition of a single capacitor had the effect of lowering the overall resonant frequency of the system. A graph of resonant frequency versus capacitance value can be constructed from equations of surface impedance that allows the determination of the

correct capacitance to achieve a specific resonant frequency. A decrease in resonant frequency was shown to the detriment of maximum absorption and hence a wider Q-factor, but still absorption coefficients in excess of 0.6 were shown over a wide bandwidth. The maximum resonant frequency shift was obtained using a 100 $\mu$ F capacitor; the change in frequency corresponded to a 39% decrease.

Further passive electronic loads were modelled and it was hence shown that a resistor and capacitor combination lead to a trade off between desired low frequency performance and Q-factor, thus a combination of resistors and capacitors was not found to be useful. Combining a shunt inductor with a capacitor however increased the system to that of two degrees of freedom, as such two resonant peaks could be observed, one as a result of the inductive load and the other as a result of the capacitive load. Applying a large enough inductance meant that the two resonant peaks could coincide with each other such that a lower frequency limit could be obtained. It was shown that resonant frequency shifts in excess of 65% could be achieved by using this technique.

Graphs were presented of component value versus resonant frequency for single capacitors and for a parallel combination of inductors and capacitors. Another graph was shown of the change in Q-factor with varying load resistance. These graphs can be used to select component values for a specific loudspeaker to fit with a desired application/ room and as such can be used to optimise the performance of the absorber and can be considered as the first steps towards a system that could actively change the passive electronic load on the terminals.

Using passive electronics to change the resonant characteristics of a loudspeaker absorber has been shown to very effective, demonstrating a large degree adjustment, suggesting suitability for room acoustic applications for the absorption of room modes.

## **7. FINAL CONCLUSIONS AND FURTHER WORK**

### **7.1 Final conclusions**

Two methods of improving membrane absorbers have been presented, through both measurement and prediction. The first method utilised the surround of a loudspeaker as the mounting for a resonating plate in the absorber. The resonating mass was shown to move pistonically such that its moving mass was increased, thus lowering its resonant frequency. Results and predictions both showed that the fundamental resonant frequency of the absorber could be dramatically lowered using this technique with shifts of 42% measured for a hardboard plate. It was shown that a lower frequency absorber system could be formed using the same materials and enclosure but simply changing the mounting conditions of the plate. Results and predictions demonstrated that it is possible to create an absorber with a pistonically mounted plate that resonates at lower frequency than a clamped mounted plate even when the depth of the backing was a third

of that used in the clamped case. This demonstrated a useful application of this mounting technique, allowing membrane absorbers to be built with much smaller dimensions whilst still exhibiting the same low frequency behaviour. Another advantage of mounting a plate or membrane using loudspeaker surround is that enables more accurate prediction of the system's resonant frequency before the absorber is built, this means that it can be designed for a specific application and the user can be confident that it will be tuned to the right frequency when it is built. It was shown that measurements on the pistonically mounted plate yielded results that matched favourably to predictions using both the standard membrane absorber design equations and a transfer matrix model. Conversely the clamped condition produced sizable errors in the resonant frequencies predicted when compared with measurements as expected.

The second method of improving membrane absorbers used a complete loudspeaker system in reverse such that sound incident to the diaphragm forced it into oscillation in sympathy to the amplitude and frequency of the incident wave; the energy of such oscillation was then absorbed by porous damping in the loudspeaker cabinet. Results showed that high absorption coefficients could be obtained at the system's fundamental resonance. It was further showed that the addition of a passive electronic load across the loudspeaker terminals enabled the resonant characteristics of the absorber to be changed. Adding a reactive component had the effect of altering the resonant frequency where as the addition of resistive components changed the magnitude of absorption and the Q-factor of the system's resonance. An equivalent circuit model was demonstrated that allowed many design permutations to be modelled. This model enabled the optimisation of an absorber given a specific driver. It was shown both experimentally and through predictions that it is possible to achieve a variable frequency membrane absorber with resonant frequency shifts of up to 39% using a single capacitor. Predictions also showed that changes between maximum and minimum resonant frequencies of over 65% were possible with the addition of capacitor and inductor in parallel. Connecting a variable capacitor in series with a variable inductor was shown to produce an absorber with an effective absorption bandwidth of 2.5 octaves; a useful case for room acoustic applications. The addition of a resistor enabled changes in Q-factor of 38%. Thus a highly variable absorber system was presented with the ability to tune the absorber for a specific application. Using a loudspeaker as an absorber



consequently means it could be transferred to a different room and be tuned to be maximally efficient, without having to change its physical construction.

## **7.2 Further work**

Further areas of research subsequent to this thesis would be to turn the aforementioned improved membrane absorbers into marketable products. Mounting a plate/membrane onto a loudspeaker surround has been shown to produce good results and a low frequency shift in resonant frequency, a problem with this is that loudspeakers are often circular; this is an impractical shape if attempting to treat an entire room, as circles do not tessellate. A further disadvantage to using a loudspeaker surround itself is that manufacturing costs would be high relative to currently available designs. Consequently it would be profitable to examine methods of manufacturing membrane absorbers that could utilise the principles of pistonic oscillation of the loudspeaker surround system without using surrounds themselves. Rectangular absorbers could be made which exhibit the advantages of pistonic movement but also achieve economy of manufacture and area. One method that could be adopted would be to manufacture membrane out of a molded rubber compound such that the 'surround' mounting is molded from the same piece of rubber as the membrane itself. This would greatly reduce manufacturing costs and would allow pistonic oscillation of the membrane. It would also mean that absorbers could be made to any shape or size relatively easily.

Using a loudspeaker as a membrane absorber could be very useful and opens up several avenues of further research. Firstly a product could be marketed as an add-on to a loudspeaker to enable a user to turn any loudspeaker into an optimised passive absorber. The box of electronics could contain a DSP chip allowing the determination of the small signal parameters of the loudspeaker which it could subsequently be used to perform calculations given the cabinet size to determine the range of available resonant frequencies available with the specific loudspeaker. With passive electronics within the box the user would simply have to turn a knob to tune it to the right frequency (a variable reactive load) and turn a knob to change the Q-factor. Extensions to this could be to provide a microphone and a deterministic noise source generator allowing the measurement of a room's frequency response at the location of the absorber. A DSP chip could again be used to determine the most problematic frequency range and could

adjust the electronic load accordingly to deal with the problem most efficiently. The additional box could allow any obsolete loudspeaker to be used as a controlled absorber within a room. In a typical studio setup there is often a selection of different loudspeakers used at different times and for different projects, the additional box would allow any of them to be turned into controlled absorbers when not being used.

Further extensions to this work could also be to design a ‘semi active’ absorber system which could utilise a microphone to continually sample the frequency response just in front of the absorber and change the passive electronic load in real time such that the most efficient absorption could always be achieved.

Further work could also include the investigation of mounting Helmholtz absorbers on a loudspeaker surround to extend the low frequency performance still further.

**REFERENCES**

- [1] H. Kuttruff, *Room Acoustics*, 4th edn, Spon Press (2000).
- [2] M. Barron, “The subjective effects of first reflections in concert halls – the need for lateral reflections”, *J. Sound Vib.*, 15, pp475-494, (1971).
- [3] F. A. Everest, *Master Handbook of Acoustics*, 4th edn McGraw-Hill, (2001).
- [4] T. J. Cox and P. D’Antonio, “Room Optimizer: A Computer Program to Optimize the Placement Listener, Loudspeakers, Acoustical Surface Treatment, and Room Dimensions in Critical Listening Rooms”, *Proc. 103<sup>rd</sup> Convention Audio Eng. Soc*, Reprint 4555 (1997).
- [5] M. Karjalainen, P. Antsalo, A. Mäkivirta and V. Välimäki, “Perception of Temporal Decay of Low-Frequency Room Modes”, *Poster 116<sup>th</sup> Convention Audio Eng. Soc* (2004).
- [6] M. R. Avis, “The Active Control of Low Frequency Room Modes”, PhD thesis, University of Salford, UK (1995).
- [7] L. Cremer and H. A. Müller, *Principles and Applications of Room Acoustics, Vol 2*. Applied Science Publishers translated by T. J. Schultz (1987).
- [8] T. J. Cox and P. D’Antonio, *Acoustic Absorbers and Diffusers*, Spon Press (2003).
- [9] K. V. Horoshenkov, “Characterisation of Acoustic Porous Materials”, *Proc. IoA (UK)*, 28 (1) pp15-38, (2006).
- [10] M. E. Delany and E. N. Bazley, “Acoustical properties of fibrous absorbent materials”, *Appl. Acoust.*, 3, pp105-116, (1970).
- [11] ISO 9053:1991 “Acoustics - Materials for acoustical applications - Determination of airflow resistance”.

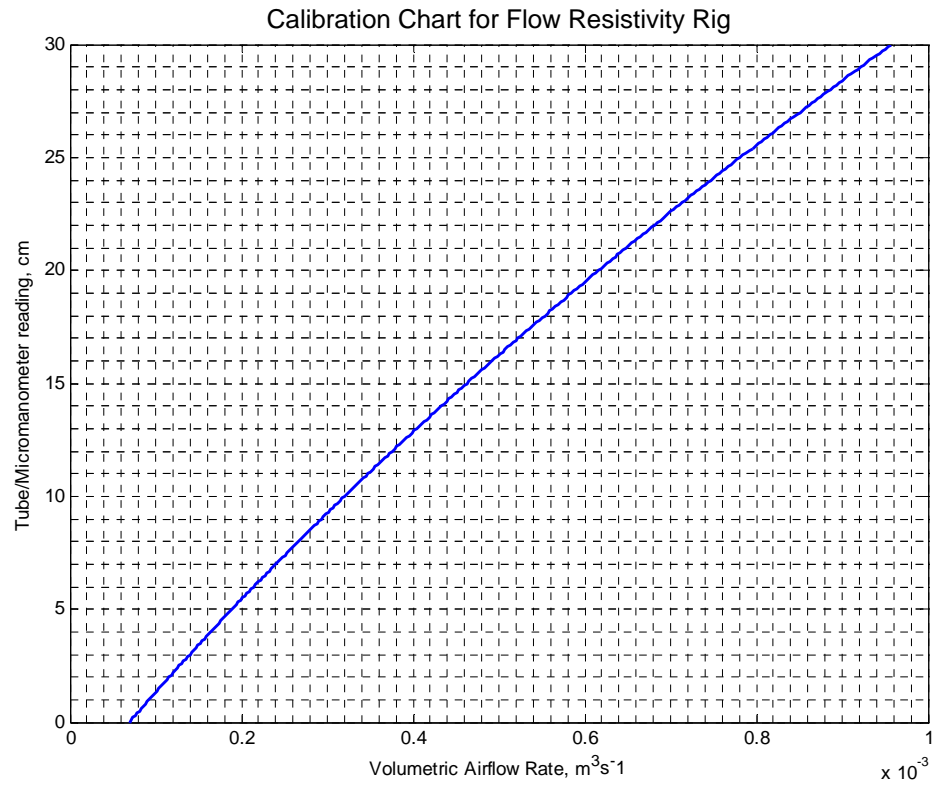
- [12] R. Kirby and A. Cummings , “Prediction of the bulk acoustic properties of fibrous materials at low frequencies”, *Appl. Acoust.*, 56 pp101-125, (1999).
- [13] J. F Allard and Y. Champoux , “New empirical equations for sound propagation in rigid frame fibrous materials”, *J. Acoust. Soc. Am.*, 91(6) pp3346-3353, (1992).
- [14] J. F. Allard, *Propagation of Sound in Porous Media: Modelling Sound Absorbing Materials*, Elsevier Applied Science (1993).
- [15] L.E Kinsler, A.R. Frey, A.B. Coppens and J.V. Sanders, *Fundamentals of Acoustics*, 3<sup>rd</sup> Edition, Wiley and Sons 1982.
- [16] R. D. Ford and M. A. McCormick, “Panel Sound Absorbers”, *J. Sound. Vib.*, 10(3), pp411-423 (1969).
- [17] F.P. Mechel, “Panel Absorber”, *J. Sound. Vib.*, 248(1), pp 43-70 (2001).
- [18] W. C. Sabine, *Collected Papers on Acoustics*, Harvard University Press (1922), republished, Acoustical Society of America (1993).
- [19] ISO 354:2003 “Acoustics — Measurement of sound absorption in a reverberation room”.
- [20] ISO 10534-1:2001 “Acoustics — Determination of sound absorption coefficient and impedance in impedance tubes — Part 1: Standing Wave Method”.
- [21] ISO 10534-2:2001 “Acoustics — Determination of sound absorption coefficient and impedance in impedance tubes — Part 2: Transfer-function method”.
- [22] D. D. Rife and J. Vanderkooy, “Transfer-function measurement with maximum length sequences”, *J. Audio Eng. Soc.*, 37(6) pp419-444, (1989).

- [23] Y. Cho, "Least Squares Estimation of Acoustic Reflection Coefficient", PhD thesis, University of Southampton, UK (2005).
- [24] A. Liessa, *Vibration of Plates*, Acoustical Society of America (1969), Originally issued by NASA, (1973).
- [25] F.P. Mechel, *Formulas of Acoustics*, Springer-Verlag, (2002).
- [26] D. D. Rife, MLSSA SPO Reference Manual Version 4WI Rev 8, DRA Laboratories, copyright 1991-2005.
- [27] M. Rossi, *Acoustics and Electroacoustics*, Artech house, (1988).
- [28] K. Sato and M. Koyasu, "On the new reverberation chamber with nonparallel walls (studies on the measurement of absorption coefficient by the reverberation chamber method II)", *J. Phys. Soc. Japan* 14(5) pp. 670-677, (1959).
- [29] K. Stahl, "Synthesis of loudspeaker mechanical properties by electrical means: A new way of controlling low-frequency loudspeaker behaviour", *J. Audio Eng. Soc.*, vol 29(9), pp. 598-596, (1981).
- [30] L.L Beranek, *Acoustics*, Acoustical Society of America, (1996).
- [31] A.N. Thiele, "Loudspeakers in vented Boxes", Parts I and II, *J. Audio Eng. Soc.*, 19, pp.382-392 (May 1971); pp. 478-483 (June 1971).
- [32] R.H. Small, "Direct-Radiator Loudspeaker System Analysis", *J. Audio Eng. Soc.*, 20, pp.383-395 (1972).
- [33] J.R. Wright, "An Empirical Model for Loudspeaker Motor Impedance", *J. Audio Eng. Soc.*, 38(10), pp749-754, (1991).

- [34] J. Vanderkooy, "A model of Loudspeaker Driver Impedance Incorporating Eddy Currents in the Pole Structure", *J. Audio Eng. Soc.*, 37(3), pp 119-128, (1998).
- [35] J. R. Ashley and M. D. Swan, "Experimental Determination of Low-Frequency Loudspeaker Parameters", *Loudspeakers 1, Audio Eng Soc Anthology*, (1978).
- [36] D. Clark, "Precision Measurement of Loudspeaker Parameters", *J. Audio Eng. Soc.* 45, pp.129 – 140, (1997).
- [37] J. C. Cox, "A Comparison of Loudspeaker Driver Parameter Measurement Techniques," *Proc – IMTC 85, IEEE Instrumentation and Measurement Technology Conference*, pp. 254-258, (1985).
- [38] J. Borwick, *Loudspeaker and Headphone Handbook*, 2<sup>nd</sup> edn, Butterworth-Heinemann Ltd, pp.45, (1994).
- [39] F. Lui, S. Horowitz, *et al*, "A Tunable Helmholtz Resonator", *9<sup>th</sup> AIA/CEAS Aeroacoustics Conference and Exhibit*, (2003).
- [40] H. F. Olson and E. G. May, "Electronic Sound Absorber", *J. Acoust, Soc, Am.*, 25, pp.1130-1136, (1953).
- [41] G. C. Nicholson, "The active control of acoustic absorption coefficient, reflection and transmission", *Proc. IoA (UK)*, 15(3), pp.403-409 (1993).
- [42] R. Kashani and J. Wischmeyer, "Electronic Bass Trap", *Proc. 117<sup>th</sup> Convention Audio Eng. Soc*, Reprint 6277 (2004).
- [43] J. D. Kemp and R. L Clark, "Noise reduction in a launch vehicle fairing using actively tuned loudspeakers", *J. Acoust. Soc. Am.*, 113(4) pt 1 (2003).

## APPENDIX A

Calibration chart for flow resistivity measurement apparatus:



The above line can be represented by the equation

$$q_v = 6.9240 \times 10^{-5} + 2.2803 \times 10^{-5} y + 2.2725 \times 10^{-7} y^2$$

Where  $y$ , is the manometer reading in cm.

## APPENDIX B

Verifying results from large tube with small tube results and prediction.

```

close all
clear all

[I1,Fs]=LOADIMP('bigA.wmb');           % Loading WINMLS mic1 file into matlab
[I2,Fs]=LOADIMP('bigB.wmb');
[I3,Fs]=LOADIMP('bigC.wmb');
[I4,Fs]=LOADIMP('bigD.wmb');

%_PROCESSING RESULTS FROM LARGE IMPEDANCE TUBE_%

t = [(1:length(I1))/Fs];               % Generate time series
N = length(I1);                       % Length of file in samples
w = hanning(N);                       % Generate hanning window
w(1:round(N/2)) = 1;                  % assign first half of window to unity

h1 = I1.*w;                           % Windowed impulse responses
h2 = I2.*w;
h3 = I3.*w;
h4 = I4.*w;

z1 = 0.184;                            % Position of mic 1 from the sample
z2 = 0.368;                            % Position of mic 2 from the sample
z3 = 0.9143;                           % Position of mic 3 from the sample
z4 = 1.2255;                           % Position of mic 4 from the sample
y = [z1 z2 z3 z4];                    % Array of mic positions

rho = 1.21;                            % Density of air
d = 0.3458;                            % Tube diameter
N1 = length(I1);                      % Length, in samples, of the input signal
Nft = 2^16;                            % Number of frequency points
f = (Fs*(0:(Nft-1)/2))/(Nft-1);       % Defining frequency axis
c = 343;                                % Speed of sound in air
k = (2*pi*f)/c;                       % Wavenumber in air

flength = length(f);
df = max(f)/flength;

spacingA = abs(y(2)-y(1));
spacingB = abs(y(3)-y(2));
spacingC = abs(y(4)-y(1));

fu1A = c/(2*d);                        % Tube high frequency limit as result of tube diameter
fu2A = (0.45*c)/spacingA;              % Frequency limit as a result of mic spacing
fuA = min(fu1A,fu2A);                  % Pick the lowest upeer frequency limit
flA = 0.05*c/spacingA;                 % Low frequency limit as a result of mic spacing

fu1B = c/(2*d);
fu2B = (0.45*c)/spacingB;
fuB = min(fu1B,fu2B);
flB = 0.05*c/spacingB;

fu1C = c/(2*d);
fu2C = (0.45*c)/spacingC;
fuC = min(fu1C,fu2C);

```



```

flC = 0.05*c/spacingC;

h1_fft = fft(h1,Nft);           % Fourier transform of impulse response
h1freq = h1_fft(1:((Nft)/2));   % Get rid of negative frequencies
h2_fft = fft(h2,(Nft));
h2freq = h2_fft(1:((Nft)/2));
h3_fft = fft(h3,(Nft));
h3freq = h3_fft(1:((Nft)/2));
h4_fft = fft(h4,(Nft));
h4freq = h4_fft(1:((Nft)/2));

H12 = h1freq./h2freq;           % Transfer functions
H13 = h2freq./h3freq;
H14 = h1freq./h4freq;

RA = (H12-exp(-j*k*spacingA)).*exp(2*j*k*y(2))./(exp(j*k*spacingA)-H12); % Reflection factor
zA = (rho*c)*((RA + 1)./(1 - RA)); % Surface impedance
alphaA = (1-abs(RA).^2); % Absorption coefficient

RB = (H13-exp(-j*k*spacingB)).*exp(2*j*k*y(2))./(exp(j*k*spacingB)-H13);
zB = (RB + 1)./(1 - RB);
alphaB = (1-abs(RB).^2);

RC = (H14-exp(-j*k*spacingC)).*exp(2*j*k*y(2))./(exp(j*k*spacingC)-H14);
zC = (RC + 1)./(1 - RC);
alphaC = (1-abs(RC).^2);

fuAs = fuA/df; % Maximum and minimum frequency limits in samples for eases of plotting
flAs = flA/df;
fuBs = fuB/df;
flBs = flB/df;
fuCs = fuC/df;
flCs = flC/df;

%_PROCESSING RESULTS FROM SMALL IMPEDANCE TUBE_%

[h1D,FsD]=LOADIMP('smallA.wmb');
[h2D,FsD]=LOADIMP('smallB.wmb');

z1D = 0.1; % Mic positions of small tube
z2D = 0.15;

yD = [z1D z2D]; % Mic distances from sample
spacingD = yD(2)-yD(1); % Microphone spacing

N1D = length(h1D); % Length in samples of the input signal
t = [(1:1:length(h1D))/FsD];
wD = hanning(N1D); % Generate hanning window
wD(1:round(N1D/2)) = ones(round(N1D/2),1); % Assign first half of window to unity

imp1D = h1D.*wD; %windowed impulse resopnse
imp2D = h2D.*wD;

fD = (FsD*(0:((N1D-1)/2))/(N1D-1))'; % Frequency series
k = 2*pi*fD/c;
lengthD = length(fD);
dfD = max(fD)/lengthD; % Frequency interval in samples
fu1D = 5.58*c/0.05;
fu2D = 0.45*c/spacingD;
fuD = min(min(fu1D,fu2D),fD(lengthD));

```

```

flD = 0.05*c/spacingD;
fuDs = fuD/dfD;
flDs = flD/dfD;

h1_fftD = fft(imp1D,N1D);           % FFT of impulse
h1freqD = h1_fftD(1:((N1D)/2));

h2_fftD = fft(imp2D,(N1D));
h2freqD = h2_fftD(1:((N1D)/2));

H12D = h1freqD./h2freqD;           % Transfer function

RD = (H12D-exp(-j*k*spacingD)).*exp(2*j*k*y(2))./(exp(j*k*spacingD)-H12D);
zD = (rho*c)*((RD + 1)./(1 - RD));

alphaD = (1-abs(RD).^2);

figure(1)
plot(f(flAs:fuAs),alphaA(flAs:fuAs),'r',...
     f(flBs:fuBs), alphaB(flBs:fuBs),'y',...
     f(flCs:fuCs),alphaC(flCs:fuCs),'g',...
     fD(flDs:fuDs),alphaD(flDs:fuDs),'b','LineWidth',2)
xlabel('Frequency (Hz)')
ylabel('Absorption Coefficient')
title('Mineral Wool as Measured in Large and Small Impedance Tubes','FontSize',12)
ylim([0 1])
grid on
hold on

%_DELANY AND BAZLEY PREDICTION_%

Z0 = c*rho;           %characteristic impedance of air
sigma = 25000;       % Flow resistivity of mineral wool
l = 0.055;           % Thickness of sample
f = fD

X = rho*f/sigma;     % Dimensionless quantity for Delany and Bazley
zc = rho*c*(1+0.0571*(X.^-0.754)-j*0.087*(X.^-0.732)); % Characteristic impedance of mine wool
k = (2*pi/c).*f.*(1+0.0978*(X.^-0.700)-j*0.189*(X.^-0.595)); % Complex wavenumber in min wool

z = -j*zc.*cot(k*l); % Surface impedance of mineral wool
R = (z-Z0)./(z+Z0); % Reflection factor of mineral wool
alpha = 1-abs(R).^2; % Absorption coefficient of mineral wool

figure(1)
plot(f,alpha,'k','LineWidth',2);
xlim([15 fuD])
legend('Large Tube Mic positions A and B',...
      'Large Tube Mic positions B and C',...
      'Large Tube Mic positions A and D',...
      'Small Tube Results',...
      'Prediction',4)

```

## APPENDIX C

## Comparing standard transfer function with least squares method

```

close all;
clear all;

rho = 1.21;           % Density of air (kg/m3)
c = 343;             % Speed of sound in air at 23C (m/s)
a = 0.3458/2;       % Tube radius (m)
S = pi*a^2;         % Cross-sectional area of the tube (m2)
dL = 0;             % Distance between tube end and sample
L = 2 + dL;         % Tube length (m)
z1 = 0.184 + dL;    % Distance from sample to micA
z2 = 0.368 + dL;    % Distance from sample to micB
z3 = 0.9143 + dL;   % Distance from sample to micC
z4 = 1.2255 + dL;   % Distance from sample to micD

x = [z1;z2;z3;z4];

name{1} = 'Mineral Wool'; % File name

for i=1:length(name) % Loop if processing more than one file
[I1,Fs]=LOADIMP(strcat(char(name(i)),'A.wmb')); % Loading WINMLS mic1 file into matlab
[I2,Fs]=LOADIMP(strcat(char(name(i)),'B.wmb'));
[I3,Fs]=LOADIMP(strcat(char(name(i)),'C.wmb'));
[I4,Fs]=LOADIMP(strcat(char(name(i)),'D.wmb'));

%_NORMAL TRANSFER FUNCTION TECHNIQUE_%

N1 = length(I1); % Length of impulse in samples
t = [(1:1:length(I1))/Fs]; % Time series
w = hanning(N1) % Hanning window
w(1:N1/2) = 1; % Set first half of window to unity
h1 = I1.*w; % Window impulses
h2 = I2.*w;
h3 = I3.*w;
h4 = I4.*w;

za = 0.19; % Position of mic 1 from the sample
zb = 0.375; % Position of mic 2 from the sample
zc = 0.9143; % Position of mic 3 from the sample
zd = 1.2255; % Position of mic 4 from the sample
y = [za zb zc zd]; % Array of mic positions

spacingA = abs(y(1)-y(2)); % Combinations of mic spacings
spacingB = abs(y(1)-y(3));
spacingC = abs(y(1)-y(4));

N1 = length(h1); % Length, in samples, of the input signal
Nft = 2^16; % Number of frequency points
f = (Fs*(0:(Nft-1)/2))/(Nft-1); % Defining frequency axis
c = 343; % Speed of sound in air
k = (2*pi*f)/c; % Wavenumber

flength = length(f);
df = max(f)/flength; % Frequency interval in samples

```

```

fu1A = c/(2*d);           % Frequency limits of tube
fu2A = (0.45*c)/spacingA;
fuA = min(fu1A,fu2A);
flA = 0.05*c/spacingA;
limA = [flA fuA];       % Upper and Lower frequency graph limits

fu1B = c/(2*d);
fu2B = (0.45*c)/spacingB;
fuB = min(fu1B,fu2B);
flB = 0.05*c/spacingB;
limB = [flB fuB];

fu1C = c/(2*d);
fu2C = (0.45*c)/spacingC;
fuC = min(fu1C,fu2C);
flC = 0.05*c/spacingC;
limC = [flC fuC];

h1_fft = fft(h1,Nft);    % Fourier transform of impulse response
h1freq = h1_fft(1:(Nft)/2); % Get rid of negative frequencies

h2_fft = fft(h2,(Nft));
h2freq = h2_fft(1:(Nft)/2);

h3_fft = fft(h3,(Nft));
h3freq = h3_fft(1:(Nft)/2);

h4_fft = fft(h4,(Nft));
h4freq = h4_fft(1:(Nft)/2);

H12 = h2freq./h1freq;   % Transfer function
H13 = h3freq./h1freq;
H14 = h4freq./h1freq;

RA = (H12.*(exp(j*k*y(1))-exp(j*k*y(2)))/((exp(-j*k*y(2)))-(H12.*exp(-j*k*y(1)))); % Reflection
factor
RB = (H13.*(exp(j*k*y(1))-exp(j*k*y(3)))/((exp(-j*k*y(3)))-(H13.*exp(-j*k*y(1))));
RC = (H14.*(exp(j*k*y(1))-exp(j*k*y(4)))/((exp(-j*k*y(4)))-(H14.*exp(-j*k*y(1))));

zA = (rho*c)*((RA + 1)/(1 - RA)); % Surface impedance
alphaA = (1-abs(RA).^2); % Absorption coefficient

zB = (rho*c)*((RB + 1)/(1 - RB));
alphaB = (1-abs(RB).^2);

zC = (rho*c)*((RC + 1)/(1 - RC));
alphaC = (1-abs(RC).^2);

fuAs = fuA/df;          % Frequency limits in samples
flAs = flA/df;
fuBs = fuB/df;
flBs = flB/df;
fuCs = fuC/df;
flCs = flC/df;

figure(1)
plot(f(flAs:fuAs),alphaA(flAs:fuAs),'r','LineWidth',1.5)
hold on
plot(f(flBs:fuBs),alphaB(flBs:fuBs),'k','LineWidth',1.5)
plot(f(flCs:fuCs),alphaC(flCs:fuCs),'y','LineWidth',1.5)

```

```

%_OPTIMISED METHOD OF PROCESSING RESULTS_%

maxspace = x(4)-x(1);          % Maximum microphone spacing
minspace = x(2)-x(1);          % Minimum microphone spacing
fmin = c/(20*abs(maxspace));    % Minimum frequency limit (Hz)
fmax1 = 0.45*c/(minspace);     % Maximum limit due to mic spacing
fmax2 = c/(2*a);               % Maximum limit due to tube diameter
fmax = min(fmax1,fmax2);       % Pick the lowest of high frequency limits

H12 = h2freq./h1freq;          % Transfer function between mics B/A
H13 = h3freq./h1freq;          % Mics C/A
H14 = h4freq./h1freq;          % Mics D/A

g11 = ((rho*c)/(2*S))*exp(-j*k*(L-z1)); % Green's function micA -> source1
g12 = ((rho*c)/(2*S))*exp(-j*k*(L+z1)); % Green's function micA -> source2
g21 = ((rho*c)/(2*S))*exp(-j*k*(L-z2)); % Green's function micB -> source1
g22 = ((rho*c)/(2*S))*exp(-j*k*(L+z2)); % Green's function micB -> source2
g31 = ((rho*c)/(2*S))*exp(-j*k*(L-z3)); % Green's function micC -> source1
g32 = ((rho*c)/(2*S))*exp(-j*k*(L+z3)); % Green's function micC -> source2
g41 = ((rho*c)/(2*S))*exp(-j*k*(L-z4)); % Green's function micD -> source1
g42 = ((rho*c)/(2*S))*exp(-j*k*(L+z4)); % Green's function micD -> source2

Roptimised1 = -((H12.*g11-g21).*(conj(H12.*g12-g22))+...
(H13.*g11-g31).*(conj(H13.*g12-g32))+...
(H14.*g11-g41).*(conj(H14.*g12-g42)))/...
((abs(H12.*g12-g22)).^2+(abs(H13.*g12-g32)).^2+...
(abs(H14.*g12-g42)).^2);

alpha1 = 1-abs(Roptimised1).^2; % Optimised absorption coefficient

Z1 = rho*c.*((1+Roptimised1)/(1-Roptimised1)); % impedance

figure(1)
plot(f(1:Nft/2),alpha1,'b','LineWidth',2),xlim([17 450])
legend('Standard Method [mics A-B]','Standard Method [mics A-C]','Standard Method [mics A-
D]','Optimised Mehtod')
title('Comparing Standard and Optimised Method','FontSize',12)
xlabel('Frequency, Hz'), ylabel('Absorption Coefficient')
hold on
grid on

end

```

## APPENDIX D

Comparing the original least squares technique with the extended version.

```

close all;
clear all;

rho = 1.21;           % Density of air (kg/m3)
c = 343;             % Speed of sound in air at 23C (m/s)
a = 0.3458/2;       % Tube radius (m)
S = pi*a^2;         % Cross-sectional area of the tube (m2)
dL = 0;             % Distance between tube end and sample
L = 2 + dL;         % Tube length (m)
z1 = 0.184 + dL;    % Distance from sample to micA
z2 = 0.368 + dL;    % Distance from sample to micB
z3 = 0.9143 + dL;   % Distance from sample to micC
z4 = 1.2255 + dL;   % Distance from sample to micD

x = [z1;z2;z3;z4];

name{1} = 'Mineral Wool';

for i=1:length(name)
[I1,Fs]=LOADIMP(strcat(char(name(i)),'A.wmb')); % Loading WINMLS mic1 file into matlab
[I2,Fs]=LOADIMP(strcat(char(name(i)),'B.wmb'));
[I3,Fs]=LOADIMP(strcat(char(name(i)),'C.wmb'));
[I4,Fs]=LOADIMP(strcat(char(name(i)),'D.wmb'));

N1 = length(I1);
han = hanning(N1)
han(1:N1/2) = 1;
h1 = I1.*han;
h2 = I2.*han;
h3 = I3.*han;
h4 = I4.*han;

za = 0.19;           % Position of mic 1 from the sample
zb = 0.375;         % Position of mic 2 from the sample
zc = 0.9143;        % Position of mic 3 from the sample
zd = 1.2255;        % Position of mic 4 from the sample
y = [za zb zc zd];  % Array of mic positions

spacingA = abs(y(1)-y(2));
spacingB = abs(y(1)-y(3));
spacingC = abs(y(1)-y(4));

spacingD = abs(y(2)-y(3));
spacingE = abs(y(2)-y(4));

spacingF = abs(y(3)-y(4));

rho=1.21;
d = 0.3458;         %Tube diameter
N1 = length(h1);    % Length, in samples, of the input signal
Nft = 2^16;         % Number of frequency points
f = (Fs*(0:(Nft-1)/2))/(Nft-1)); % Defining frequency axis
k = (2*pi*f)/c;

```

```

length = length(f);
df = max(f)/length;

fname1 = strcat(name(i),'A.wmb');
fname2 = strcat(name(i),'B.wmb');
fname3 = strcat(name(i),'C.wmb');
fname4 = strcat(name(i),'D.wmb');

maxspace = x(4)-x(1);           % Maximum microphone spacing
minspace = x(2)-x(1);           % Minimum microphone spacing
fmin = c/(20*abs(maxspace));    % Minimum frequency limit (Hz)
fmax1 = 0.45*c/(minspace);     % Maximum limit due to mic spacing
fmax2 = c/(2*a);                % Maximum limit due to tube diameter
fmax = min(fmax1,fmax2);       % Pick the lowest of high frequency limits

[yA, Fs] = loadimp(char(fname1)); % Load WinMLS impulse response for micA
[yB, Fs] = loadimp(char(fname2)); % MicB
[yC, Fs] = loadimp(char(fname3)); % MicC
[yD, Fs] = loadimp(char(fname4)); % MicD

N = length(yA);                 % Number of sample points
w = hanning(N);                 % Generate hanning window
w(1:N/2) = ones(N/2,1);        % Assign first half of window to unity

yA = (yA(1:N));                 % Pick the first N points of yA
yB = (yB(1:N));                 % yB
yC = (yC(1:N));                 % yC
yD = (yD(1:N));                 % yD

ywA = yA.*w;                    % Apply hanning window to micA impulse reponse
ywB = yB.*w;                    % MicB
ywC = yC.*w;                    % MicC
ywD = yD.*w;                    % MicD

t = [(1:1:length(ywA))/Fs];     % Generate time series (s)
f = (Fs*(0:(N-1)))/(N-1);      % Generate frequency series (Hz)
k = (2*pi*f(1:N/2))/c;          % Wave number array

YA = fft(ywA);                  % Fourier Transform on mic A impulse responses
YB = fft(ywB);                  % Mic B
YC = fft(ywC);                  % Mic C
YD = fft(ywD);                  % Mic D

Y1 = (YA(1:N/2));               % Pick the first N/2 points of Y1
Y2 = (YB(1:N/2));               % Y2
Y3 = (YC(1:N/2));               % Y3
Y4 = (YD(1:N/2));               % Y4

H12 = Y2./Y1;                   % Transfer function between mics B/A
H13 = Y3./Y1;                   % Mics C/A
H14 = Y4./Y1;                   % Mics D/A
H23 = Y3./Y2;                   % Mics C/B
H24 = Y4./Y2;                   % Mics D/B
H34 = Y4./Y3;                   % Mics D/C

g11 = ((rho*c)/(2*S))*exp(-j*k*(L-z1)); % Green's function micA -> source1
g12 = ((rho*c)/(2*S))*exp(-j*k*(L+z1)); % Green's function micA -> source2
g21 = ((rho*c)/(2*S))*exp(-j*k*(L-z2)); % Green's function micB -> source1
g22 = ((rho*c)/(2*S))*exp(-j*k*(L+z2)); % Green's function micB -> source2
g31 = ((rho*c)/(2*S))*exp(-j*k*(L-z3)); % Green's function micC -> source1

```

```

g32 = ((rho*c)/(2*S))*exp(-j*k*(L+z3)); % Green's function micC -> source2
g41 = ((rho*c)/(2*S))*exp(-j*k*(L-z4)); % Green's function micD -> source1
g42 = ((rho*c)/(2*S))*exp(-j*k*(L+z4)); % Green's function micD -> source2

Roptimised1 = -((H12.*g11-g21).*(conj(H12.*g12-g22))+... % Original optimised method
(H13.*g11-g31).*(conj(H13.*g12-g32))+...
(H14.*g11-g41).*(conj(H14.*g12-g42)))/...
((abs(H12.*g12-g22)).^2+(abs(H13.*g12-g32)).^2+...
(abs(H14.*g12-g42)).^2);

Roptimised2 = -((H12.*g11-g21).*(conj(H12.*g12-g22))+... % Extended optimised method
(H13.*g11-g31).*(conj(H13.*g12-g32))+...
(H14.*g11-g41).*(conj(H14.*g12-g42))+...
(H23.*g21-g31).*(conj(H23.*g22-g32))+...
(H24.*g21-g41).*(conj(H24.*g22-g42))+...
(H34.*g31-g41).*(conj(H34.*g32-g42)))/...
((abs(H12.*g12-g22)).^2+(abs(H13.*g12-g32)).^2+...
(abs(H14.*g12-g42)).^2+(abs(H23.*g22-g32)).^2+...
(abs(H24.*g22-g42)).^2+(abs(H34.*g32-g42)).^2);

alpha1 = 1-abs(Roptimised1).^2; % Absorption coefficient original
alpha2 = 1-abs(Roptimised2).^2; % Absorption coefficient extended

Z1 = rho*c.*((1+Roptimised1)/(1-Roptimised1)); % Surface impedance original
Z2 = rho*c.*((1+Roptimised2)/(1-Roptimised2)); % Surface impedance extended

figure(1)
set(gcf,'Name','Absorption Coefficient')
plot(f(1:N/2),alpha1,'b',f(1:N/2),alpha2,'r','LineWidth',2),xlim([17 450])
legend('Original Optimisation Method','Extended Optimisation Method')
grid on
title('Comparing Standard and Extended Optimised Methods','FontSize',12)
xlabel('Frequency, Hz'), ylabel('Absorption Coefficient')
hold on

end

```



## APPENDIX E

MATLAB script for processing results from accelerometer data in section 4.3

```
% ____ Processing Accelerometer Measurements ____ %

close all;
clear all;

c = 343; % Speed of sound in air
fmax = 200; % max frequency
fmin = 30; % min frequency

str(1,1:2) = 'r-'; % String to define order of colours for plot
str(2,1:2) = 'b-';

s{1} = 'acc surround'; % Input file names
s{2} = 'acc no surround';

for i = 1:length(s)
    files = s(i); % Pick successive files to process
    fname = strcat(files,'wmb'); % Add on suffix to complete file name
    [yA, Fs] = loadimp(char(fname)); % Load winMLS files

    N = length(yA); % Number of sample points
    w = hanning(N); % Generate Hanning window
    w(1:N/2) = 1; % Assign first half of window to unity

    yA = (yA(1:N)); % Pick the first N points
    ywA = yA.*w; % Apply Hanning window to mic A impulse response

    t = [(1:1:length(ywA))/Fs]; % Generate time series (s)
    f = (Fs*(0:(N-1)))/(N-1); % Generate frequency series (Hz)
    k=(2*pi*f(1:N/2))/c; % Wave number array

    YA = fft(ywA); % Fourier Transform on impulse responses
    YA = 20*log(abs(YA)); % Log of FFT

    plot(f,YA,str(i,:), 'LineWidth',2)
    hold on
    grid on
    legend('With Surround','Without Surround',4)
    xlabel('Frequency, Hz')
    ylabel('Level, dB')
    title('Acceleration Level versus Frequency For Different Mounting Conditions','FontSize',13)
    xlim([fmin fmax])
end
```

**APPENDIX F**



A: Surround mounted membrane on Large sample holder



B: Clamped membrane on large sample holder



C: Impedance tube mounting rings

The sample holder, with the sample in place between the mounting rings, was jacked into place to provide a termination at the impedance tube walls approximating a clamped condition.

## APPENDIX G

Analogue circuit analysis of absorber with and without surround.

```

close all;
clear all;

c = 343; % Speed of sound in air
rho = 1.21; % Density of air
Z0 = c*rho; % Characteristic impedance of air
f = 1:1:400; % Frequency spectrum, Hz
w = 2*pi*f; % Angular frequency
k = w/c; % Wavenumber in air
V = 0.035; % Volume of backing
a = 0.135; % Radius of plate with surround plus 1/3 of surround
SD = pi*(a^2); % Area of plate and surround

sigma = 10200; % Flow resistivity of absorbent
X = rho*f/sigma;
Z2 = rho*c*(1+0.0571*(X.^-0.754)-j*0.087*(X.^-0.732));
k2 = (2*pi/c).*f.*(1+0.0978*(X.^-0.700)-j*0.189*(X.^-0.595));
d2 = 0.15;
zs2 = -j*rho*c.*cot(k2*d2); % Delany and Bazley prediction for porous absorbent in cabinet

%_ With Surround _%

MSUR = 0.03402; % Mass of moving surround
MMEM = 0.1077; % Mass of moving hardboard
MMS = MSUR+MMEM; % Combined mass of surround and plate (hardboard),kg
RAF1 = (rho*c.*(k.^2))./(2*pi); % Radiation resistance
MAF1 = j*w.*((8*rho)/(3*(pi^2)*a)); % Radiation mass
BL = 15;
RES = 360.575;
RMS = (BL^2)/RES;
RAD = RMS/(SD^2); % Approximate resistive losses in diaphragm based on L/S data
RAB = zs2; % Resistive losses in cabinet

CMS = 205.5E-6; % Compliance of surround/plate in mechanical units
CAD = CMS*(SD^2); % Diaphragm compliance in acoustic units
CAB = V/(rho*(c^2)); % Compliance of cabinet in acoustic units

CAT = (1/(j.*w.*((CAD*CAB)/(CAD+CAB)))); % Total compliance in acoustic units
RAT = RAD+RAB+RAF1; % Total resistive damping in acoustical units
MAD = (j.*w.*((MMS/(SD^2)))) + MAF1; % Total mass impedance acoustic units

ZAF = Z0/SD;
Z = SD*(RAT + MAD + CAT + ZAF); % Total surface impedance of system

R = (Z-Z0)/(Z+Z0); % Complex reflection factor of system
alpha = 1-R.*conj(R); % Absorption coefficient

figure(1)
plot(f,alpha,'b','LineWidth',2)
hold on

%_ Without Surround _%

a = 0.14;

```

```

SD = pi*(a^2);
MMEM2 = 0.173;
MMS = MMEM2/5;           % Combined mass of surround and plate (hardboard),kg

RES = 360.575;
RMS = (BL^2)/RES;
RAD = RMS/(SD^2);       % Resistive losses in diaphragm
RAB = zs2;              % Resistive losses in cabinet

E = 0.1e6;              % Youngs Modulus
mu = 0.7;              % Poisson Ratio
h = 3.2e-3;            % Thickness of plate
CMS = 180*(1-(mu^2))*(a^2)/(E*(h^3)); % Compliance of surround/plate in mechanical units
CAD = CMS*(SD^2);      % Diaphragm compliance in acoustic units
CAB = V/(rho*(c^2));   % Compliance of cabinet in acoustic units

CAT = 1./(j.*w.*((CAD*CAB)/(CAD+CAB))); % Total compliance in acoustic units
RAT = RAD+RAB+RAF1;    % Total resistive damping in acoustical units
MAD = (j.*w.*(MMS/(SD^2)))+MAF1; % Total mass impedance acoustic units
ZAF = Z0/SD;
Z = SD*(RAT + MAD + CAT + ZAF); % Total surface impedance of system

R = (Z-Z0)/(Z+Z0);     % Complex reflection factor of system
alpha = 1-R.*conj(R); % Absorption coefficient

figure(1)
plot(f,alpha,'r','LineWidth',2)
title('Equivalent Circuit Model of Membrane Absorber With and Without Surround
Mounting','FontSize',13)
legend('With Surround','Without Surround')
xlabel('Frequency, Hz'),ylabel('Absorption Coefficient')
ylim([0 1.1])
grid on

```

## APPENDIX H

MATLAB script for comparing impedance tube results with transfer matrix models for hardboard and vinyl rubber membranes.

```

close all;
clear all;

rho = 1.21;           % Density of air (kg/m3)
c = 343;             % Speed of sound in air at 23C (m/s)
Z0 = rho*c;         % Characteristic impedance of air
a = 0.3458;         % Tube radius (m)
S = pi*a^2;         % Cross-sectional area of the tube (m2)
dL = 0;             % Distance between tube end and sample
L = 2 + dL;         % Tube length (m)
z1 = 0.184 + dL;    % Distance from sample to micA
z2 = 0.368 + dL;    % Distance from sample to micB
z3 = 0.9143 + dL;   % Distance from sample to micC
z4 = 1.2255 + dL;   % Distance from sample to micD
x = [z1;z2;z3;z4];

name{1} = 'With Surround Min Wool';    % File names
name{2} = 'No Surround Min Wool';
name{3} = 'With Surround Hardboard';
name{4} = 'No Surround Hardboard';

str(1,1:2) = 'r-';    % String of colours for plotting
str(2,1:2) = 'b-';
str(3,1:2) = 'r-';
str(4,1:2) = 'b-';

for i = 1:length(name)
    fname1 = strcat(name(i),'A.wmb');
    fname2 = strcat(name(i),'B.wmb');
    fname3 = strcat(name(i),'C.wmb');
    fname4 = strcat(name(i),'D.wmb');

    maxspace = x(4)-x(1);    % Maximum microphone spacing
    minspace = x(2)-x(1);    % Minimum microphone spacing
    fmin = c/(20*abs(maxspace)); % Minimum frequency limit (Hz)
    fmax1 = 0.45*c/(minspace); % Maximum limit due to mic spacing
    fmax2 = c/(2*a);         % Maximum limit due to tube diameter
    fmax = min(fmax1,fmax2); % Pick the lowest of high frequency limits

    [yA, Fs] = loadimp(char(fname1)); % Load WinMLS impulse response for micA
    [yB, Fs] = loadimp(char(fname2)); % MicB
    [yC, Fs] = loadimp(char(fname3)); % MicC
    [yD, Fs] = loadimp(char(fname4)); % MicD

    N = length(yA);          % Number of sample points
    w = hanning(N);          % Generate Hanning window
    w(1:N/2) = ones(N/2,1); % Assign first half of window to unity
    yA = (yA(1:N));          % Pick the first N points of yA
    yB = (yB(1:N));          % yB
    yC = (yC(1:N));          % yC
    yD = (yD(1:N));          % yD

```

```

ywA = yA.*w;           % Apply Hanning window to micA impulse response
ywB = yB.*w;           % MicB
ywC = yC.*w;           % MicC
ywD = yD.*w;           % MicD

f = (Fs*(0:(N-1))/(N-1)); % Generate frequency series (Hz)
k = (2*pi*f(1:N/2))/c;   % Wave number array

YA = fft(ywA);          % Fourier Transform on mic A impulse responses
YB = fft(ywB);          % Mic B
YC = fft(ywC);          % Mic C
YD = fft(ywD);          % Mic D

Y1 = (YA(1:N/2));      % Pick the first N/2 points of YA
Y2 = (YB(1:N/2));      % YB
Y3 = (YC(1:N/2));      % YC
Y4 = (YD(1:N/2));      % YD

H12 = Y2./Y1;          % Transfer function between mics B/A
H13 = Y3./Y1;          % Mics C/A
H14 = Y4./Y1;          % Mics D/A
H23 = Y3./Y2;          % Mics C/B
H24 = Y4./Y2;          % Mics D/B
H34 = Y4./Y3;          % Mics D/C

g11 = ((rho*c)/(2*S))*exp(-j*k*(L-z1)); % Green's function micA -> source1
g12 = ((rho*c)/(2*S))*exp(-j*k*(L+z1)); % Green's function micA -> source2
g21 = ((rho*c)/(2*S))*exp(-j*k*(L-z2)); % Green's function micB -> source1
g22 = ((rho*c)/(2*S))*exp(-j*k*(L+z2)); % Green's function micB -> source2
g31 = ((rho*c)/(2*S))*exp(-j*k*(L-z3)); % Green's function micC -> source1
g32 = ((rho*c)/(2*S))*exp(-j*k*(L+z3)); % Green's function micC -> source2
g41 = ((rho*c)/(2*S))*exp(-j*k*(L-z4)); % Green's function micD -> source1
g42 = ((rho*c)/(2*S))*exp(-j*k*(L+z4)); % Green's function micD -> source2

Roptimised = -((H12.*g11-g21).*(conj(H12.*g12-g22))+...% Optimised reflection factor from impedance
tube measurements
(H13.*g11-g31).*(conj(H13.*g12-g32))+...
(H14.*g11-g41).*(conj(H14.*g12-g42))+...
(H23.*g21-g31).*(conj(H23.*g22-g32))+...
(H24.*g21-g41).*(conj(H24.*g22-g42))+...
(H34.*g31-g41).*(conj(H34.*g32-g42)))/...
((abs(H12.*g12-g22)).^2+(abs(H13.*g12-g32)).^2+...
(abs(H14.*g12-g42)).^2+(abs(H23.*g22-g32)).^2+...
(abs(H24.*g22-g42)).^2+(abs(H34.*g32-g42)).^2);

alpha = 1-abs(Roptimised).^2; % Absorption coefficient from impedance tube measurements
Z = Z0.*((1+Roptimised)/(1-Roptimised)); % Surface impedance from impedance tube measurements

figure(1)
if i<=2
    subplot(2,1,1)
    plot(f(1:N/2),alpha,str(i,:), 'LineWidth',2)
    hold on
else
    figure(1)
    subplot(2,1,2)
    plot(f(1:N/2),alpha,str(i,:), 'LineWidth',2)
    hold on
end
end

```

```

%_ TRANSFER MATRIX MODEL _%

d2 = 0.15;           % Depth of absorbent
d1 = 0.15;           % Air gap depth
mV = 2.81;           % Acoustic mass per unit area of membrane (vinyl)
mH = 2.57;           % Acoustic mass per unit area of membrane (hardboard)
f = (1:1:300)';      % Array of frequencies
w = 2*pi.*f;         % Angular frequency
rm = 10;             % Resistive losses due to mounting of the membrane
k1 = w/c;            % Wavenumber

sigma = 10200;       % Flow resistivity of absorbent
X = rho*f/sigma;     % Unitless quantity for Delany and Bazley prediction
Z2 = Z0*(1+0.0571*(X.^-0.754)-j*0.087*(X.^-0.732));
k2 = (2*pi/c).*f.*(1+0.0978*(X.^-0.700)-j*0.189*(X.^-0.595));

zs2 = -j*Z2.*cot(k2*d2);
zs3 = (-j*zs2.*Z0.*cot(k1*d1)+Z0.^2)./(zs2 -j*Z0.*cot(k1*d1));

zs4V = zs3 + j*w*mV +rm;           %Final surface impedance of vinyl rubber
zs4H = zs3 + j*w*mH +rm;           %Final surface impedance of hardboard

RV = (zs4V - Z0)/(zs4V + Z0);      % Reflection factor for vinyl rubber
alphaV = 1-(abs(RV).^2);           % Absorption coefficient for vinyl rubber

RH = (zs4H - Z0)/(zs4H + Z0);      % Reflection factor for hardboard
alphaH = 1-(abs(RH).^2);           % Absorption coefficient for hardboard

figure(1)
set(gcf,'Name','Absorption Coefficient')
subplot(2,1,1)
plot(f,alphaV,'g','LineWidth',2)
xlabel('Frequency, Hz'),ylabel('absorption coefficient')
title('Vinyl Rubber')
legend('With Surround','Without Surround','Transfer Matrix Model')
axis([20 150 0 1])
grid on
subplot(2,1,2)
plot(f,alphaH,'g','LineWidth',2)
xlabel('Frequency, Hz'),ylabel('absorption coefficient')
title('Hardboard')
legend('With Surround','Without Surround','Transfer Matrix Model')
axis([20 150 0 1])
grid on

```

## APPENDIX I

### Rules for equivalent circuit nomenclature:

In general the symbols are written in the form  $A_{xyz}$  :

$A$  refers to the quantity, i.e. Mass ( $M$ ), Resistance ( $R$ ), Compliance ( $C$ ), Impedance ( $Z$ )... etc

$x$  refers to the units or type of quantity i.e. Electrical ( $E$ ), Mechanical ( $M$ ) or Acoustic ( $A$ )

$y$  refers to other information regarding the value e.g.

Subscript:  $B$ , refers to the back of the diaphragm (the cabinet)

$D$ , refers to the diaphragm without an air load

$S$ , refers to the diaphragm with an air load

$T$ , refers to a total

$V$ , refers to a variable component

For example: The total acoustic compliance is written as:  $C_{AB}$

The mechanical mass of the diaphragm with an air load is written as,

$M_{MS}$

The total damping in acoustic units is written as,  $R_{AT}$



## APPENDIX J

## Comparing impedance tube results with lumped parameter predictions

```

close all;
clear all;

rho = 1.21;           % Density of air (kg/m3)
c = 344;             % Speed of sound in air at 23C (m/s)
a = 0.3458;         % Tube diameter (m)
S = pi*(a/2)^2;     % Cross-sectional area of the tube (m2)
dL = 0;             % Distance between tube end and sample
L = 2 + dL;         % Tube length (m)
z1 = 0.184 + dL;    % Distance from sample to micA
z2 = 0.368 + dL;    % Distance from sample to micB
z3 = 0.9143 + dL;   % Distance from sample to micC
z4 = 1.2255 + dL;   % Distance from sample to micD
x = [z1;z2;z3;z4];

values(1) = 1e6;     % Approximation to resistance of open circuit case
files{1} = 'Open Circuit';

for i = 1:length(files)
    fname1 = strcat(files(i),'A.wmb');
    fname2 = strcat(files(i),'B.wmb');
    fname3 = strcat(files(i),'C.wmb');
    fname4 = strcat(files(i),'D.wmb');

    maxspace = x(4)-x(1); % Maximum microphone spacing
    minspace = x(2)-x(1); % Minimum microphone spacing
    fmin = c/(20*abs(maxspace)); % Minimum frequency limit (Hz)
    fmax1 = 0.45*c/(minspace); % Maximum limit due to mic spacing
    fmax2 = c/(2*a); % Maximum limit due to tube diameter
    fmax = min(fmax1,fmax2); % Pick the lowest of high frequency limits

    [yA, Fs] = loadimp(char(fname1)); % Load WinMLS impulse response for micA
    [yB, Fs] = loadimp(char(fname2)); % MicB
    [yC, Fs] = loadimp(char(fname3)); % MicC
    [yD, Fs] = loadimp(char(fname4)); % MicD

    N = length(yA); % Number of sample points
    w = hanning(N); % Generate hanning window
    w(1:N/2) = 1; % Assign first half of window to unity

    yA = (yA(1:N)); % Pick the first N points of yA
    yB = (yB(1:N)); % yB
    yC = (yC(1:N)); % yC
    yD = (yD(1:N)); % yD

    ywA = yA.*w; % Apply hanning window to micA impulse reponse
    ywB = yB.*w; % MicB
    ywC = yC.*w; % MicC
    ywD = yD.*w; % MicD

    t = [(1:length(ywA))/Fs]; % Generate time series (s)
    f = (Fs*(0:(N-1))/(N-1)); % Generate frequency series (Hz)
    k = (2*pi.*f(1:N/2))./c; % Wave number array

```

```

YA = fft(ywA);           % Fourier Transform on mic A impulse responses
YB = fft(ywB);           % Mic B
YC = fft(ywC);           % Mic C
YD = fft(ywD);           % Mic D

Y1 = (YA(1:N/2));        % Pick the first N/2 points of YA
Y2 = (YB(1:N/2));        % YB
Y3 = (YC(1:N/2));        % YC
Y4 = (YD(1:N/2));        % YD

H12 = Y2./Y1;            % Transfer function between mics B/A
H13 = Y3./Y1;            % Mics C/A
H14 = Y4./Y1;            % Mics D/A
H23 = Y3./Y2;            % Mics C/B
H24 = Y4./Y2;            % Mics D/B
H34 = Y4./Y3;            % Mics D/C

g11 = ((rho*c)/(2*S))*exp(-j*k*(L-z1)); % Green's function micA -> source1
g12 = ((rho*c)/(2*S))*exp(-j*k*(L+z1)); % Green's function micA -> source2
g21 = ((rho*c)/(2*S))*exp(-j*k*(L-z2)); % Green's function micB -> source1
g22 = ((rho*c)/(2*S))*exp(-j*k*(L+z2)); % Green's function micB -> source2
g31 = ((rho*c)/(2*S))*exp(-j*k*(L-z3)); % Green's function micC -> source1
g32 = ((rho*c)/(2*S))*exp(-j*k*(L+z3)); % Green's function micC -> source2
g41 = ((rho*c)/(2*S))*exp(-j*k*(L-z4)); % Green's function micD -> source1
g42 = ((rho*c)/(2*S))*exp(-j*k*(L+z4)); % Green's function micD -> source2

Roptimised = -((H12.*g11-g21).*(conj(H12.*g12-g22))+...
(H13.*g11-g31).*(conj(H13.*g12-g32))+...
(H14.*g11-g41).*(conj(H14.*g12-g42))+...
(H23.*g21-g31).*(conj(H23.*g22-g32))+...
(H24.*g21-g41).*(conj(H24.*g22-g42))+...
(H34.*g31-g41).*(conj(H34.*g32-g42)))/...
((abs(H12.*g12-g22)).^2+(abs(H13.*g12-g32)).^2+...
(abs(H14.*g12-g42)).^2+(abs(H23.*g22-g32)).^2+...
(abs(H24.*g22-g42)).^2+(abs(H34.*g32-g42)).^2);

alpha = 1-abs(Roptimised).^2;

str(1,1:2) = 'r-';
str(2,1:2) = 'b-';

Z = rho*c.*((1+Roptimised)/(1-Roptimised)); % Impedance

figure(1)
plot(f(1:N/2),alpha,'r','LineWidth',2)
xlim([20 400]),ylim([0 1.1])
hold on

end

% __ LUMPED PARAMETER PREDICTION __%

% Loudspeaker Parameters
a = 0.1355;           % Radius of diaphragm
L1 = 0.907e-3;        % Electrical inductance of voice coil [1]
L2 = 1.595e-3;        % Electrical inductance of voice coil [2]
R2 = 5.02;
BL = 20.169;          % Force factor of driver
SD = pi*(a^2);        % Area of diaphragm
RE = 12.415;          % Electrical resistance of driver

```

```

MMS = 28.152e-3;           % Moving mass of diaphragm (with air load)
RES = 360.575;           % Damping of diaphragm in electrical units
CMS = 385.276e-6;       % Mechanical compliance of driver with air load
LE=L1;
f = 20:1000;
w = 2*pi*f;
k = w./c;
x = 0.38;                % Width of cabinet/sample holder
y = 0.505;              % Height of cabinet/sample holder
d = 0.226;              % Depth of cabinet/sample holder
V = x*y*d;              % Volume of cabinet/sample holder
Z0 = c*rho;             % Characteristic impedance of air

RMS = (BL^2)/RES;       % Mechanical damping/resistance of diaphragm with airload
RAD = RMS/(SD^2);      % Resistance/damping of diaphragm in acoustic units
RAF = 0;

sigma = 10200;          % Flow resistivity of absorbent
X = rho*f/sigma;        % Delany and Bazley prediction for absorbent in cabinet
Z0 = rho*c;
d2 = 0.3;
Z2 = rho*c*(1+0.0571*(X.^-0.754)-j*0.087*(X.^-0.732));
k2 = k.*(1+0.0978*(X.^-0.700)-j*0.189*(X.^-0.595));

RAB = -j*rho*c.*cot(k2*d2);
CAD = CMS*(SD^2);      % Compliance of diaphragm in acoustic units
CAB = V/(rho*(c^2));   % Compliance in acoustic units of cabinet
ZAF = Z0/SD;

val = values';          % Array of resistance values
for i = 1:length(val)

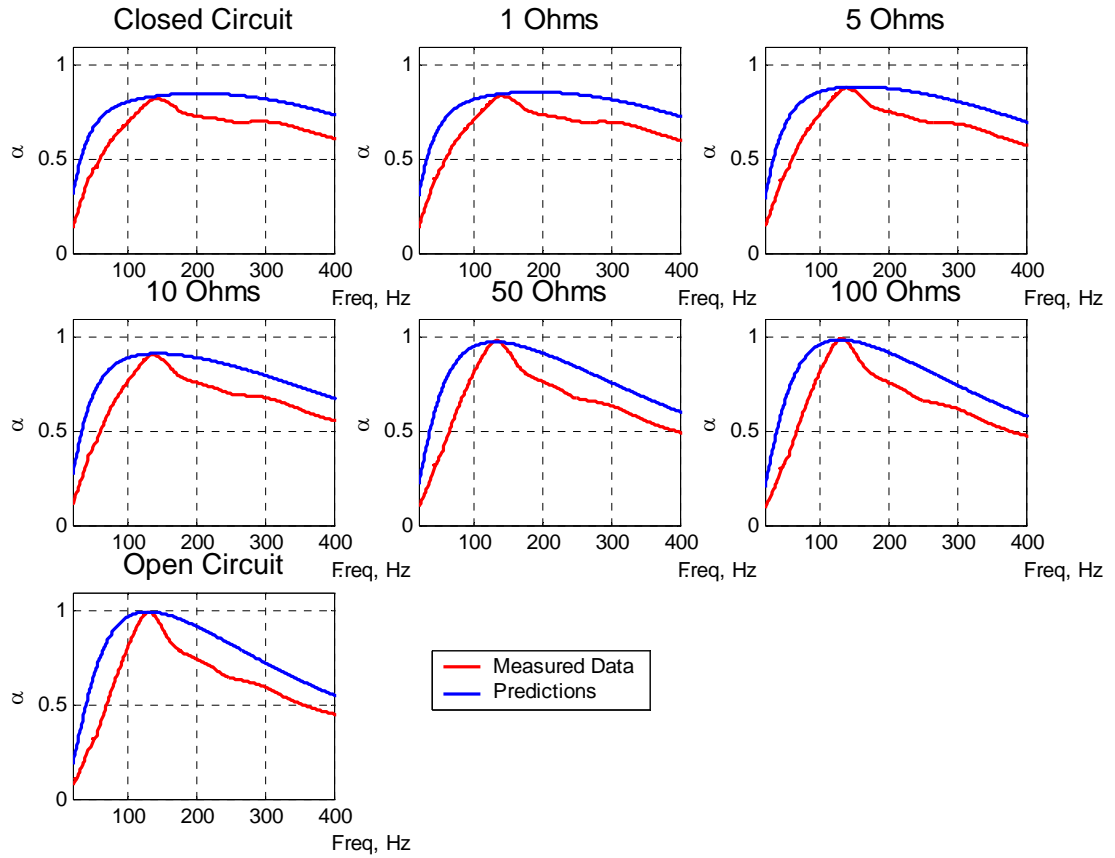
    REV = val(i);       % Variable resistance values
    z1 = 1./(j*w*(((SD^2)*LE)/(BL^2))); % Impedance due to electrical inductance in acoustic units
    z2 = (BL^2)/(RE*(SD^2)); % Impedance due to electrical resistance in acoustic units
    z3 = (BL^2)/(REV*(SD^2)); % Impedance due to variable resistance in acoustic units
    z4 = ((BL^2)/(R2*(SD^2)))+(1./(j.*w.*(((SD^2).*L2)/(BL^2))));
    ZEA = 1./((1./z1)+(1./z2)+(1./z3)+(1./z4)); % Combined impedance due to electronic
components in acoustic units
    CAT = (1./(j*w.*((CAD*CAB)/(CAD+CAB)))); % Combined acoustic compliance of entire system
    RAT = RAD+RAB;      % Comined acoustic damping of entire system
    MAF1 = j*w.*((8*rho)/(3*(pi^2)*a)); % Radiation impedance of a baffled piston
    MAT = (j.*w.*(MMS/(SD^2)))-MAF1; % Combined mass loading of entire system (minus air load
as MMS was measured in free field)
    Z = SD*(ZEA + RAT + MAT + CAT + ZAF); % Specific acoustic impedance of entire system
    R = (Z-Z0)/(Z+Z0);
    alpha = 1-R.*conj(R);

figure(1)
plot(f,alpha,'b','LineWidth',1.5)
xlabel('Frequency, Hz'),ylabel('Absorption Coefficient')
title('Using a Loudspeaker as an Absorber', 'FontSize',13)
legend('Results from Impedance Tube', 'Equivalent Circuit Prediction')
grid on
end

```

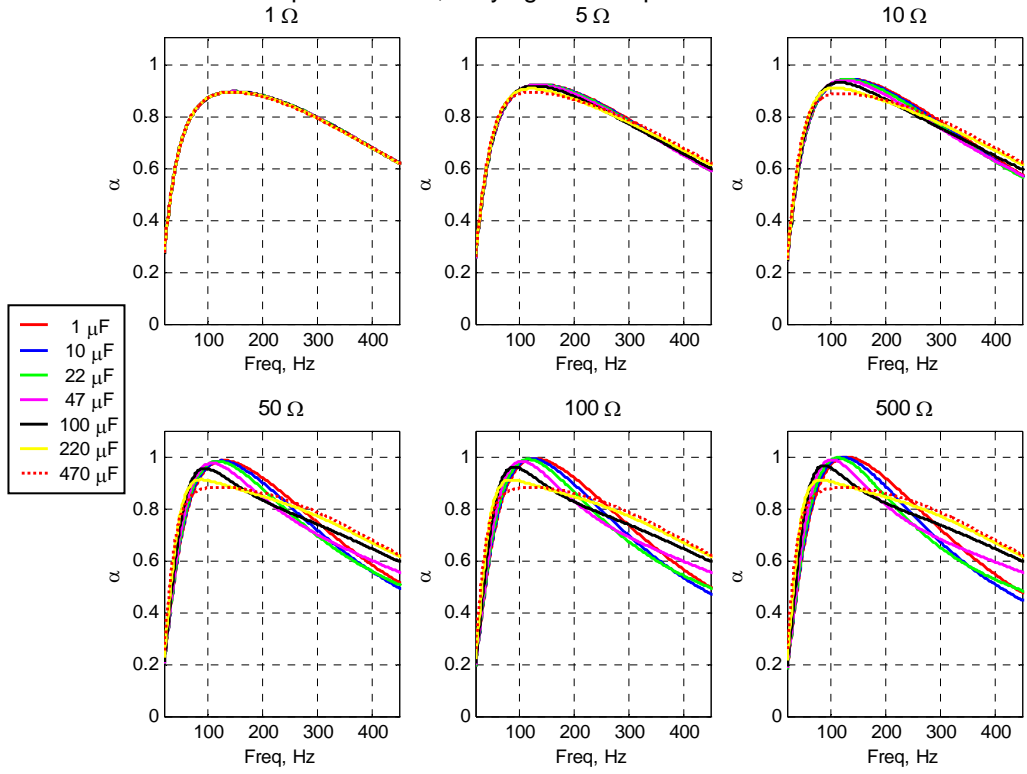
### APPENDIX K

Comparing impedance tube measurements with predictions from the equivalent circuit model for each load resistance connected to terminals.



### APPENDIX L

Predicted Absorption Curves, Varying Load Capacitance and Resistance in Parallel



**BIBLIOGRAPHY**

- F. Alton Everest, *Master Handbook of Acoustics*, 4<sup>th</sup> edn., McGraw-Hill, (2001).
- M. Barron, *Auditorium Acoustics and Architectural Design*, E and F. N. Spon (1993).
- L. L. Beranek, *Acoustics*, Acoustical Society of America, (1996).
- J. Borwick, *Loudspeaker and Headphone handbook*, 2<sup>nd</sup> edn, Focal Press, (1994).
- J. Borwick, *Loudspeaker and Headphone handbook*, 3<sup>rd</sup> edn, Focal Press (2001).
- M. Colloms, *High Performance Loudspeakers*, 6<sup>th</sup> edn, John Wiley and sons (2005).
- T. J. Cox and P. D'Antonio, *Acoustic absorbers and diffusers*, Spon Press (2004).
- F. Fahy, *Foundations of Engineering Acoustics*, Academic Press, (2001)
- F. A. Fischer, *Fundamentals of Electroacoustics*, Interscience Publishers, inc., New York, (1955).
- L.E. Kinsler, A. R. Frey, A. B. Copens and J. V. Sanders, *Fundamentals of Acoustics*, 3<sup>rd</sup> edn, John Wiley and Sons (1982).
- H. Kuttruff , *Room Acoustics*, 4<sup>th</sup> edn., Spon press (2000).
- F. P. Mechel, *Formulas of Acoustics*, Springer, (2002).
- P. M. Morse and K. U. Ingard, *Theoretical Acoustics*, McGraw-Hill, (1968).
- M. Rossi, *Acoustics and Electroacoustics*, Artech House, (1988).
- I. R. Sinclair (ed), *Audio and Hi-Fi Handbook*, 2<sup>nd</sup> edn, Butterworth-Heinemann, (1993).
- M. C. M. Wright (ed), *Lecture Notes on the Mathematics of Acoustics*, Imperial College Press, (2005).